

A NEW, IMPROVED PRECATALYST FOR SUZUKI-MIYAJIMA CROSS-  
COUPLING REACTIONS

by

Danielle Marie Norton

A thesis submitted to the Department of Chemistry

In conformity with the requirements for

the degree of Master of Science

Queen's University

Kingston, Ontario, Canada

(July, 2009)

Copyright © Danielle Marie Norton, 2009

## Abstract

Carbon-carbon bond formation is one of the most important reactions in organic chemistry, and the Suzuki-Miyaura cross-coupling reaction has become a forerunner in this area. Considerable research has been directed at the mechanistic aspects and synthetic utility of the reaction; however, little attention has been given to the formation of the putative PdL<sub>2</sub> catalysts. Due to their high reactivities, these catalysts are typically difficult to store and therefore are often generated *in situ* in unknown yields and at unknown rates via any number of available palladium precursors. This thesis describes research directed towards determining the optimum conditions to quantitatively generate compounds of the type Pd(0)L<sub>n</sub> (L = PMePh<sub>2</sub>, PPh<sub>3</sub>, PCy<sub>3</sub>, PMeBu<sup>t</sup><sub>2</sub>, PBu<sup>t</sup><sub>3</sub>, dppe, dppp, dppf) from Pd(η<sup>5</sup>-C<sub>5</sub>H<sub>5</sub>)(η<sup>3</sup>-1-Ph-C<sub>3</sub>H<sub>4</sub>). Pd(η<sup>5</sup>-C<sub>5</sub>H<sub>5</sub>)(η<sup>3</sup>-1-Ph-C<sub>3</sub>H<sub>4</sub>) has been found to be a superior precursor for synthesizing catalytically active PdL<sub>2</sub> compounds due to its ease in handling and reactivity with tertiary phosphines.

Furthermore, investigations into the role of water in the transmetallation step of the Suzuki-Miyaura reaction are presented. The research indicates that water is necessary to effect the transmetallation step when coupling [NBu<sub>4</sub>][PhBF<sub>3</sub>] with 4-bromotoluene in toluene; however, the amount of water above one equivalent has no significant effect on the rate or yield of the reaction.

## Acknowledgements

I would like to begin by thanking Dr. Michael Baird for the opportunity to be a part of his research group. I have truly appreciated his guidance and patience.

I would also like to thank Dr. Phillip Jessop for his advice, Dr. Françoise Sauriol for her assistance with the NMR experiments, and Dr. Ruiyao Wang for the crystallographic work.

The Baird group has made the lab a truly enjoyable place to work. I would like to thank all past and present group members, especially Shay, Heidi, Andrew and Kevin, for all the good times. I would like to single out Dr. Emily Mitchell for getting this project started and for always being available and willing to provide advice.

Finally, I would like to thank my family and friends for all their support and understanding throughout the course of my studies. I would like to thank my friend Tony for regularly making the 3+ hour drive up to visit, despite 401 construction and horrible weather conditions. I would like to thank my parents, Cathie and Kerry, and my brother, Rob, for all their encouragement. Without them, I would not be where I am today.

## Table of Contents

Abstract .....	ii
Acknowledgements .....	iii
Table of Contents .....	iv
List of Figures .....	viii
List of Tables .....	xii
List of Symbols and Abbreviations.....	xiii
Chapter 1 Introduction .....	1
1.1 Cross-Coupling Reactions.....	1
1.1.1 Development of Cross-Coupling Reactions .....	2
1.1.2 Palladium-catalyzed Cross-Coupling Reactions .....	4
1.2 The Suzuki-Miyaura Reaction .....	6
1.2.1 Mechanism.....	8
1.2.1.1 Oxidative Addition .....	9
1.2.1.2 Transmetalation .....	11
1.2.1.3 Reductive Elimination .....	14
1.2.2 Reagents.....	15
1.2.2.1 Aryl Electrophiles .....	15
1.2.2.2 Organoboron Reagents .....	16
1.3 Palladium(0) Catalysts .....	18
1.3.1 Ligand Selection .....	18
1.3.2 Catalyst Generation .....	20
1.3.2.1 Pd(PPh <sub>3</sub> ) <sub>4</sub> .....	20

1.3.2.2 Pd(OAc) <sub>2</sub> .....	22
1.3.2.3 PdCl <sub>2</sub> (PPh <sub>3</sub> ) <sub>2</sub> .....	23
1.3.2.4 Pd(dba) <sub>2</sub> /Pd <sub>2</sub> (dba) <sub>3</sub> .....	25
1.4 Research Aims .....	27
1.4.1 Generation of PdL <sub>2</sub> .....	27
1.4.2 Studies of Transmetallation.....	29
Chapter 2 Experimental.....	30
2.1.1 Physical and Analytical Methods.....	30
2.1.2 Chemical Supplies .....	30
2.2 Preparation of Reagents .....	31
2.2.1 Synthesis of [Pd(η <sup>3</sup> -1-Ph-C <sub>3</sub> H <sub>4</sub> )Cl] <sub>2</sub> .....	31
2.2.2 Synthesis of Pd(η <sup>3</sup> -1-Ph-C <sub>3</sub> H <sub>4</sub> )(η <sup>5</sup> -C <sub>5</sub> H <sub>5</sub> ).....	32
2.2.3 Synthesis of Pd(PCy <sub>3</sub> ) <sub>2</sub> .....	33
2.2.4 Synthesis of <i>trans</i> -Pd(4-CH <sub>3</sub> C <sub>6</sub> H <sub>5</sub> )(Br)(PCy <sub>3</sub> ) <sub>2</sub> .....	34
2.2.5 Independent Synthesis of 4-methyl biphenyl.....	34
2.2.6 Synthesis of [NBu <sub>4</sub> ][PhBF <sub>3</sub> ].....	35
2.2.7 Drying of K <sub>2</sub> CO <sub>3</sub> .....	36
2.3 In Situ Generation of PdL <sub>n</sub> from Pd(η <sup>3</sup> -1-Ph-C <sub>3</sub> H <sub>4</sub> )(η <sup>5</sup> -C <sub>5</sub> H <sub>5</sub> ).....	36
2.3.1 Monodentate Phosphines .....	37
2.3.1.1 L = PMePh <sub>2</sub> .....	37
2.3.1.2 L = PPh <sub>3</sub> .....	38
2.3.1.3 L = PMeBu <sup>t</sup> <sub>2</sub> .....	38
2.3.1.4 L = PCy <sub>3</sub> .....	39

2.3.1.5 L = $\text{PBU}_3^t$ .....	39
2.3.1.6 Isolation of $\text{Pd}_2(\text{PPh}_3)_2(\mu\text{-C}_5\text{H}_5)(\mu\text{-1-Ph-C}_3\text{H}_4)$ .....	39
2.3.2 Bidentate Phosphines .....	39
2.3.2.1 L = dppe.....	40
2.3.2.2 L = dppp.....	40
2.3.2.3 L = dppf.....	40
2.4 Oxidative Addition Experiments.....	40
2.4.1 Oxidative Addition to $\text{PdL}_n$ Generated <i>in situ</i> (L = $\text{PMePh}_2$ , $\text{PPh}_3$ , $\text{PCy}_3$ , $\text{PMeBu}_2^t$ , $\text{PBU}_3^t$ , dppe, dppp) .....	40
2.4.2 Oxidative Addition to Isolated $\text{PdL}_2$ (L = dppf).....	41
2.5 Studies of Transmetalation .....	42
2.5.1 Investigations into the Role of $\text{H}_2\text{O}$ .....	42
Chapter 3 Results and Discussion.....	44
3.1 <i>In Situ</i> Generation of $\text{Pd}(0)\text{L}_n$ from $\text{Pd}(\eta^5\text{-C}_5\text{H}_5)(\eta^3\text{-1-Ph-C}_3\text{H}_4)$ .....	44
3.1.1 Properties of $\text{Pd}(\eta^5\text{-C}_5\text{H}_5)(\eta^3\text{-1-Ph-C}_3\text{H}_4)$ .....	44
3.1.2 Reactions of $\text{Pd}(\eta^5\text{-C}_5\text{H}_5)(\eta^3\text{-1-Ph-C}_3\text{H}_4)$ with Monodentate Phosphines .....	46
3.1.2.1 L = $\text{PMeBu}_2^t$ .....	50
3.1.2.2 L = $\text{PBU}_3^t$ .....	52
3.1.2.3 L = $\text{PPh}_3$ .....	55
3.1.2.4 L = $\text{PMePh}_2$ .....	62
3.1.2.5 L = $\text{PCy}_3$ .....	66
3.1.3 Reactions of $\text{Pd}(\eta^5\text{-C}_5\text{H}_5)(\eta^3\text{-1-Ph-C}_3\text{H}_4)$ with Bidentate Phosphines .	69

3.1.4 Comparison of the Reactivities of Pd( $\eta^5$ -C <sub>5</sub> H <sub>5</sub> )( $\eta^3$ -1-Ph-C <sub>3</sub> H <sub>4</sub> ) and Pd( $\eta^5$ -C <sub>5</sub> H <sub>5</sub> )( $\eta^3$ -C <sub>3</sub> H <sub>5</sub> ) with Monodentate Phosphines .....	71
3.2 Oxidative Addition Experiments.....	74
3.2.1 Oxidative Addition to <i>In Situ</i> Generated PdL <sub>n</sub> .....	74
3.3 Investigations into the Role of Water in Transmetallation.....	79
3.3.1 Attempts at Anhydrous Cross-Coupling .....	84
3.3.2 Cross-Coupling with Controlled H <sub>2</sub> O Addition .....	85
3.4 Summary and Conclusions .....	88
References .....	90
Appendix A. Crystal Structure Data for Pd( $\eta^5$ -C <sub>5</sub> H <sub>5</sub> )( $\eta^3$ -1-Ph-C <sub>3</sub> H <sub>4</sub> ) .....	97
Appendix B. Calibration Curves and a Sample Gas Chromatograph .....	111

## List of Figures

Figure 1. General cross-coupling reaction for C-C bond formation.....	1
Figure 2. Carbon-carbon bond formation using Mg and Li reagents.....	2
Figure 3. Representative Ni-catalyzed cross-coupling of Grignard reagents at $sp^2$ -carbons, as reported by Kumada <i>et al.</i> (top) and Corriu and Masse (bottom) .....	3
Figure 4. Comparison of Ni and Pd for the synthesis of conjugated dienes .....	4
Figure 5. Representative cross-coupling of organostannanes.....	5
Figure 6. General Stille cross-coupling reaction .....	5
Figure 7. Diene synthesis using organoboron reagents .....	7
Figure 8. General SM cross-coupling reaction.....	7
Figure 9. General accepted catalytic cycle of the SM reaction .....	8
Figure 10. Proposed transition states for oxidative addition of aryl electrophiles .	9
Figure 11. Proposed mechanism of <i>cis-trans</i> isomerization .....	10
Figure 12. Proposed processes to transmetallation (L omitted).....	11
Figure 13. Exchange equilibria of $[RBF_3]^-$ in the presence of $OH^-$ .....	12
Figure 14. Proposed transition state of reductive elimination of Ar-Ar' .....	14
Figure 15. Organoboron compounds.....	17
Figure 16. Oxidative addition to monoligated Pd(0).....	19
Figure 17. Proposed species arising from a solution of Pd(Ar)(X)(PR <sub>3</sub> ) .....	19
Figure 18. Dissociation of Pd(PPh <sub>3</sub> ) <sub>4</sub> in solution.....	21
Figure 19. Proposed mechanism for aryl-aryl exchange .....	22
Figure 20. Proposed formation of Pd(0) species from Pd(OAc) <sub>2</sub> and PPh <sub>3</sub> .....	23



Figure 21. Anionic species produced from $\text{PdX}_2(\text{PPh}_3)_2 + 2 \text{e}^-$ , for (a) $\text{X} = \text{Cl}^-$ and (b) $\text{X} = \text{Br}^-$ .....	24
Figure 22. Coordination of dba to $\text{Pd}(0)$ .....	26
Figure 23. $\text{Pd}(\eta^5\text{-C}_5\text{H}_5)(\eta^3\text{-1-Ph-C}_3\text{H}_4)$ .....	27
Figure 24. Intermediates in the generation of $\text{PdL}_2$ from $\text{Pd}(\eta^5\text{-C}_5\text{H}_5)(\eta^3\text{-C}_3\text{H}_5)$ .	28
Figure 25. Molecular Structure of $\text{Pd}(\eta^5\text{-C}_5\text{H}_5)(\eta^3\text{-1-Ph-C}_3\text{H}_4)$ (50 % probability level).....	45
Figure 26. Proposed mechanism for the formation of $\text{PdL}_2$ from $\text{Pd}(\eta^5\text{-C}_5\text{H}_5)(\eta^3\text{-2-Me-C}_3\text{H}_4)$ .....	46
Figure 27. Proposed mechanism for the generation of $\text{Pd}_2(\text{PPh}_3)_2(\mu\text{-C}_5\text{H}_5)(\mu\text{-2-Me-C}_3\text{H}_4)$ .....	47
Figure 28. Proposed mechanism of $\text{PdL}_n$ formation from $\text{Pd}(\eta^5\text{-C}_5\text{H}_5)(\eta^3\text{-1-Ph-C}_3\text{H}_4)$ .....	48
Figure 29. $^1\text{H}$ NMR ( $-20\text{ }^\circ\text{C}$ , 500 MHz, $\text{tol-d}_8$ ) of $\sigma$ -allyl intermediate produced from the reaction of $\text{Pd}(\eta^5\text{-C}_5\text{H}_5)(\eta^3\text{-1-Ph-C}_3\text{H}_4)$ with two equivalents $\text{PMeBu}^t_2$ (* free $\text{PMeBu}^t_2$ ).....	51
Figure 30. Stacked plots of $^{31}\text{P}$ NMR spectra (202.3 MHz, $\text{tol-d}_8$ ) for the reaction of $\text{Pd}(\eta^5\text{-C}_5\text{H}_5)(\eta^3\text{-1-Ph-C}_3\text{H}_4)$ with two equivalents of $\text{PBu}^t_3$ at $25\text{ }^\circ\text{C}$ .....	54
Figure 31. $^{31}\text{P}$ NMR spectrum (242.9 MHz, $\text{tol-d}_8$ ) of a reaction of $\text{Pd}(\eta^5\text{-C}_5\text{H}_5)(\eta^3\text{-1-Ph-C}_3\text{H}_4)$ with two equivalents $\text{PPh}_3$ at $25\text{ }^\circ\text{C}$ (20 min after mixing) .....	55

Figure 32. $^1\text{H}$ NMR spectra (600 MHz, $\text{C}_7\text{D}_8$ ) of the allyl region of a crude sample of $\text{Pd}_2(\text{PPh}_3)_2(\mu\text{-C}_5\text{H}_5)(\mu\text{-1-Ph-C}_3\text{H}_4)$ .....	59
Figure 33. COSY spectrum (600 MHz, $\text{tol-d}_8$ ) of the allyl region of a crude sample of $\text{Pd}_2(\text{PPh}_3)_2(\mu\text{-C}_5\text{H}_5)(\mu\text{-1-Ph-C}_3\text{H}_4)$ .....	60
Figure 34. Stacked plots of $^{31}\text{P}$ NMR spectrum (202.3 MHz) of reaction of $\text{Pd}(\eta^5\text{-C}_5\text{H}_5)(\eta^3\text{-1-Ph-C}_3\text{H}_4)$ with two equivalents $\text{PMePh}_2$ at $25^\circ\text{C}$ .....	63
Figure 35. Stacked $^{31}\text{P}$ NMR (202.5 MHz, $\text{tol-d}_8$ ) spectra of (a) the 3:1 and (b) the 2:1 $\text{PMePh}_2$ systems at $-80^\circ\text{C}$ .....	66
Figure 36. $^1\text{H}$ NMR spectrum (300 MHz, $\text{tol-d}_8$ ) of the $\sigma$ -allyl species, produced in the reaction of $\text{Pd}(\eta^5\text{-C}_5\text{H}_5)(\eta^3\text{-1-Ph-C}_3\text{H}_4)$ with two equivalents $\text{PCy}_3$ at $25^\circ\text{C}$ (3 h after mixing).....	67
Figure 37. $^1\text{H}$ NMR spectrum (500 MHz, $\text{tol-d}_8$ ) of the reaction of four equivalents $\text{PhI}$ with <i>in situ</i> generated $\text{Pd}(\text{PMeBu}^t)_3$ 10 minutes after mixing.....	76
Figure 38. Proposed pathway for the formation of $\text{Pd}_2(\mu\text{-I})_2(\text{P}^t\text{Bu}_3)_2$ .....	77
Figure 39. $^{31}\text{P}$ - $^{31}\text{P}$ correlation spectrum (242.9 MHz, $\text{CD}_2\text{Cl}_2$ ) of the reaction of four equivalents $\text{PhI}$ with <i>in situ</i> generated $\text{Pd}(\text{dppe})_2$ .....	78
Figure 40. Quaternization of $\text{RB}(\text{OH})_2$ in the presence of aqueous $\text{K}_2\text{CO}_3$ .....	79
Figure 41. Proposed four-centered transition state of transmetallation .....	80
Figure 42. Representative couplings of $[\text{ArBF}_3]^-$ with $\text{ArX}$ , illustrating the necessity of base.....	81
Figure 43. Cross-coupling reaction of $\text{Pd}(\text{Tol})(\text{Br})(\text{PCy}_3)_2$ and $[\text{NBu}_4][\text{PhBF}_3]$ .....	83
Figure 44. Biphenyl Calibration Curve .....	112

Figure 45. Methylbiphenyl Calibration Curve .....	112
Figure 46. Representative chromatograph: reaction of Pd(Tol)(Br)(PCy <sub>3</sub> ) <sub>2</sub> and [NBu <sub>4</sub> ][PhBF <sub>3</sub> ] in the presence of 3.75 eq H <sub>2</sub> O (table 1, entry 5)....	113

## List of Tables

Table 1. Summary of attempted cross-coupling experiments with Pd(4- CH <sub>3</sub> C <sub>6</sub> H <sub>5</sub> )(Br)(PCy <sub>3</sub> ) <sub>2</sub> and [NBu <sub>4</sub> ][PhBF <sub>3</sub> ].....	42
Table 2. GC instrument conditions used for all analyses.....	43
Table 3. Select bond lengths for Pd(η <sup>5</sup> -C <sub>5</sub> H <sub>5</sub> )(η <sup>3</sup> -1-Ph-C <sub>3</sub> H <sub>4</sub> ).....	45
Table 4. Timelines for the formation of Pd(0)L <sub>n</sub> from monodentate phosphines L .....	49
Table 5. <sup>1</sup> H and <sup>31</sup> P NMR chemical shifts of η <sup>5</sup> -CpPd(η <sup>1</sup> -1-Ph-C <sub>3</sub> H <sub>4</sub> )(PMeBu <sup>t</sup> <sub>2</sub> ) in toluene-d <sub>8</sub> .....	51
Table 6. <sup>1</sup> H and <sup>31</sup> P NMR chemical shifts of η <sup>5</sup> -CpPd(η <sup>1</sup> -1-Ph-C <sub>3</sub> H <sub>4</sub> )(PBu <sup>t</sup> <sub>3</sub> ) in toluene-d <sub>8</sub> .....	53
Table 7. <sup>1</sup> H and <sup>31</sup> P NMR chemical shifts of η <sup>5</sup> -CpPd(η <sup>1</sup> -1-Ph-C <sub>3</sub> H <sub>4</sub> )(PPh <sub>3</sub> ) in toluene-d <sub>8</sub> .....	56
Table 8. <sup>1</sup> H and <sup>31</sup> P NMR chemical shifts of Pd <sub>2</sub> (PPh <sub>3</sub> ) <sub>2</sub> (μ-C <sub>5</sub> H <sub>5</sub> )(μ-1-Ph-C <sub>3</sub> H <sub>4</sub> ) in toluene-d <sub>8</sub> .....	57
Table 9. <sup>1</sup> H and <sup>31</sup> P NMR chemical shifts of η <sup>5</sup> -CpPd(η <sup>1</sup> -1-Ph-C <sub>3</sub> H <sub>4</sub> )(PMePh <sub>2</sub> ) in toluene-d <sub>8</sub> .....	63
Table 10. <sup>1</sup> H and <sup>31</sup> P NMR chemical shifts of η <sup>5</sup> -CpPd(η <sup>1</sup> -1-Ph-C <sub>3</sub> H <sub>4</sub> )(PCy <sub>3</sub> ) in toluene-d <sub>8</sub> .....	68
Table 11. Timelines for the formation of Pd(0)L <sub>2</sub> from bidentate phosphines L ..	70
Table 12. Percent yields of 4-methylbiphenyl .....	85

## List of Symbols and Abbreviations

acac	acetylacetonate
allyl	propenyl group
Ar	aryl group
Å	Ångström
Bu <sup>t</sup>	tert-butyl group
°C	degrees Celsius
C <sub>6</sub> D <sub>6</sub>	deuterated benzene
COSY	correlation spectroscopy
Cp	cyclopentadienyl group ( $\eta^5$ -C <sub>5</sub> H <sub>5</sub> )
Cy	cyclohexyl group
$\delta$	chemical shift
d	doublet
dba	dibenzylideneacetone
DFT	density functional theory
DMF	dimethylformamide
dppe	1,1'-bis(diphenylphosphino)ethane
dppf	1,1'-bis(diphenylphosphino)ferrocene
dppp	1,1'-bis(diphenylphosphino)propane
eq	equivalents
g	grams
GC	gas chromatography

$\eta$	hapticity
h	hour
$J$	coupling constant
m	multiplet
M	moles/litre
Me	methyl group
mg	milligram
MHz	megahertz
min	minutes
$\mu\text{L}$	microlitres
mL	millilitres
mol	moles
NMR	nuclear magnetic resonance
NOESY	nuclear overhauser effect spectroscopy
OAc	acetate
OTf	triflate
Ph	phenyl group
R	alkyl group
s	singlet
t	triplet
THF	tetrahydrofuran
Tol	<i>para</i> -tolyl group (4-CH <sub>3</sub> -C <sub>6</sub> H <sub>5</sub> )

# Chapter 1

## Introduction

### 1.1 Cross-Coupling Reactions

Carbon-carbon bond forming reactions are some of the most important reactions in organic chemistry, and cross-coupling reactions have revolutionized this field by vastly expanding the available methodologies for synthesizing everything from basic to complex organic molecules.<sup>1</sup> In the general case, an organometallic nucleophile (R-m) reacts with an organic electrophile (R'-X) in the presence of a transition metal catalyst (M) to generate the coupled product R-R' (Figure 1).<sup>1</sup>

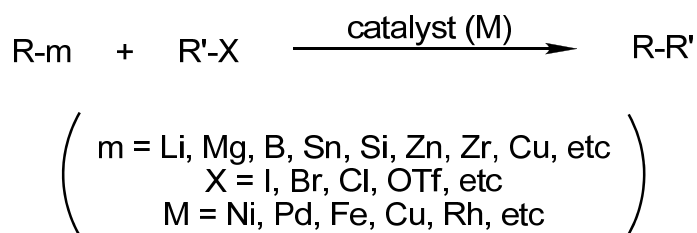


**Figure 1. General cross-coupling reaction for C-C bond formation**

The limitations on the organic groups, R and R', are reaction specific, varying with the nature of m, X and M.<sup>1,2</sup> The wide range of available reagents and catalysts has allowed recent research to expand cross-coupling reactions to include other bond forming reactions, such as C-N, C-O, and C-S bonds.<sup>1,2</sup>

### 1.1.1 Development of Cross-Coupling Reactions

Carbon-carbon bonds have traditionally been formed through the reaction of organic halides (RX) with Grignard (R'MgX) or organolithium (R'Li) reagents (Figure 2).<sup>3</sup> The extremely electropositive nature of Li and Mg results in a very polar R'-M bond and creates an exceptionally nucleophilic R' group.

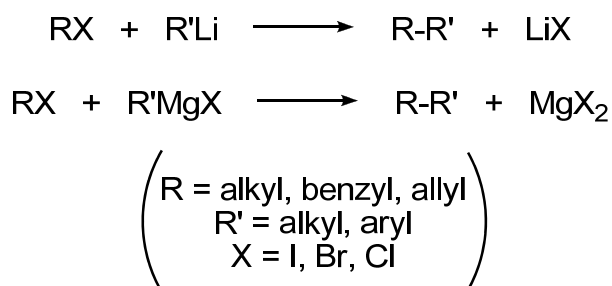


**Figure 2. Carbon-carbon bond formation using Mg and Li reagents**

The scope of these reactions is severely limited due to a number of factors. The preferred S<sub>N</sub>2 mechanism of these reactions restricts R to relatively unhindered sp<sup>3</sup>-carbons.<sup>3</sup> The highly nucleophilic and basic R' group may react with unprotected electrophilic and acidic functionalities, restricting functional group compatibility. As well, metal-halogen exchange may lead to significant amounts of homo-coupled products, R-R and R'-R'.<sup>3</sup>

In the early 1970's, the organic portion of RX was expanded to include sp<sup>2</sup>-carbons when Grignard reagents were coupled with 1-alkenyl or aryl bromides or chlorides in the presence of nickel catalysts (Figure 3).<sup>4</sup>



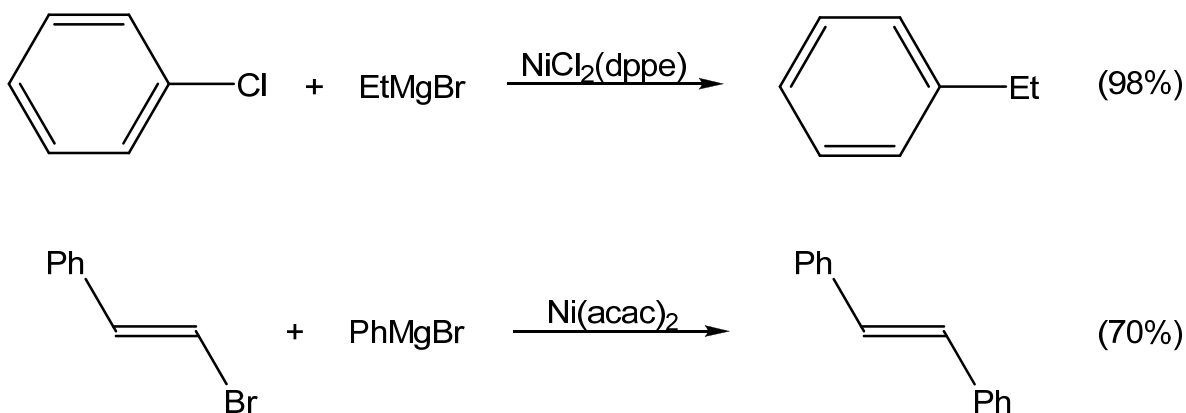


**Figure 3. Representative Ni-catalyzed cross-coupling of Grignard reagents at  $sp^2$ -carbons, as reported by Kumada *et al.* (top) and Corriu and Masse (bottom)**

While this early Ni-research, commonly referred to as the Kumada-Tamao-Corriu reaction, still utilized highly reactive organolithium and magnesium reagents, it marked a milestone in carbon-carbon bond formation as it was essentially the dawn of modern transition metal catalyzed cross-coupling reactions.<sup>1a,3</sup> Work in the subsequent decades moved towards expanding the available organometallic reagents towards less electropositive metals.

The development of new organometallic reagents came hand in hand with the development of new catalytic systems. The key property necessary for a potential catalyst is the ability of the metal centre to undergo a simultaneous two-electron change via an oxidative addition-reductive elimination couple.<sup>1a</sup> While an array of metals meet this criterion, the group 10 transition metals, and more particularly palladium, were found to make highly efficient catalysts.

### 1.1.2 Palladium-catalyzed Cross-Coupling Reactions

While Ni-catalyzed cross-coupling reactions were still being developed, experiments performed with Pd catalysts found that they too were capable of coupling organic halides with Grignard and organolithium reagents.<sup>3,5</sup> Little attention was paid to these early successes as the products of these reactions were obtainable by the more affordable Ni-catalyzed Kumada-Tamao-Corriu reaction. It was not until Negishi replaced Mg with Al in the synthesis of conjugated dienes (Figure 4) that a distinct advantage of Pd over Ni became apparent: Pd was capable of oxidative addition of vinyl halides with essentially 100% retention of configuration.<sup>3,5</sup>

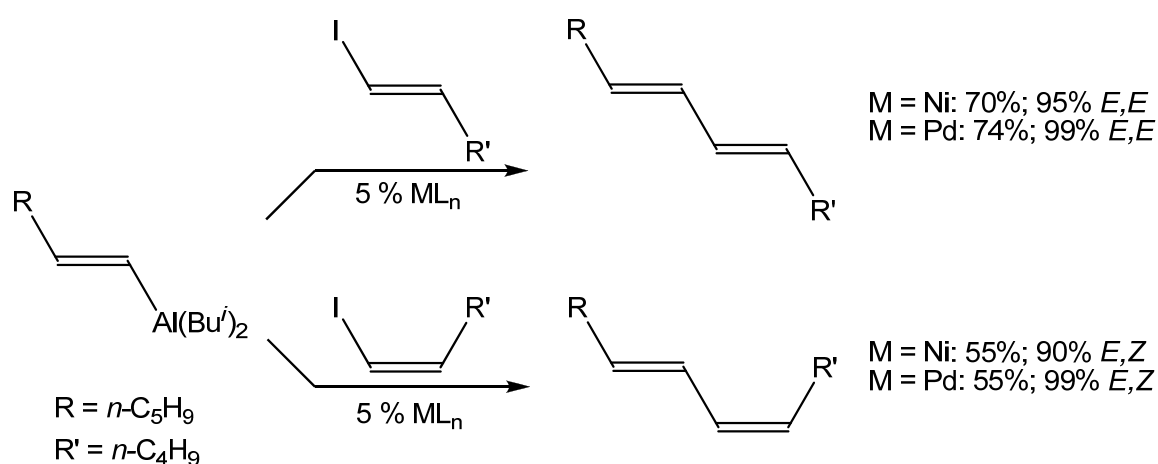
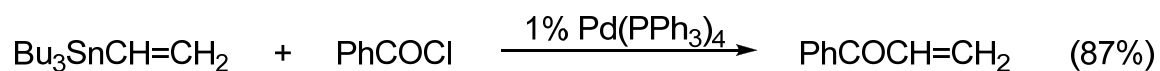


Figure 4. Comparison of Ni and Pd for the synthesis of conjugated dienes

Following Negishi's success with organic aluminum reagents, the efficiency and utility of palladium catalysts was further demonstrated by the development of and success with organic zirconium and zinc reagents.<sup>1a,c,3</sup> The

expansion of organometallic reagents did not end in there, and in the late 1970's Migita and Kosugi first employed organostannanes for the alkylation, arylation, and vinylation of acyl chlorides in the presence of catalytic amounts of tetrakis(triphenylphosphine) palladium(0) (Figure 5).<sup>6</sup>



**Figure 5. Representative cross-coupling of organostannanes**

This first use of organotin reagents laid the ground work for what would soon be a vital synthetic method for organic syntheses: the Stille reaction (Figure 6). It was Stille's subsequent and extensive work with organostannanes that extended their applicability to the coupling of a wide range of organic groups.<sup>7</sup>

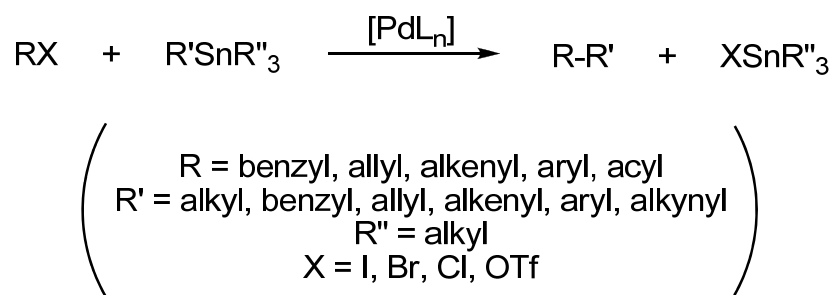


**Figure 6. General Stille cross-coupling reaction**

In the above reaction, the ligands, L, are most commonly tertiary phosphines as they are one of the strongest donors to the group 10 metals in the 2+ oxidation state.<sup>8</sup> For R", *n*-Bu groups are almost always employed due to their relatively slow transfer from Sn to Pd. The approximate order of effectiveness of transfer from Sn is alkynyl > alkenyl > aryl > methyl > alkyl.<sup>7</sup>

The widespread use of the Stille reaction can be attributed to the convenience of organotin reagents and the broad range of compatible reagents. Organotin reagents are air and moisture stable, making them easy to synthesize and store.<sup>7</sup> As well, organotin reagents are tolerant of a wide range of functional groups, expanding the available organic portion and reducing the need for protecting groups.<sup>7</sup> Despite the significant advantages of the Stille reaction, its large scale practicality is severely limited by the high toxicity of organotin reagents.<sup>1,9</sup> Future developments in cross-coupling reactions therefore expanded to the use of more "environmentally-friendly" organometallic reagents.

## **1.2 The Suzuki-Miyaura Reaction**

At the time of Stille's review in 1986,<sup>7</sup> Suzuki and Miyaura had already published several papers regarding their successful syntheses of dienes through the coupling of 1-alkenyl halides with 1-alkenyl boranes in the presence of tetrakis(triphenylphosphine)palladium and base (Figure 7).<sup>10</sup>

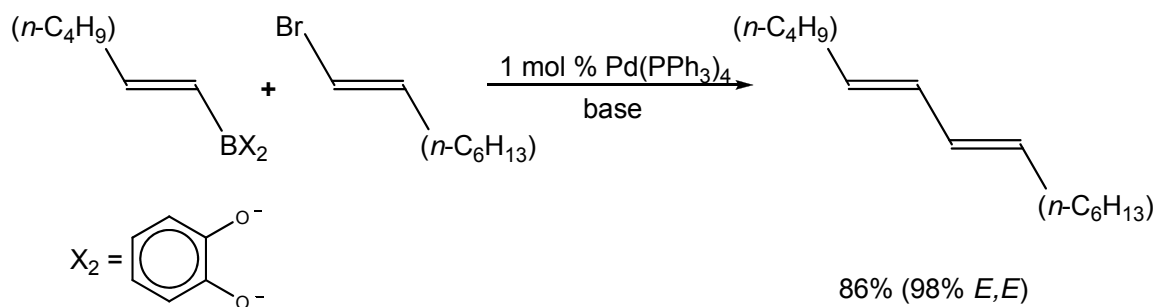


**Figure 7. Diene synthesis using organoboron reagents**

These reactions saw non-toxic organoboron compounds replacing the toxic organotin reagents of the Stille reaction. Subsequent research showed that an array of organoboron compounds, mainly boronic acids and esters, could couple under mild reaction conditions and tolerate a wide variety of functional groups.<sup>9</sup> The cross-coupling of organoboron reagents to organic electrophiles is known as the Suzuki-Miyaura (SM) reaction (Figure 8).<sup>9</sup>

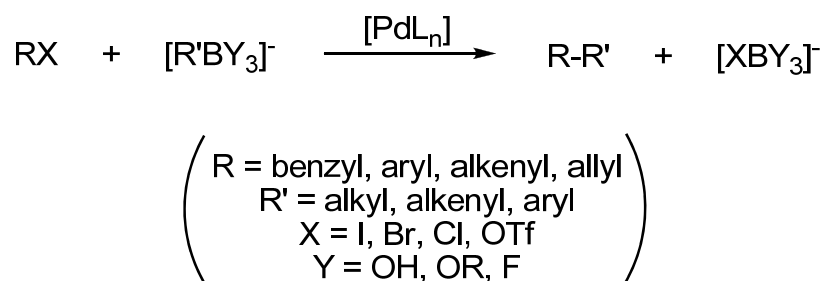


**Figure 8. General SM cross-coupling reaction**

The SM reaction is most commonly employed to synthesize biaryls by coupling an aryl electrophile with an aryl boron compound.<sup>9</sup> The boron compound exists as a borate species in the coupling reaction, a feature which will be discussed in greater detail later on in this work.

### 1.2.1 Mechanism

The SM reaction shares the same basic mechanism as most Pd-catalyzed cross-coupling reactions. The generally accepted catalytic cycle (Figure 9), begins with the generation of the catalytically active species  $\text{Pd}(0)\text{L}_2$ , followed by oxidative addition of the organic electrophile, then transmetallation with the organoborate complex, and ultimately reductive elimination to yield the coupled product and regenerate the catalyst.<sup>1a,c,9b,c,e</sup>

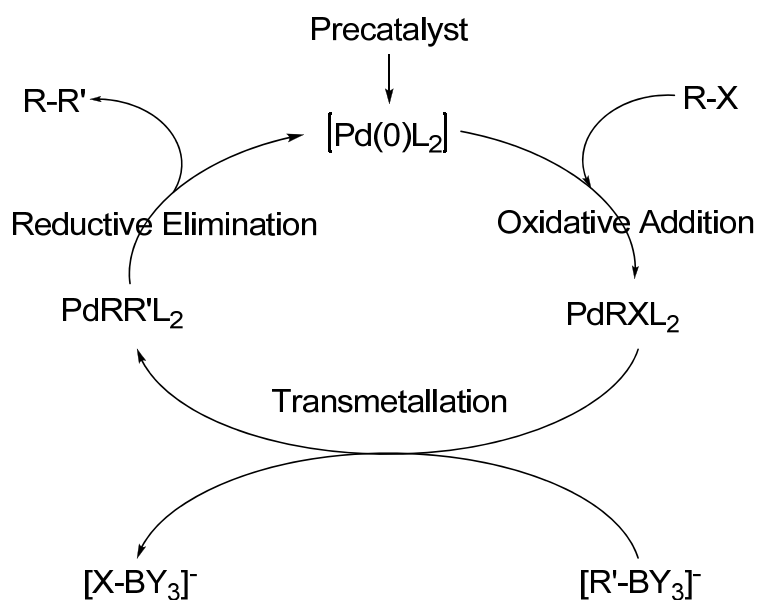


Figure 9. General accepted catalytic cycle of the SM reaction

### 1.2.1.1 Oxidative Addition

The oxidative addition product,  $\text{PdRXL}_2$ , is the only observable species in the mechanistic pathway, essentially making the oxidative addition step the best understood step in the cross-coupling mechanism. Oxidative addition is often the rate determining step when using less reactive organic electrophiles, such as aryl bromides and chlorides.<sup>9e, 11,12</sup>

Oxidative addition of aryl electrophiles precedes via a 3-centred transition state (Figure 10) which contains either ionic (**A**) or neutral (**B**) character.<sup>1b,13</sup>

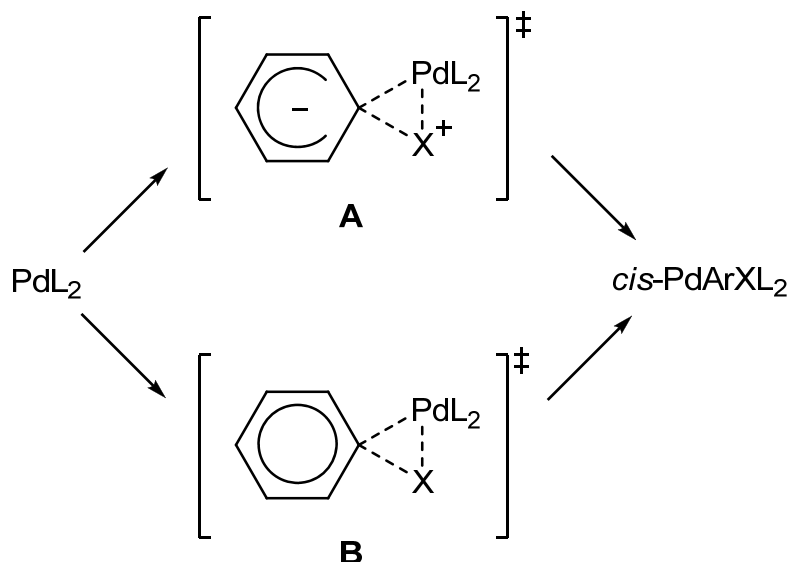


Figure 10. Proposed transition states for oxidative addition of aryl electrophiles

Studies carried out by Amatore and Pflüger support the idea of a neutral transition state and lead to the conclusion of a concerted process to oxidative addition.<sup>13a</sup> This concerted addition is an associative reaction in which Ar-X first

binds to PdL<sub>2</sub> as a  $\sigma$  complex, and then undergoes C-X bond breaking as a result of strong back donation from Pd(0) into the C-X  $\sigma^*$  orbital.<sup>14</sup>

The resulting PdRXL<sub>2</sub> product is initially in the *cis*-geometry; however, it is *trans*-PdRXL<sub>2</sub> which is almost always observed and/or isolated.<sup>13-15</sup> Kinetic studies carried out by Casado and Espinet on the oxidative addition of C<sub>6</sub>Cl<sub>2</sub>F<sub>3</sub>I to Pd(PPh<sub>3</sub>)<sub>4</sub> reveal four parallel pathways to the *cis-trans* isomerization (Figure 11).<sup>13b</sup> Two pathways involve the formation of pentacoordinated species, followed by two consecutive Berry pseudorotations and dissociation (A and B). The other two pathways involve associative replacement of the PPh<sub>3</sub> ligand *cis* to the iodide ligand (C and D). Exchange between a bridging and terminal iodide, followed by displacement by PPh<sub>3</sub>, ultimately leads to the formation of the *trans* product.

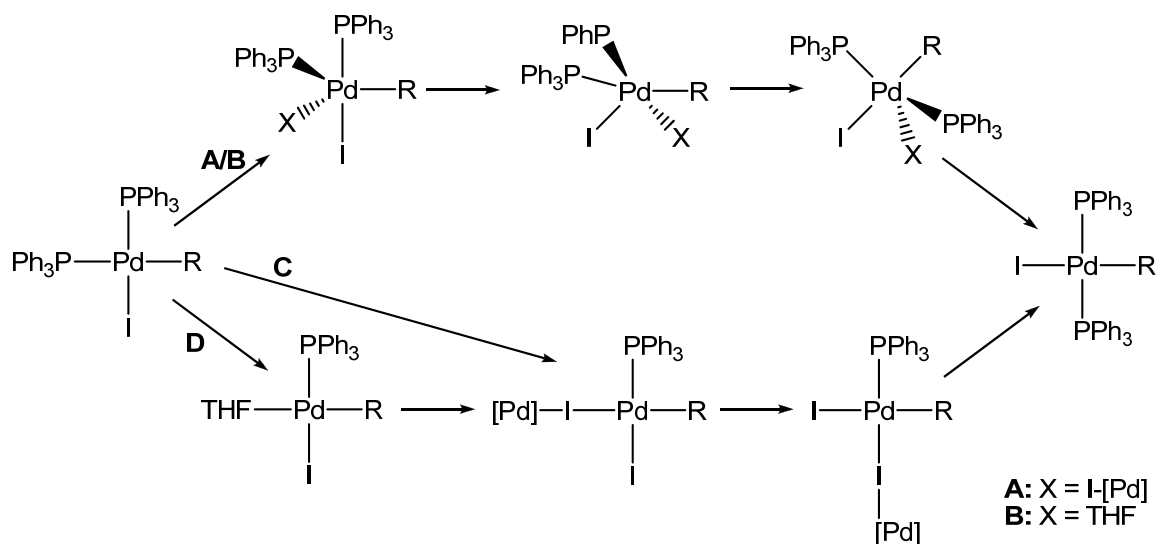


Figure 11. Proposed mechanism of *cis-trans* isomerization



### 1.2.1.2 Transmetalation

As illustrated in Figure 8 and 9, it is a borate species which participates in SM cross-coupling reactions. This species is necessary to effect the transmetalation step and is, in fact, a part of only one of three proposed pathways (Figure 12) for the generation of  $\text{PdRR}'\text{L}_2$ , the species which ultimately undergoes reductive elimination.<sup>9,16</sup>

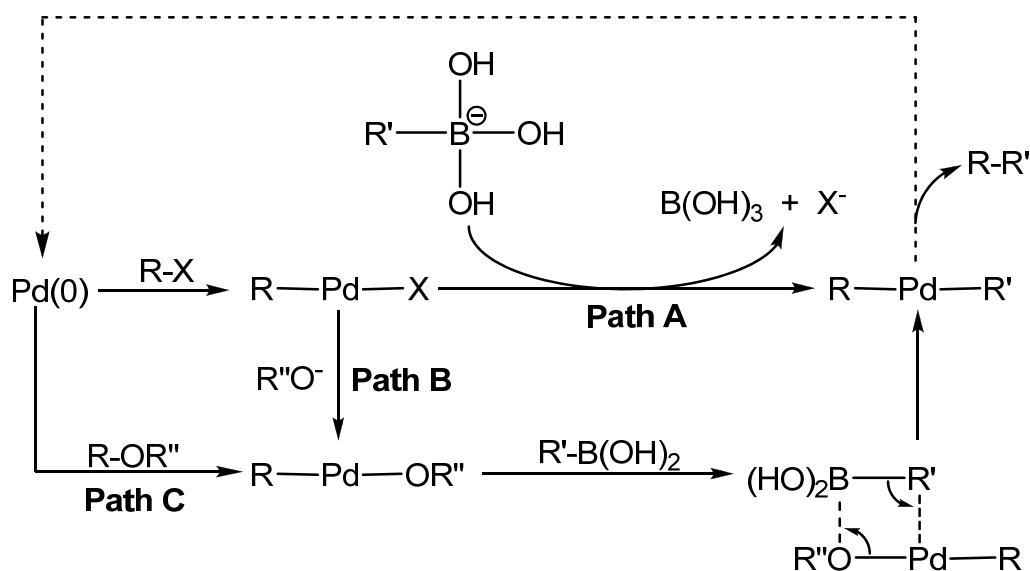
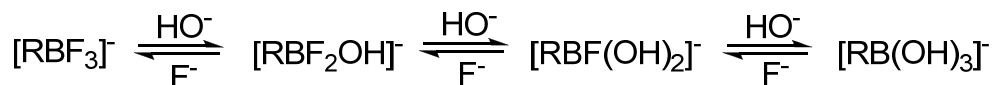


Figure 12. Proposed processes to transmetalation (L omitted)

In Path A, the role of the base is to form the 4-coordinate  $\text{RB(OH)}_3^-$  species. Quaternization of boron increases the nucleophilicity of the organic group and allows it to be effectively transferred to the Pd(II) centre.<sup>9c,e,16,17</sup> It has been shown experimentally that  $[\text{RB(OH)}_3]^-$  forms upon the treatment of  $\text{RB(OH)}_2$  with NaOH.<sup>16c</sup> These results are predicted by DFT calculations which reveal that

the coordination is essentially barrierless.<sup>16e</sup> DFT calculations indicate that this quaternization is necessary, as  $[\text{RB}(\text{OH})_3]^-$  must displace  $\text{X}^-$  in the coordination sphere of Pd for the organic group to be transferred.<sup>16e</sup> Kinetic studies by Matos and Soderquist support this proposal as they suggest the formation of a 4-centered transition state with a bridging hydroxyl group between boron and palladium, similar to that shown for Paths B and C in Figure 12.<sup>16c</sup>

Recent work on  $[\text{RBF}_3]^-$  as a coupling partner further establishes the need for the bridging hydroxyl group.<sup>18</sup> While Wright *et al.* proposed that  $\text{OH}^-$  replacement on  $\text{RB}(\text{OH})_2$  by  $\text{F}^-$  would increase the efficiency of coupling,<sup>19</sup> numerous groups have shown that  $[\text{RBF}_3]^-$  compounds only couple in the presence of water and/or base.<sup>18</sup> These studies have demonstrated that an equilibrium exists as in Figure 13, with any of the hydroxyl containing species being capable of participating in transmetallation.<sup>18a-c</sup>



**Figure 13. Exchange equilibria of  $[\text{RBF}_3]^-$  in the presence of  $\text{OH}^-$**

Path B was first proposed by Miyaura *et al.* after attempts to couple (*E*)- $\beta$ -styryl bromide with lithium (1-hexenylmethyl)disiamylborate were unsuccessful.<sup>16a</sup> The role of the base in any SM reaction was assumed to be more than just quaternizing the boron since the reactions failed with a known

borate species. It was therefore proposed that the base interacts with the Pd(II) oxidative addition product, replacing the halide.<sup>9b,c,16a</sup>

While Path B cannot definitively be ruled out, both experimental studies and DFT calculations suggest that it is not the main process of transmetallation. Aliprantis and Canary were unable to identify any Pd(R)(OR')L<sub>2</sub> intermediates in aliquots of an SM reaction mixture by ESI-MS.<sup>16b</sup> While Matos and Soderquist were able to generate Pd(OH)(Ph)(PPh<sub>3</sub>)<sub>2</sub> by treating Pd(Br)(Ph)(PPh<sub>3</sub>)<sub>2</sub> with NaOH, a significant amount of O=PPh<sub>3</sub> formed, which is typically not seen under experimental SM conditions.<sup>16c</sup> As well, DFT calculations were unable to locate a transition state for the direct replacement of Br<sup>-</sup> by OH<sup>-</sup> in the coordination sphere of Pd.<sup>16e</sup> Instead, the calculations predicted a transition state with OH<sup>-</sup> bound to a phosphine ligand, [PdR'(PR<sub>3</sub>)(PR<sub>3</sub>OH)Br]<sup>-</sup>, which could then transfer the OH<sup>-</sup> to Pd with concomitant release of Br<sup>-</sup>. This would result in the generation of a large amount of phosphine oxide, as was seen in the Matos and Soderquist studies. These studies suggest that while Path B may be partially involved in transmetallation, it is unlikely to be the key process. By reconsidering these studies and those studies with [RBF<sub>3</sub>]<sup>-</sup> previously discussed, it is possible that the lack of success Miyaura *et al.* experienced coupling with lithium (1-hexenylmethyl)disiamylborate may be due to the absence of an appropriate group for bridging to Pd.

Experimental evidence supports Path C, as coupling with boronic acids and esters occurs in the absence of base when Pd(R)(OR')L<sub>2</sub> can be generated

directly *via* oxidative addition.<sup>16d,20</sup> DFT calculations predict this pathway to be successful when Path B is not, as Path C bypasses halide displacement and therefore does not lead to phosphine oxidation.<sup>16e</sup>

### 1.2.1.3 Reductive Elimination

Reductive elimination is the process which releases the coupled product, R-R', from the Pd(II) complex PdRR'L<sub>2</sub> and regenerates the catalytically active Pd(0)L<sub>2</sub> species. Reductive elimination is the inverse process of oxidative addition, and as such, occurs by a process analogous to concerted addition.<sup>9a</sup> It involves a non-polar, non-radical three-centered transition state as illustrated in Figure 14.<sup>9a,14</sup> Just as oxidative addition produces a *cis* product, the aryl groups must be in the *cis* geometry for reductive elimination to occur.<sup>9a,14</sup>

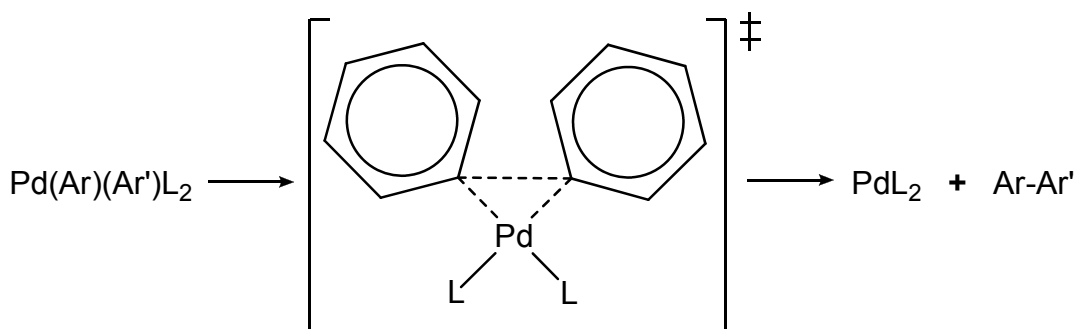


Figure 14. Proposed transition state of reductive elimination of Ar-Ar'

## 1.2.2 Reagents

### 1.2.2.1 Aryl Electrophiles

For the SM reaction, aryl halides and triflates comprise the most common organic electrophiles. The reactivity of the aryl electrophile to oxidative addition is controlled by the C-X bond strength, making aryl iodides the most reactive, followed by aryl bromides and triflates, and lastly aryl chlorides.<sup>21</sup> The C-X bond strength can be decreased by placing electron-withdrawing groups on the aryl portion, increasing the reactivity of the aryl electrophile to oxidative addition.<sup>22</sup> *Ortho* and *para* substituents are better activators than *meta* substituents; however, *ortho* substituents may cause steric interactions which can in fact hinder oxidative addition.<sup>9e,22</sup> This difference in reactivities typically causes the aryl electrophile to dictate the rate determining step.<sup>9e,11,12</sup> In the case of aryl iodides, oxidative addition occurs quickly, leaving transmetalation as the rate determining step. For aryl chlorides, the reverse is true. Due to the intermediate reactivity of aryl bromides and triflates, the rate determining step is dependent on the substituents on the aryl group.<sup>9e,11,12</sup>

The high costs associated with the synthesis of aryl iodides, bromides and triflates make aryl chlorides a very appealing electrophile for large-scale applications of the SM reaction.<sup>1b,9e</sup> Unfortunately, the low reactivity of aryl chlorides makes them essentially unreactive to oxidative addition excepting in select cases when the aryl chloride is activated and a highly reactive catalyst is employed.<sup>1b,9e</sup> Since activation places limitations on the available aryl portion,

significant developments are being made in order to produce catalysts and ligands which are capable of oxidatively adding aryl chlorides under mild conditions. This work will be discussed in greater detail later on in this work.

Other groups are looking to overcome the costs of aryl iodides, bromides and triflates by researching the potential use of other aryl sulphonates, such as aryl tosylates.<sup>23</sup>

### **1.2.2.2 Organoboron Reagents**

Boronic acids are chemically stable and can be handled in air; however, they are susceptible to B-C bond oxidation with time which limits their long-term storage in air.<sup>17</sup> Boronic acids typically exist as a mixture of cyclic and linear oligomeric anhydrides, with the most common of these structures being cyclic six-membered boroxine compounds (Figure 15). These anhydrides are still fully capable of participating in the SM reaction; however, an excess of “boronic acid” must be used due to the unknown stoichiometry<sup>9b,c,e,17</sup> Aryl boronic acids are also particularly prone to protodeboronation, the process in which a proton displaces boron from a boronic acid, during the coupling process.<sup>18b</sup>

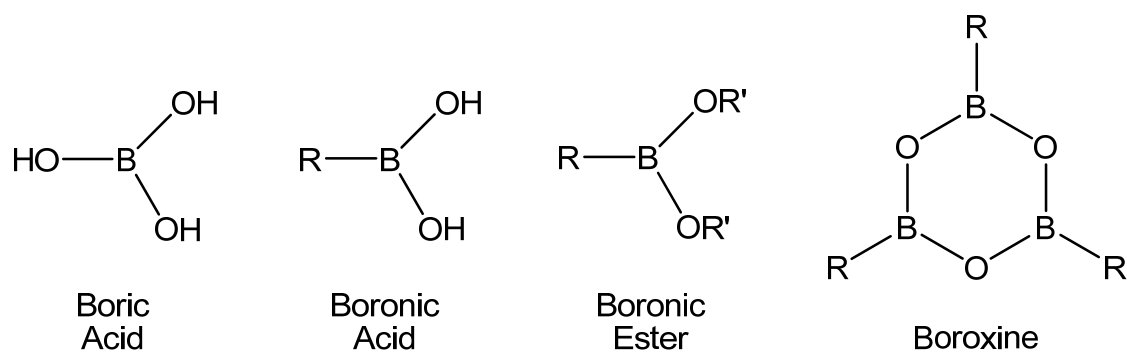


**Figure 15. Organoboron compounds**

For the above discussed reasons, boronic acids are not the ideal organoboron reagent for a large number of SM reactions. There are a variety of other organoboron compounds that are of synthetic utility. Boronic esters are less polar, easier to handle, and most can be easily purified by distillation.<sup>17</sup> However, they result in poor atom economy and suffer from rapid hydrolysis back to the boronic acid.<sup>17,18b</sup>

Trifluoroborate salts are air-stable, crystalline solids which can easily be purified by recrystallization.<sup>1b,c,17,18a-c</sup> As they already possess a quaternized boron, the use of base is not always a requirement.<sup>18a-c</sup> This is beneficial in some instances as base can lead to saponification of esters, racemization of optically active compounds, aldol condensations, and hydrolytic B-C cleavage.<sup>9c</sup> A wide range of trifluoroborate compounds are commercially available as the potassium salts. While these salts suffer from insolubility in most organic solvents, this problem can be overcome by a simple counter-ion exchange with a compound such as tetrabutylammonium bromide.<sup>9b,18d</sup>

## 1.3 Palladium(0) Catalysts

### 1.3.1 Ligand Selection

The most widely used catalysts for SM reactions are of the type Pd(0)L<sub>2</sub>. The reactivity of the catalyst is tuned by the steric and electronic properties of the phosphine ligands utilized.

The electron donating ability of L has its greatest effect on the oxidative addition of ArX to Pd(0). Electron rich, strong  $\sigma$ -donors, such as PCy<sub>3</sub>, PMeBu<sup>t</sup><sub>2</sub> and PBu<sup>t</sup><sub>3</sub>, increase the rate of oxidative addition by increasing the electron density around the Pd centre. An electron-rich Pd(0) centre experiences a greater driving force for oxidation.<sup>24</sup> The reverse is true for reductive elimination, in that it is more difficult to reduce a Pd(II) centre with an increased electron density.<sup>25</sup> Electron rich ligands therefore generally result in slower reductive elimination of Ar-Ar'. Strong  $\sigma$ -donation also increases the strength of the P-Pd bond, helping to stabilize Pd intermediates generated during the course of the reaction.<sup>26</sup> It is believed that precipitation of Pd, and therefore loss of the catalyst from solution, can be attributed to the formation of unstable Pd intermediates.<sup>26</sup>

It has been found that an increase in the bulk of L increases the reductive elimination of Ar-Ar' from Pd(Ar)(Ar')L<sub>2</sub>.<sup>2,24-26</sup> It is generally accepted that this effect is due to the driving force to reduce the steric congestion around the Pd(II) centre.<sup>25</sup> Bulky L can, however, interfere with oxidative addition and transmetallation due to steric interactions with incoming reagents.<sup>25</sup>



For extremely bulky phosphines, such as  $\text{P}^t\text{Bu}_3$ , with a cone angle of  $182^\circ$ ,<sup>27</sup> research has indicated that the catalytically active compound is a monoligated PdL species as opposed to the traditionally proposed  $\text{PdL}_2$ .<sup>28</sup> This PdL species is more reactive towards oxidative addition, being capable of adding aryl chlorides and deactivated aryl bromides. Oxidative addition of ArX produces a T-shaped  $\text{Pd}(\text{Ar})(\text{X})\text{L}$  complex (Figure 16).<sup>29</sup>

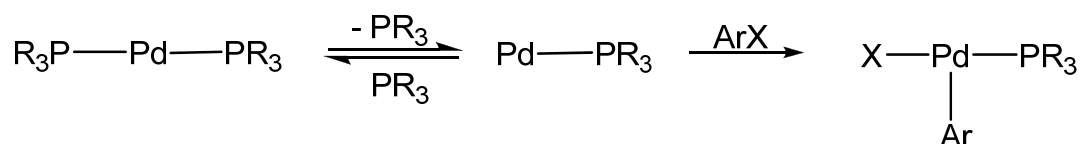


**Figure 16. Oxidative addition to monoligated Pd(0)**

In the absence of an organoboron compound to couple with, and depending on reaction conditions, these  $\text{Pd}(\text{Ar})(\text{X})\text{L}$  species may dimerize, ultimately leading to homo-coupling and regeneration of PdL (Figure 17).<sup>28,29</sup>

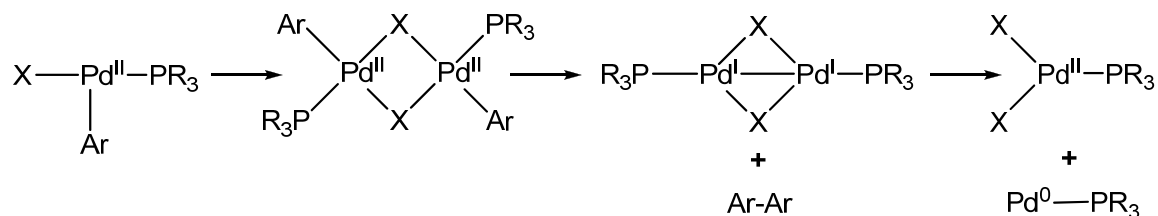


**Figure 17. Proposed species arising from a solution of  $\text{Pd}(\text{Ar})(\text{X})(\text{PR}_3)$**

Should an appropriate organoboron species be present, the Pd(Ar)(X)L species is more reactive than Pd(Ar)(X)L<sub>2</sub> to transmetallation due to a decrease in steric interaction with the incoming reagent.<sup>2,30</sup> The T-shaped Pd(Ar)(Ar')L species resulting from transmetallation is quite reactive to reductive elimination of Ar-Ar'.<sup>31</sup> This is counter-intuitive considering the general acceptance that steric congestion increases the rate of reductive elimination of Ar-Ar' from Pd(Ar)(Ar')L<sub>2</sub>. Theoretical studies predict that in some cases reductive elimination may in fact be favoured from a tricoordinate Pd(II) species.<sup>31</sup>

### 1.3.2 Catalyst Generation

The putative catalytic species, PdL<sub>2</sub> or PdL, are typically generated *in situ* due to their extreme air-sensitivity, as well as their tendency to increase its coordination number (with CO, alkenes, alkynes, phosphines, etc) and to form palladium-palladium clusters.<sup>32</sup> As there are a large number of available precursors to this catalytic species, only those most commonly used and studied will be briefly discussed.

#### 1.3.2.1 Pd(PPh<sub>3</sub>)<sub>4</sub>

Pd(PPh<sub>3</sub>)<sub>4</sub> was the first Pd catalyst used for cross-coupling reactions<sup>1a,5</sup> and remains the most commonly used general precatalyst.<sup>9c,e</sup> In solution, Pd(PPh<sub>3</sub>)<sub>4</sub> dissociates into Pd(PPh<sub>3</sub>)<sub>3</sub> and free PPh<sub>3</sub>. While this tris species is the major Pd(PPh<sub>3</sub>)<sub>n</sub> species existing in solution, it must further dissociate into the catalytically active Pd(PPh<sub>3</sub>)<sub>2</sub> species and another equivalent of free PPh<sub>3</sub> in order for oxidative addition to occur (Figure 18).<sup>33</sup>

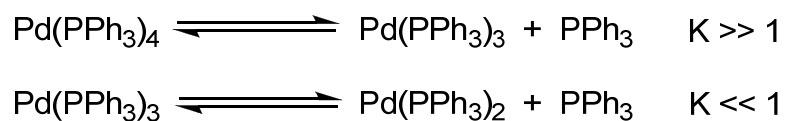


**Figure 18. Dissociation of Pd(PPh<sub>3</sub>)<sub>4</sub> in solution**

Despite the popularity of Pd(PPh<sub>3</sub>)<sub>4</sub>, this precatalyst suffers from several drawbacks. Due to the air-sensitivity of the compound, handling and storage are inconvenient. There are also a number of disadvantages which arise in the oxidative addition of ArX. As the rate of oxidative addition is inversely proportional to the amount of free ligand in solution, free PPh<sub>3</sub> generated during dissociation to the catalytically active Pd(PPh<sub>3</sub>)<sub>2</sub> species hinders oxidative addition.<sup>13a</sup> As well, the PPh<sub>3</sub> ligands do not produce a catalytic species reactive enough to oxidatively add aryl chlorides or inactivated aryl bromides, preventing coupling with these aryl halides.<sup>21b</sup>

Aryl-aryl exchange is a possible side reaction when working with Pd(PPh<sub>3</sub>)<sub>4</sub>.<sup>1b,9c</sup> In this process, a phenyl group from the phosphine exchanges with the aryl group on the oxidative addition product prior to transmetallation.<sup>1b,9c,34a</sup> This exchange leads to the coupling of phosphine-bound aryls and therefore creates scrambled products.<sup>9c,e,34b</sup> Mechanistic studies of this exchange suggest that reductive elimination occurs to form a phosphonium salt, followed by oxidative addition of a different P-C bond (Figure 19).<sup>34a</sup>

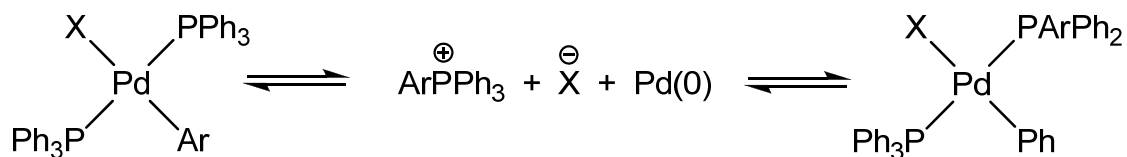


Figure 19. Proposed mechanism for aryl-aryl exchange

### 1.3.2.2 Pd(OAc)<sub>2</sub>

The air and moisture stability of Pd(OAc)<sub>2</sub> make it easy to handle and store and therefore make it an attractive precatalyst for many applications. As the active catalyst is a Pd(0) complex, the Pd(II) of Pd(OAc)<sub>2</sub> must first be reduced before oxidative addition can occur. This reduction is assumed to be performed by the phosphine, but it is unknown to what extent this reduction occurs.<sup>35</sup>

Kinetic studies performed by Amatore *et al.*<sup>35a,b</sup> on the Pd(OAc)<sub>2</sub>/PPh<sub>3</sub> system (Figure 20) demonstrate that Pd(OAc)<sub>2</sub>(PPh<sub>3</sub>)<sub>2</sub> is initially formed regardless of the Pd:PPh<sub>3</sub> ratio, but that this species is unstable and undergoes a spontaneous intramolecular reaction to generate a Pd(0) species capable of oxidatively adding ArX. The structure is believed to be that of Pd(PPh<sub>3</sub>)(OAc)<sup>-</sup>, therefore requiring an additional PPh<sub>3</sub> ligand for a stable oxidative addition product to be formed. Should ArX and PPh<sub>3</sub> not be available, this Pd(0) species will further decompose into an unidentified species incapable of undergoing oxidative addition. Alternatively, excess PPh<sub>3</sub> can also generate the stable

$\text{Pd}(\text{PPh}_3)_3(\text{OAc})^-$  species which is capable of undergoing oxidative addition of  $\text{ArX}$  by dissociation into  $\text{Pd}(\text{PPh}_3)_2(\text{OAc})^-$  and  $\text{PPh}_3$ .<sup>35b</sup>

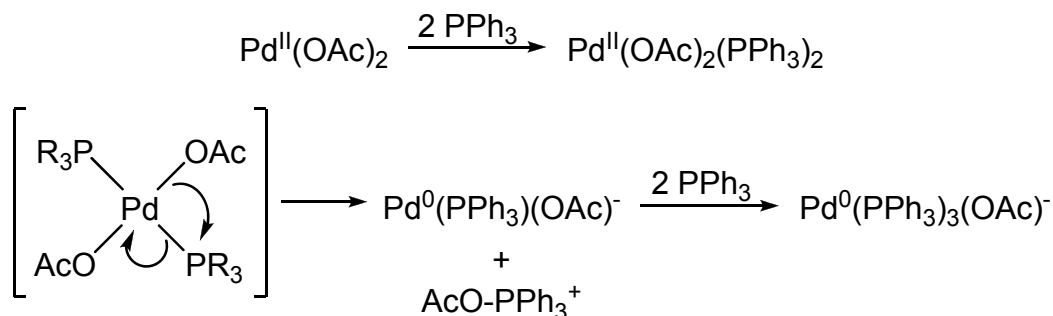


**Figure 20. Proposed formation of Pd(0) species from  $\text{Pd}(\text{OAc})_2$  and  $\text{PPh}_3$**

Since the mechanism of Pd(0) formation involves acetate attacking the phosphine (Figure 20), sterically demanding R groups make this attack unfavourable and severely limit the reduction of the Pd(II) centre. Studies have shown that the optimum cone angle of the phosphine be  $129^\circ$ , comparable to that of  $\text{PEt}_3$ .<sup>35b</sup> Because of this, not all phosphines possess the same ability to reduce Pd(II) and therefore it is often unknown to what extent the catalytically active Pd(0) species may be generated.<sup>35</sup> As well, an extra equivalent of ligand is required beyond that necessary to produce a stable Pd(0) species, an undesirable necessity when expensive ligands are being employed.

### 1.3.2.3 $\text{PdCl}_2(\text{PPh}_3)_2$

$\text{PdCl}_2(\text{PPh}_3)_2$  is stable in solution and will never spontaneously evolve to produce a catalytically active Pd(0) species.<sup>12,36</sup> Unlike  $\text{Pd}(\text{OAc})_2$ , the phosphine

ligand is already coordinated and therefore reduction is typically performed by electrochemical means or by external chemical reducers such as hydrides, Grignards, or organolithiums.<sup>12,36,37</sup>

$\text{PdCl}_2(\text{PPh}_3)_2$  is often used as an alternative to  $\text{Pd}(\text{PPh}_3)_4$  and was once considered to be superior due the expectancy to quantitatively generate  $\text{Pd}(\text{PPh}_3)_2$ . Studies performed by Amatore *et al.* using electrochemical reduction indicate that  $\text{Pd}(\text{PPh}_3)_2$  is not directly formed, but instead a rapid equilibrium of three different anionic  $\text{Pd}(0)$  species is produced (Figure 21 (a)).<sup>12,36</sup> For  $\text{X}=\text{Br}$ , only two anionic  $\text{Pd}(0)$  species are in equilibrium (Figure 21 (b)). Both systems were found to be capable of reacting with  $\text{PhI}$  to form the oxidative addition product  $\text{PdPhI}(\text{PPh}_3)_2$ .

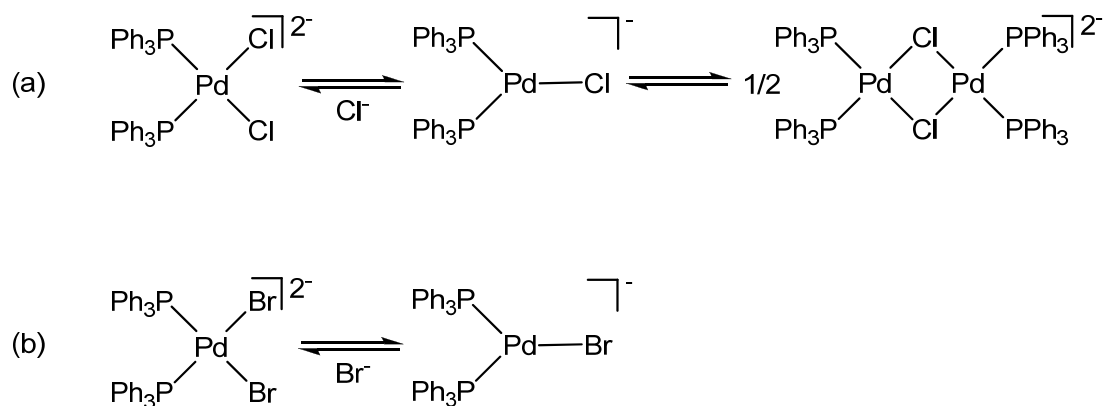


**Figure 21.** Anionic species produced from  $\text{PdX}_2(\text{PPh}_3)_2 + 2 \text{e}^-$ , for (a)  $\text{X} = \text{Cl}^-$  and (b)  $\text{X} = \text{Br}^-$

Studies have found that the halides help to stabilize  $\text{Pd}(\text{PPh}_3)_2$ , decreasing its reactivity.<sup>36</sup> Despite this decrease in reactivity, kinetic studies on

the oxidative addition of PhI to the anionic Pd(0) complexes generated electrochemically from PdCl<sub>2</sub>(PPh<sub>3</sub>)<sub>2</sub> found the system to experience an increased rate of oxidative addition as compared to Pd(PPh<sub>3</sub>)<sub>4</sub>.<sup>36</sup> This increased rate is attributed to the by-passing of ligand dissociation necessary in the Pd(PPh<sub>3</sub>)<sub>4</sub> system.<sup>36</sup>

#### 1.3.2.4 Pd(dba)<sub>2</sub>/Pd<sub>2</sub>(dba)<sub>3</sub>

Pd(dba)<sub>2</sub> (dba = *trans, trans*-dibenzylideneacetone) was first used as a precatalyst in 1978 by Fiaud *et al.*<sup>38</sup> Pd(dba)<sub>2</sub> was selected as the chiral phosphine ligand DIOP (DIOP = 4,5-bis(diphenylphosphinomethyl)-2,2-dimethyldioxolane) was required and it was assumed that dba would be a very labile ligand, easily generating Pd(DIOP)<sub>2</sub>. The reactions were successful and Pd(dba)<sub>2</sub>/Pd<sub>2</sub>(dba)<sub>3</sub> became widely used Pd-precatalysts for cross-coupling reactions.

Much of the popularity of Pd(dba)<sub>2</sub> arises from the assumption that the active catalyst, PdL<sub>2</sub>, is quantitatively generated *in situ* from two equivalents of ligand. Work by Amatore *et al.*<sup>12,33,39a</sup> has illustrated that this is not the case and that the dba ligand is not as easily displaced as previously thought. Studies to determine if Pd(dba)<sub>2</sub> + 2 PPh<sub>3</sub> was equivalent to Pd(PPh<sub>3</sub>)<sub>2</sub> and if Pd(dba)<sub>2</sub> + 4 PPh<sub>3</sub> was equivalent to Pd(PPh<sub>3</sub>)<sub>4</sub>, quickly found that the systems were not equivalent, as 6-8 eq of PPh<sub>3</sub> were necessary in order to completely displace both dba ligands from the Pd centre.<sup>33</sup> It was also found that Pd(PPh<sub>3</sub>)<sub>4</sub>

produced a faster rate of oxidative addition of PhI than  $\text{Pd}(\text{dba})_2$  with both two and four equivalents of  $\text{PPh}_3$ .<sup>33</sup>

Subsequent studies investigating both monodentate (L) and bidentate (L-L) ligands found that while the first dba is easily displaced by a phosphine ligand, the second remains bound forming  $\text{Pd}(0)(\text{dba})\text{L}_2$  or  $\text{Pd}(0)(\text{dba})(\text{L-L})$  species regardless of the ligand employed (Figure 22).<sup>39a</sup>

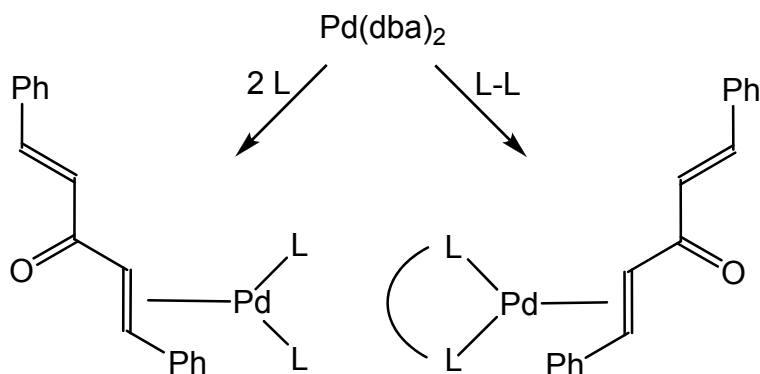


**Figure 22. Coordination of dba to Pd(0)**

For monodentate phosphine ligands, only the  $\text{Pd}(0)\text{L}_2$  species is capable of oxidative addition;<sup>39a</sup> therefore, the coordination of dba decreases the concentration of the catalytically active species and dictates the rate of oxidative addition. For bidentate ligands, both  $\text{Pd}(\text{L-L})$  and  $\text{Pd}(\text{dba})(\text{L-L})$  are capable of oxidative addition, but  $\text{Pd}(\text{L-L})$  is more reactive.<sup>39a</sup>



## 1.4 Research Aims

### 1.4.1 Generation of PdL<sub>2</sub>

The objective of this thesis is to investigate Pd( $\eta^5$ -C<sub>5</sub>H<sub>5</sub>)( $\eta^3$ -1-Ph-C<sub>3</sub>H<sub>4</sub>) (Figure 23) as a precatalyst for the generation of catalytically active Pd(0)L<sub>2</sub> species.

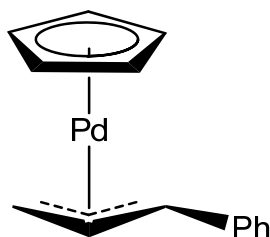
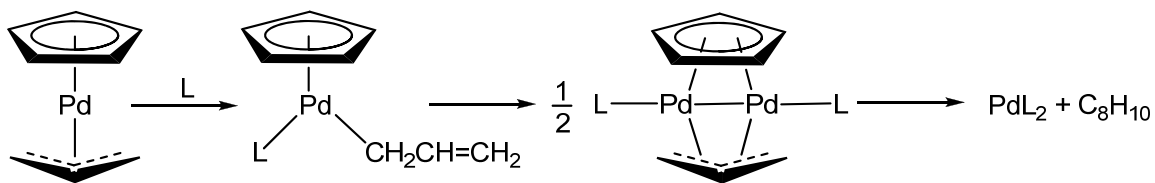


Figure 23. Pd( $\eta^5$ -C<sub>5</sub>H<sub>5</sub>)( $\eta^3$ -1-Ph-C<sub>3</sub>H<sub>4</sub>)

This palladium compound was selected due to the success of the analogous compound Pd( $\eta^5$ -C<sub>5</sub>H<sub>5</sub>)( $\eta^3$ -C<sub>3</sub>H<sub>5</sub>).<sup>40-42</sup> Studies have found that in the presence of L, Pd( $\eta^5$ -C<sub>5</sub>H<sub>5</sub>)( $\eta^3$ -C<sub>3</sub>H<sub>5</sub>) easily generates Pd(0)L<sub>2</sub>, proceeding through well characterized intermediates and reductively eliminating C<sub>8</sub>H<sub>10</sub> in the process (Figure 24).<sup>40,41</sup>



**Figure 24. Intermediates in the generation of PdL<sub>2</sub> from Pd(η<sup>5</sup>-C<sub>5</sub>H<sub>5</sub>)(η<sup>3</sup>-C<sub>3</sub>H<sub>5</sub>)**

While Pd(η<sup>5</sup>-C<sub>5</sub>H<sub>5</sub>)(η<sup>3</sup>-C<sub>3</sub>H<sub>5</sub>) shows a considerable amount of promise, having shown to be more effective at generating Pd(0)L<sub>2</sub> than Pd<sub>2</sub>dba<sub>3</sub> or Pd(OAc)<sub>2</sub>,<sup>42d,43</sup> it begins to decompose within days at room temperature and toluene-d<sub>8</sub> solutions precipitate palladium black within a matter of hours.<sup>44</sup> This compound is also volatile, condensing in vacuum traps while attempting to remove solvent during purification.<sup>44</sup> The phenyl derivative Pd(η<sup>5</sup>-C<sub>5</sub>H<sub>5</sub>)(η<sup>3</sup>-1-Ph-C<sub>3</sub>H<sub>4</sub>) was selected as it is expected to be less volatile than Pd(η<sup>5</sup>-C<sub>5</sub>H<sub>5</sub>)(η<sup>3</sup>-C<sub>3</sub>H<sub>5</sub>) and was hoped that it would react in a similar fashion with L.

The minimum time at a reasonable temperature to generate Pd(0)L<sub>2</sub> from Pd(η<sup>5</sup>-C<sub>5</sub>H<sub>5</sub>)(η<sup>3</sup>-1-Ph-C<sub>3</sub>H<sub>4</sub>) with a number of monodentate and bidentate tertiary phosphines will be monitored by <sup>1</sup>H and <sup>31</sup>P NMR spectroscopy. The intermediates to this formation are expected to be analogous to those formed in Figure 24, and will be spectroscopically identified when possible. In order to confidently assert that a catalytically active species is in fact generated, oxidative addition of C<sub>6</sub>H<sub>5</sub>I to *in situ* generated Pd(0)L<sub>n</sub> will be performed.

### 1.4.2 Studies of Transmetallation

Due to the inherent problems with boronic acids and esters previously discussed, an increased focus has been placed on the use of trifluoroborate species for SM reactions. While the necessity for  $\text{H}_2\text{O}/\text{OH}^-$  in such systems to orchestrate the  $\text{F}^-/\text{OH}^-$  exchange has been demonstrated,<sup>18</sup> no studies have systematically investigated the exact amount of  $\text{H}_2\text{O}$  necessary for efficient transmetallation to occur.

This thesis will examine the role of  $\text{H}_2\text{O}$  in transmetallation through the cross-coupling of  $\text{Pd}(p\text{-Tol})(\text{Br})(\text{PCy}_3)_2$  with  $[\text{NBu}_4][\text{PhBF}_3]$ . The equivalents of  $\text{H}_2\text{O}$  to  $[\text{NBu}_4][\text{PhBF}_3]$  will be varied, with other reaction conditions being kept constant as a control. Progress of the reactions will be monitored by  $^1\text{H}$  and  $^{31}\text{P}$  NMR spectroscopy, and yields will be determined by gas chromatography. The results should provide insight into optimizing reaction conditions for coupling with trifluoroborate species.

## Chapter 2

### Experimental

#### 2.1.1 Physical and Analytical Methods

Unless otherwise indicated, syntheses were carried out under a dry, deoxygenated argon or nitrogen atmosphere using standard Schlenk line techniques or an MBraun Labmaster glove box, respectively. Anhydrous solvents (THF, diethyl ether, dichloromethane, hexanes, and toluene) were purchased packaged under nitrogen and were dried by passage through columns of activated alumina (Innovative Technology Solvent Purification System).

NMR spectra were recorded using Bruker AV 300, AV 500 and AV 600 spectrometers.  $^{31}\text{P}$  NMR spectra were run at 121.5 MHz, 202.3 MHz or 242.9 MHz and are referenced with respect to external 85 %  $\text{H}_3\text{PO}_4$ .  $^1\text{H}$  NMR data are referenced to TMS via the residual protons signals of the deuterated solvents.

GC analyses were conducted on a Varian 3900 GC equipped with a CP-8400 autosampler, a CP-1177 injector, an FID detector and a Varian WCOT Fused Silica column (CP-Sil 8CB, 25 m x 0.32 mm ID, DF = 0.52).

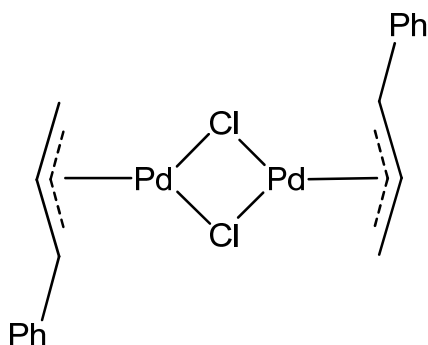
#### 2.1.2 Chemical Supplies

All chemicals were purchased from Sigma Aldrich and used without purifications, unless stated otherwise. Deuterated solvents were purchased from Cambridge Isotope Laboratories, dried, degassed under vacuum and stored over 4 Å molecular sieves. Toluene- $\text{d}_8$  was dried over sodium metal,

dichloromethane- $d_2$  was dried over calcium hydride, and benzene- $d_6$  was dried by passage through a small column of activated alumina.  $PdCl_2$  was obtained on loan courtesy of Johnson Matthey.  $PMePh_2$ ,  $PCy_3$ ,  $PMeBu^t_2$ ,  $PBu^t_3$ ,  $dppe$ ,  $dppp$  and  $dppf$  were obtained from Strem and used without purification.  $Pd(\eta^3-C_3H_5)(\eta^5-C_5H_5)$  was synthesized by E. A. Mitchell according to the method described by Otsuka *et al.*<sup>45a</sup>

## 2.2 Preparation of Reagents

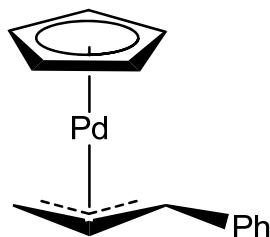
### 2.2.1 Synthesis of $[Pd(\eta^3-1-Ph-C_3H_4)Cl]_2$



This compound was prepared according to the procedure described by Auburn *et al.*<sup>45b</sup> The reaction was carried out in air using wet solvents.  $PdCl_2$  (0.5 g, 2.8 mmol) and  $LiCl$  (0.5 g, 11.8 mmol) were stirred in hot distilled water (0.7 mL) for 1.5 h. A solution of cinnamyl chloride (1.6 mL, 10.9 mmol) in 95 % ethanol (5.6 mL) was added to the stirring solution.  $CO_{(g)}$  was bubbled through the solution for 3 h, during which time an oily orange-yellow product began to form. The flow of  $CO_{(g)}$  was discontinued and the solution was left stirring for 48 h at 25 °C under a  $CO$  atmosphere. Immediately prior to filtration, the solution

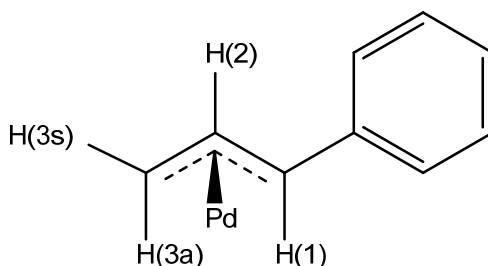
was stirred for 1.5 h at 0 °C. The product was collected by suction filtration and washed with cold methanol (5 mL). The product was recrystallized from chloroform by addition of diethyl ether, yielding a yellow crystalline solid. Yield: 0.679 g, 92 %.  $^1\text{H NMR}$  ( $\text{CDCl}_3$ , 300 MHz):  $\delta$  3.05 (d,  $J$  11.7 Hz, 1H), 3.98 (d,  $J$  6.6 Hz, 1H), 4.64 (d,  $J$  11.5 Hz, 1H), 5.81 (td,  $J$  11.5 Hz, 6.7 Hz, 1H), 7.27 (t,  $J$  7.1 Hz, 2H), 7.34 (t,  $J$  7.1 Hz, 1H), 7.50 (d,  $J$  7.1 Hz, 2H). Lit.<sup>45b</sup>:  $^1\text{H NMR}$  ( $\text{dmsO-d}_6$ ):  $\delta$  3.83 (d,  $J$  10 Hz, 2H), 5.13 (d,  $J$  12 Hz, 1H), 6.40 (dt, 12 Hz, 10 Hz, 1H), 7.0-7.8 (m, 5H)

### 2.2.2 Synthesis of $\text{Pd}(\eta^3\text{-1-Ph-C}_3\text{H}_4)(\eta^5\text{-C}_5\text{H}_5)$



This compound was prepared according to the procedure described by Welch *et al.*<sup>45c</sup> NaCp (0.258 g, 2.90 mmol) suspended in THF (25 mL) was added to a solution of  $[\text{Pd}(\eta^3\text{-1-Ph-C}_3\text{H}_4)\text{Cl}]_2$  (0.601 g, 1.16 mmol) in THF (20 mL). The resulting deep purple solution was stirred for 1.5 h. The solvent was removed under vacuum and the product was extracted using three 20 mL portions of hexanes. The filtrate was reduced under vacuum, yielding an oily purple solid. The solid was dissolved in a minimum of hexanes and purple-red crystals were collected at -40 °C. Yield: 0.565 g, 84 %. A crystal was selected for X-ray crystallographic studies (data in Appendix A).  $^1\text{H NMR}$  ( $\text{C}_7\text{D}_8$ , 600

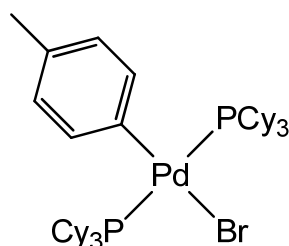
MHz):  $\delta$  2.16 (d,  $J$  10.5 Hz, 1H, H(3a)), 3.36 (d,  $J$  6.1 Hz, 1H, H(3s)), 3.84 (d,  $J$  9.8 Hz, 1H, H(1)), 5.14 (ddd,  $J$  10.5 Hz, 9.8 Hz, 6.1 Hz, 1H, H(2)), 5.63 (s, 5H, C<sub>5</sub>H<sub>5</sub>), 6.98 - 7.03 (m, 3H), 7.24-7.27 (m, 2H)). Lit.<sup>45c</sup>: <sup>1</sup>H NMR (dms<sub>o</sub>-d<sub>6</sub>):  $\delta$  2.35 (d,  $J$  10.5 Hz, 1H), 3.60 (d,  $J$  6.2 Hz, 1H), 4.14 (d,  $J$  9.8 Hz, 1H), 5.55 (m, 1H), 5.56 (s, 5H), 7.17-7.58 (m, 5H).



### 2.2.3 Synthesis of Pd(PCy<sub>3</sub>)<sub>2</sub>

PCy<sub>3</sub> (0.335 g, 1.2 x 10<sup>-3</sup> mol) dissolved in toluene (5 mL) was added to a solution of Pd( $\eta^3$ -1-Ph-C<sub>3</sub>H<sub>4</sub>)( $\eta^5$ -C<sub>5</sub>H<sub>5</sub>) (0.170 g, 5.9 x 10<sup>-4</sup> mol) in toluene (10 mL). The solution was stirred at 75 °C for 1 h. Toluene was removed *in vacuo* and the brown solid was washed with cold, deoxygenated MeOH (2 x 5 mL). The product was dried under vacuum and stored under nitrogen. Yield: 0.205 g, 52%. <sup>1</sup>H NMR (C<sub>7</sub>D<sub>8</sub>, 500 MHz):  $\delta$  1.1-2.2 (m). <sup>31</sup>P (C<sub>7</sub>D<sub>8</sub>, 202.3 MHz):  $\delta$  40.2 (s). Lit.<sup>45c</sup>: <sup>1</sup>H NMR (C<sub>6</sub>D<sub>6</sub>):  $\delta$  1.21-2.22(m). Lit.<sup>40</sup>: <sup>31</sup>P (C<sub>7</sub>D<sub>8</sub>):  $\delta$  39.2

#### 2.2.4 Synthesis of *trans*-Pd(4-CH<sub>3</sub>C<sub>6</sub>H<sub>5</sub>)(Br)(PCy<sub>3</sub>)<sub>2</sub>



Pd(PCy<sub>3</sub>)<sub>2</sub> (0.119 g, 1.78 x 10<sup>-4</sup> mol) was combined with 4-bromotoluene (0.108 g, 6.31 x 10<sup>-4</sup> mol) and dissolved in toluene (15 mL). The solution was stirred for 4 h at 25 °C. The solvent was reduced under vacuum to a volume of approximately 2 mL. Acetone (15 mL) was added by syringe to the stirring solution, precipitating a light beige solid. The product was collected by suction filtration and washed with cold acetone (2 mL). Yield: 0.092 g, 62 %. <sup>1</sup>H NMR (C<sub>6</sub>D<sub>6</sub>, 600 MHz): δ 1.09-2.36 (m, 66H), 2.25 (s, 3H), 6.92 (d, *J* 7.6 Hz, 2H), 7.52 (d, *J* 7.6 Hz, 2H). <sup>31</sup>P NMR (C<sub>6</sub>D<sub>6</sub>, 242.9 MHz): δ 20.1. Anal: Found C 61.14, H 8.85. Calculated C 61.60, H 8.79.

#### 2.2.5 Independent Synthesis of 4-methyl biphenyl

PMeBu<sub>2</sub><sup>t</sup> (20 μL, 1.03 x 10<sup>-4</sup> mol) was added to a Schlenk containing Pd(η<sup>5</sup>-C<sub>5</sub>H<sub>5</sub>)(η<sup>3</sup>-1-Ph-C<sub>3</sub>H<sub>4</sub>) (0.014 g, 4.85 x 10<sup>-5</sup> mol) dissolved in toluene (1 mL), and the solution was stirred at 70 °C for 45 min. The solvent was removed under reduced pressure. PhB(OH)<sub>2</sub> (0.185 g, 1.52 x 10<sup>-3</sup> mol) and K<sub>2</sub>CO<sub>3</sub> (0.420 g, 3.04 x 10<sup>-3</sup> mol) were added to the Schlenk, along with DMF (4 mL) and H<sub>2</sub>O (4 mL). In a separate Schlenk, 4-bromotoluene was dissolved in toluene (0.5 mL). Both Schlenks were purged with argon. The 4-bromotoluene solution was added



to the PhB(OH)<sub>2</sub> solution. The biphasic system was stirred for 48 h at 80 °C. The product was extracted with hexanes (3 x 5 mL) and the combined organic layers were dried over MgSO<sub>4</sub>. Upon reduction in volume, the hexanes solution was applied to an alumina column (15 cm high, 2 cm diameter), and the product was eluted with an 85:15 hexanes:Et<sub>2</sub>O solution. 4-methyl biphenyl came off the column as a colourless, UV active fraction and was isolated as a white powder by removal of the solvent *in vacuo*. Yield: 0.066 g, 39 %. <sup>1</sup>H NMR (CD<sub>2</sub>Cl<sub>2</sub>, 600 MHz): δ 2.39 (s; 3H), 7.26 (d, *J* 7.8 Hz; 2H), 7.32 (t, *J* 7.4 Hz; 1H), 7.42 (t, *J* 7.5 Hz; 2H), 7.50 (d, *J* 8.1 Hz; 2H), 7.59 (d, *J* 8.4 Hz; 2H). Lit.<sup>45d</sup>: <sup>1</sup>H NMR (CDCl<sub>3</sub>): δ 2.38 (s, 3H), 7.37 (m, 9H).

### 2.2.6 Synthesis of [NBu<sub>4</sub>][PhBF<sub>3</sub>]

This compound was prepared, with minor modifications, according to the procedure described by Batey *et al.*<sup>18d</sup> In air, Bu<sub>4</sub>NBr (1.377 g, 4.27 x 10<sup>-3</sup> mol) was suspended in H<sub>2</sub>O (3 mL) and added to a suspension of PhBF<sub>3</sub>K (0.786 g, 4.27 x 10<sup>-3</sup> mol) in MeOH (1.5 mL). The mixture was stirred with mild heating for 30 min, followed by stirring at 25 °C for 30 min. The product oiled out and was collect by extraction with CH<sub>2</sub>Cl<sub>2</sub> (4 x 10 mL). The combined organic layers were dried over MgSO<sub>4</sub> and the solvent was removed under reduced pressure to yield the product as a white oily solid. Under argon, the product was recrystallized from dry CH<sub>2</sub>Cl<sub>2</sub> by addition of dry hexanes, yielding a white crystalline powder. Yield: 1.392 g, 84 %. <sup>1</sup>H NMR (CD<sub>2</sub>Cl<sub>2</sub>, 500 MHz): δ 0.99 (t, *J* 7.3 Hz, 12H), 1.37 (m, 8 H), 1.52 (m, 8H), 3.04 (m, 8H), 7.10 (t, *J* 7.2 Hz, 1H), 7.17 (t, *J* 7.2 Hz, 2H),

7.48 (d,  $J$  6.9 Hz, 2H). Lit.<sup>18d</sup>:  $^1\text{H}$  NMR ( $\text{CDCl}_3$ ): 0.89 (t,  $J$  7.0 Hz, 12H), 1.18-1.40 (m, 16H), 2.80-2.90 (m, 8H), 7.00-7.15 (m, 3H), 7.51 (d,  $J$  6.5 Hz, 2H).

### 2.2.7 Drying of $\text{K}_2\text{CO}_3$

Finely powdered, anhydrous  $\text{K}_2\text{CO}_3$  was placed in a Schlenk, and left under vacuum for 3 days in an oil bath at 150 °C. The Schlenk and solid were then flame dried using a propane torch while a vacuum was applied. An IR spectrum of the solid did not reveal an O-H stretch.

### 2.3 In Situ Generation of $\text{PdL}_n$ from $\text{Pd}(\eta^3\text{-1-Ph-C}_3\text{H}_4)(\eta^5\text{-C}_5\text{H}_5)$

In order to maximize the precision with which reactants were combined, stock solutions of  $\text{Pd}(\eta^3\text{-1-Ph-C}_3\text{H}_4)(\eta^5\text{-C}_5\text{H}_5)$  (0.136 M; 0.039 g in 1 mL) and phosphines L (0.136 M or 0.272 M) were prepared in toluene- $d_8$ , unless otherwise noted. Solutions were stored under nitrogen at -35 °C. NMR tubes equipped with Teflon caps were utilized for all NMR experiments. Reactions were monitored every 15 to 30 min by  $^1\text{H}$  and  $^{31}\text{P}$  NMR for the first 5 h, at which point they were checked every 12 to 18 h. For experiments at higher temperatures, heating was performed using a combination of oil baths and the heaters of the spectrometers. The objective was to establish the minimum time at a reasonable temperature to generate  $\text{PdL}_n$ ; determined by the disappearance of the strong Cp singlets of the starting material and all intermediates, and the full development of the  $\text{PdL}_n$  resonance in the  $^{31}\text{P}$  NMR.

### 2.3.1 Monodentate Phosphines

Experiments investigated 2:1 ratios of L:Pd at 25, 50 and 75 °C. In a typical experiment, 0.25 mL of 0.272 M ( $6.8 \times 10^{-5}$  mol) L was injected into a capped NMR tube containing 0.25 mL of 0.136 M ( $3.4 \times 10^{-5}$  mol) Pd( $\eta^3$ -1-Ph-C<sub>3</sub>H<sub>4</sub>)( $\eta^5$ -C<sub>5</sub>H<sub>5</sub>). Deviations from and/or additions to this general procedure are noted below.

#### 2.3.1.1 L = PMePh<sub>2</sub>

A stock solution of PMePh<sub>2</sub> was not prepared. For a typical 2:1 experiment, 14.5  $\mu$ L ( $6.8 \times 10^{-5}$  mol) PMePh<sub>2</sub> was injected into a capped NMR tube containing 0.25 mL of 0.136 M Pd( $\eta^3$ -1-Ph-C<sub>3</sub>H<sub>4</sub>)( $\eta^5$ -C<sub>5</sub>H<sub>5</sub>) and 0.25 mL toluene-d<sub>8</sub>. In addition to the 2:1 ratio, a 3:1 ratio was also investigated at 25 °C. For this experiment, 21.8  $\mu$ L ( $1.02 \times 10^{-4}$  mol) PMePh<sub>2</sub> was injected into an NMR tube containing 0.25 mL of 0.136 M Pd( $\eta^3$ -1-Ph-C<sub>3</sub>H<sub>4</sub>)( $\eta^5$ -C<sub>5</sub>H<sub>5</sub>) and 0.25 mL toluene-d<sub>8</sub>. Upon complete reaction to form Pd(PMePh<sub>2</sub>)<sub>n</sub>, both the 2:1 and 3:1 systems were investigated by <sup>1</sup>H and <sup>31</sup>P NMR at -50 and -80 °C.

For low temperature studies on a fresh sample, the sample was prepared as above for the 2:1 system; however, the Pd( $\eta^3$ -1-Ph-C<sub>3</sub>H<sub>4</sub>)( $\eta^5$ -C<sub>5</sub>H<sub>5</sub>) solution was cooled in an acetone/dry ice bath at -78 °C prior to injection of PMePh<sub>2</sub>. The reaction was monitored by <sup>1</sup>H and <sup>31</sup>P NMR on an instrument precooled to -70 °C and gradually warmed up to 25 °C.

### 2.3.1.2 L = PPh<sub>3</sub>

A stock solution of 0.272 M PPh<sub>3</sub> was prepared by dissolving 0.071 g of PPh<sub>3</sub> in 1 mL toluene-d<sub>8</sub>.

In addition to the 2:1 experiments outlined in 2.3.1, experiments at the 3:1 ratio were also investigated. 0.30 mL of 0.272 M ( $8.16 \times 10^{-5}$  mol) PPh<sub>3</sub> was injected into a solution of 0.20 mL 0.136 M ( $2.72 \times 10^{-5}$  mol) Pd( $\eta^3$ -1-Ph-C<sub>3</sub>H<sub>4</sub>)( $\eta^5$ -C<sub>5</sub>H<sub>5</sub>), and was monitored at 25 °C. Upon complete reaction to form Pd(PPh<sub>3</sub>)<sub>n</sub>, both the 2:1 and 3:1 systems were investigated by <sup>1</sup>H and <sup>31</sup>P NMR at -50 and -80 °C.

### 2.3.1.3 L = PMeBu<sup>t</sup><sub>2</sub>

A stock solution of PMeBu<sup>t</sup><sub>2</sub> was not prepared. For a typical experiment, 13.2 μL ( $6.8 \times 10^{-5}$  mol) PMeBu<sup>t</sup><sub>2</sub> was injected into a capped NMR tube containing 0.25 mL of 0.136 M Pd( $\eta^3$ -1-Ph-C<sub>3</sub>H<sub>4</sub>)( $\eta^5$ -C<sub>5</sub>H<sub>5</sub>) and 0.25 mL toluene-d<sub>8</sub>. Experiments were performed at 25 and 50 °C.

For low temperature studies, a fresh sample was prepared as above; however, the Pd( $\eta^3$ -1-Ph-C<sub>3</sub>H<sub>4</sub>)( $\eta^5$ -C<sub>5</sub>H<sub>5</sub>)/toluene-d<sub>8</sub> solution was cooled to -78 °C in an acetone/dry ice bath prior to injection of PMeBu<sup>t</sup><sub>2</sub>. The reaction was monitored by <sup>1</sup>H and <sup>31</sup>P NMR on an instrument precooled to -70 °C and gradually warmed up to 25 °C.

#### 2.3.1.4 L = PCy<sub>3</sub>

A stock solution of 0.272 M PCy<sub>3</sub> was prepared by dissolving 0.076 g of PCy<sub>3</sub> in 1 mL toluene-d<sub>8</sub>. Experiments were carried out as outlined in 2.3.1.

#### 2.3.1.5 L = PBu<sup>t</sup><sub>3</sub>

A stock solution of 0.272 M PBu<sup>t</sup><sub>3</sub> was prepared by dissolving 0.055 g of PBu<sup>t</sup><sub>3</sub> in 1 mL toluene-d<sub>8</sub>. Experiments were carried out as outlined in 2.3.1.

#### 2.3.1.6 Isolation of Pd<sub>2</sub>(PPh<sub>3</sub>)<sub>2</sub>(μ-C<sub>5</sub>H<sub>5</sub>)(μ-1-Ph-C<sub>3</sub>H<sub>4</sub>)

Pd(η<sup>3</sup>-1-Ph-C<sub>3</sub>H<sub>4</sub>)(η<sup>5</sup>-C<sub>5</sub>H<sub>5</sub>) (0.045 g, 1.56 x 10<sup>-4</sup> mol) and PPh<sub>3</sub> (0.050 g, 1.91 x 10<sup>-4</sup> mol) were dissolved in hexanes (10 mL) and stirred at 25 °C for 1 h. The light brown precipitate was collected by syringing off the hexanes solution and washed with additional hexanes (2 x 5 mL). The residue was dried *in vacuo*. Analysis was performed in toluene-d<sub>8</sub> using <sup>1</sup>H, <sup>1</sup>H{<sup>31</sup>P} and <sup>31</sup>P NMR spectroscopy, COSY, and NOESY.

#### 2.3.2 Bidentate Phosphines

Experiments investigated both 1:1 and 2:1 ratios of L:Pd at 25, 50 and 75 °C. In a typical 1:1 experiment, 0.25 mL of 0.136 M (3.4 x 10<sup>-5</sup> mol) L was injected into a capped NMR tube containing 0.25 mL of 0.136 M (3.4 x 10<sup>-5</sup> mol) Pd(η<sup>3</sup>-1-Ph-C<sub>3</sub>H<sub>4</sub>)(η<sup>5</sup>-C<sub>5</sub>H<sub>5</sub>). In a typical 2:1 experiment, 0.40 mL of 0.136 M (5.44 x 10<sup>-5</sup> mol) L was injected into a capped NMR tube containing 0.20 mL of 0.136 M (2.72 x 10<sup>-5</sup> mol) Pd(η<sup>3</sup>-1-Ph-C<sub>3</sub>H<sub>4</sub>)(η<sup>5</sup>-C<sub>5</sub>H<sub>5</sub>). Deviations from and/or additions to this general procedure are noted below.

### 2.3.2.1 L = dppe

A stock solution of 0.136 M dppe was prepared by dissolving 0.054 g of dppe in 1 mL toluene- $d_8$ .

The 2:1 ratio was only investigated at 25 °C. In addition to the experiments outlined in 2.3.2, low temperature NMR studies were performed on both the 1:1 and 2:1 systems. Once the systems had completely reacted to form  $\text{Pd}(\text{dppe})_n$ ,  $^1\text{H}$  and  $^{31}\text{P}$  NMR spectra were taken at -50 and -70 °C.

### 2.3.2.2 L = dppp

A stock solution of 0.136 M dppp was prepared by dissolving 0.056 g of dppp in 1 mL toluene- $d_8$ . The 2:1 ratio was only investigated at 25 and 75 °C.

### 2.3.2.3 L = dppf

Due to poor solubility of dppf in toluene, 0.136 M stock solutions of dppf and  $\text{Pd}(\eta^3\text{-1-Ph-C}_3\text{H}_4)(\eta^5\text{-C}_5\text{H}_5)$  were prepared in  $\text{C}_6\text{D}_6$  (0.075 g of dppf in 1 mL  $\text{C}_6\text{D}_6$ ; 0.039 g of  $\text{Pd}(\eta^3\text{-1-Ph-C}_3\text{H}_4)(\eta^5\text{-C}_5\text{H}_5)$  in 1 mL  $\text{C}_6\text{D}_6$ ).

Both the 1:1 and 2:1 systems were only investigated at 25 and 75 °C.

## 2.4 Oxidative Addition Experiments

### 2.4.1 Oxidative Addition to $\text{PdL}_n$ Generated *in situ* (L = $\text{PMePh}_2$ , $\text{PPh}_3$ , $\text{PCy}_3$ , $\text{PMeBu}^t_2$ , $\text{PBU}^t_3$ , dppe, dppp)

In a typical experiment, 4 eq. of PhI was injected into a sample of  $\text{PdL}_n$  generated at the time and temperature determined from experiments described

in 2.3. The product formed was identified by  $^1\text{H}$  and  $^{31}\text{P}$  NMR, COSY, and for L = dppe and dppp,  $^{31}\text{P}$ - $^{31}\text{P}$  correlation spectroscopy.

For L =  $\text{PMePh}_2$  and  $\text{PPh}_3$ , both the 2:1 and 3:1 L:Pd ratios were investigated. For L = dppe and dppp, only the 2:1 L:Pd ratio was investigated. For L =  $\text{PMePh}_2$ ,  $\text{PPh}_3$ , dppe and dppp, the oxidative addition products precipitated out of their toluene- $\text{d}_8$  solutions, and therefore were collected and redissolved in  $\text{CD}_2\text{Cl}_2$  for identification. For L =  $\text{PCy}_3$ ,  $\text{PMeBu}^t_2$ , and  $\text{PBU}^t_3$ , the oxidative addition products were identified directly.

Quantitative information was gathered for L =  $\text{PCy}_3$  and  $\text{PMeBu}^t_2$  by generating  $\text{PdL}_n$  as above and inserting sealed capillaries containing TOPB in toluene- $\text{d}_8$  into the NMR tubes. Inverse-gated  $^{31}\text{P}$  NMR spectra ( $d_1 = 45$  s) were taken both prior to and following the injection of PhI ( $20 \mu\text{L}$ ,  $1.80 \times 10^{-4}$  mol). Yields were determined to be 99% for both products.

#### 2.4.2 Oxidative Addition to Isolated $\text{PdL}_2$ (L = dppf)

For dppf,  $\text{Pd}(\text{dppf})_2$  was generated at the time and temperature determined from experiments described in 2.3.2 using the 2:1 ratio of dppf:Pd; however,  $\text{Pd}(\text{dppf})_2$  precipitated out of the  $\text{C}_6\text{D}_6$  solution. It was collected and dried *in situ*, and the residue was dissolved in a minimum of THF. PhI ( $15 \mu\text{L}$ ,  $1.35 \times 10^{-4}$  mol) was added and the solution was stirred for 18 h at  $25^\circ\text{C}$ . THF was removed at reduced pressures and the residue was redissolved in  $\text{C}_6\text{D}_6$  for identification by  $^1\text{H}$  and  $^{31}\text{P}$  NMR, COSY, and  $^{31}\text{P}$ - $^{31}\text{P}$  correlation spectroscopy.

## 2.5 Studies of Transmetallation

### 2.5.1 Investigations into the Role of H<sub>2</sub>O

A stock solution of 0.006 M *trans*-Pd(4-CH<sub>3</sub>C<sub>6</sub>H<sub>5</sub>)(Br)(PCy<sub>3</sub>)<sub>2</sub> (0.030 g) and 0.009 M [NBu<sub>4</sub>][PhBF<sub>3</sub>] (0.021 g) was prepared in dry toluene-d<sub>8</sub> (6 mL). In a typical experiment, 0.50 mL of this stock solution (3.0 x 10<sup>-6</sup> mol *trans*-Pd(4-CH<sub>3</sub>C<sub>6</sub>H<sub>5</sub>)(Br)(PCy<sub>3</sub>)<sub>2</sub> and 4.5 x 10<sup>-6</sup> mol [NBu<sub>4</sub>][PhBF<sub>3</sub>]) was placed in an NMR tube and the sample was treated according to the conditions in Table 1.

**Table 1. Summary of attempted cross-coupling experiments with Pd(4-CH<sub>3</sub>C<sub>6</sub>H<sub>5</sub>)(Br)(PCy<sub>3</sub>)<sub>2</sub> and [NBu<sub>4</sub>][PhBF<sub>3</sub>]**

Entry	Iterations	Additional Reagents <sup>a</sup>	Temperature (°C)
1	2	-	80/reflux
2	1	3.1 eq K <sub>2</sub> CO <sub>3</sub> (2 mg, 1.4 x 10 <sup>-5</sup> mol)	80/reflux
3	1	3.1 eq K <sub>2</sub> CO <sub>3</sub> + 3.3 eq TBAB (5 mg, 1.5 x 10 <sup>-5</sup> mol)	80/reflux
4	3	1.3 eq H <sub>2</sub> O (0.1 μL, 5.6 x 10 <sup>-5</sup> mol)	90 – 95
5	3	3.8 eq H <sub>2</sub> O (0.3 μL, 1.7 x 10 <sup>-5</sup> mol)	90 – 95
6	3	xs <sup>c</sup> H <sub>2</sub> O (5.0 μL, 2.8 x 10 <sup>-4</sup> mol)	90 – 95

(a) The number of equivalents is compared to [NBu<sub>4</sub>][PhBF<sub>3</sub>] (4.5 x 10<sup>-6</sup> mol)

(b) TBAB = tetrabutylammonium bromide

(c) At the temperatures investigated, 0.50 mL toluene can only dissolve approximately 1.5 – 2.0 μL H<sub>2</sub>O (8.3 x 10<sup>-5</sup> – 1.1 x 10<sup>-4</sup> mol)<sup>46</sup>

Samples were heated in an oil bath and the progress of the reaction was monitored by <sup>1</sup>H and <sup>31</sup>P NMR spectroscopy. The reaction was deemed



complete when Pd(4-CH<sub>3</sub>C<sub>6</sub>H<sub>5</sub>)(Br)(PCy<sub>3</sub>)<sub>2</sub> and/or [NBu<sub>4</sub>][PhBF<sub>3</sub>] was no longer observable in the NMR spectra. Yields were determined by gas chromatography.

Samples were diluted to 1 mL and 1 μL injections were introduced into the injection port. The GC instrument conditions are outlined in Table 2.

**Table 2. GC instrument conditions used for all analyses**

Component	Temperature (°C)	Temperature Ramp
Column Oven	120	Hold 3 min
	200	20 °C/min; hold 5 min
Injector	270	-
FID	300	-

## Chapter 3

### Results and Discussion

#### 3.1 *In Situ* Generation of Pd(0)L<sub>n</sub> from Pd(η<sup>5</sup>-C<sub>5</sub>H<sub>5</sub>)(η<sup>3</sup>-1-Ph-C<sub>3</sub>H<sub>4</sub>)

##### 3.1.1 Properties of Pd(η<sup>5</sup>-C<sub>5</sub>H<sub>5</sub>)(η<sup>3</sup>-1-Ph-C<sub>3</sub>H<sub>4</sub>)

Pd(η<sup>5</sup>-C<sub>5</sub>H<sub>5</sub>)(η<sup>3</sup>-1-Ph-C<sub>3</sub>H<sub>4</sub>) was obtained in 78 % yield as a red, crystalline solid in two steps starting from PdCl<sub>2</sub>. It had minimal vapour pressure and was sufficiently robust that it remained unchanged in appearance as a crystalline solid on standing in air at room temperature for several days, while solutions in toluene-d<sub>8</sub> were stable at room temperature in air for at least 24 h. Therefore, it is more easily synthesized and handled than is Pd(η<sup>5</sup>-C<sub>5</sub>H<sub>5</sub>)(η<sup>3</sup>-C<sub>3</sub>H<sub>5</sub>).

The X-ray crystal structure of Pd(η<sup>5</sup>-C<sub>5</sub>H<sub>5</sub>)(η<sup>3</sup>-1-Ph-C<sub>3</sub>H<sub>4</sub>) was determined (Figure 25), and although this structure can be found in the literature,<sup>45c</sup> the structure presented herein is of a different space group and corrects for previous disorder found in the Cp ring. A list of select bond lengths can be found in Table 3, with complete structural data provided in Appendix A.

Pd(η<sup>5</sup>-C<sub>5</sub>H<sub>5</sub>)(η<sup>3</sup>-1-Ph-C<sub>3</sub>H<sub>4</sub>) is a sandwich structure with an angle of 19.93(22)° between the planes of the allyl and Cp ligands. The C-C bond lengths of the allyl group are identical within experimental error (1.408(4), 1.400(4)); however, the Pd-allyl bond lengths demonstrate asymmetry in the binding of the allyl ligand. The Pd-C(8) bond is significantly longer than the Pd-C(6) bond by 0.051 Å, causing the group to hinge away from the Pd centre on the side of the

phenyl substituent. The Cp ring also hinges away from Pd on that side, with longer Pd-ring bonds to C(1) (2.353(3)) and C(2) (2.403(3)) than to C(3) (2.293(3)) and C(4) (2.303(3)). This is in contrast with the structure of Pd( $\eta^5$ -C<sub>5</sub>H<sub>5</sub>)( $\eta^3$ -C<sub>3</sub>H<sub>5</sub>) which symmetrically binds both the allyl (Pd-C(6) 2.07; Pd-C(8) 2.13) and Cp (Pd-C(1)/C(2)/C(3) 2.27; Pd-C(4)/C(5) 2.25) ligands.<sup>49</sup>

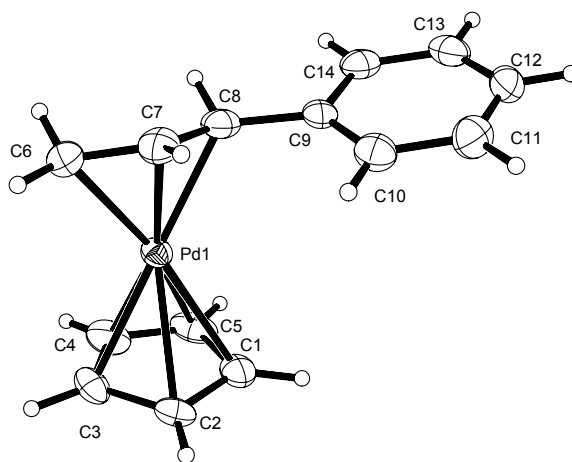


**Figure 25. Molecular Structure of Pd( $\eta^5$ -C<sub>5</sub>H<sub>5</sub>)( $\eta^3$ -1-Ph-C<sub>3</sub>H<sub>4</sub>) (50 % probability level)**

**Table 3. Select bond lengths for Pd( $\eta^5$ -C<sub>5</sub>H<sub>5</sub>)( $\eta^3$ -1-Ph-C<sub>3</sub>H<sub>4</sub>)**

Bond	Bond Length (Å)	Bond	Bond Length (Å)
Pd(1)-C(7)	2.072(3)	C(1)-C(2)	1.398(4)
Pd(1)-C(6)	2.123(3)	C(1)-C(5)	1.433(5)
Pd(1)-C(8)	2.174(3)	C(2)-C(3)	1.406(4)
Pd(1)-C(3)	2.293(3)	C(3)-C(4)	1.425(4)
Pd(1)-C(4)	2.303(3)	C(4)-C(5)	1.388(5)
Pd(1)-C(5)	2.313(3)	C(6)-C(7)	1.408(4)
Pd(1)-C(1)	2.353(3)	C(7)-C(8)	1.400(4)
Pd(1)-C(2)	2.403(3)	C(8)-C(9)	1.476(4)

### 3.1.2 Reactions of $\text{Pd}(\eta^5\text{-C}_5\text{H}_5)(\eta^3\text{-1-Ph-C}_3\text{H}_4)$ with Monodentate Phosphines

Generation of  $\text{Pd}(0)\text{L}_n$  species from compounds of the type  $\text{Pd}(\eta^5\text{-C}_5\text{H}_5)(\eta^3\text{-2-R-C}_3\text{H}_4)$  ( $\text{R} = \text{H, Me, Bu}^t$ ) in the presence of monodentate phosphines and phosphites has been well studied by Werner *et al.*<sup>41</sup> Initial kinetic studies on the ligand displacement of  $\text{Pd}(\eta^5\text{-C}_5\text{H}_5)(\eta^3\text{-2-Me-C}_3\text{H}_4)$  by phosphites revealed a multi-step mechanism, and subsequent low temperature NMR experiments were able to capture intermediates of the type  $(\eta^5\text{-C}_5\text{H}_5)\text{Pd}(\eta^1\text{-2-Me-C}_3\text{H}_4)\text{L}$ .<sup>41b</sup> This led to the proposed mechanism illustrated in Figure 26.

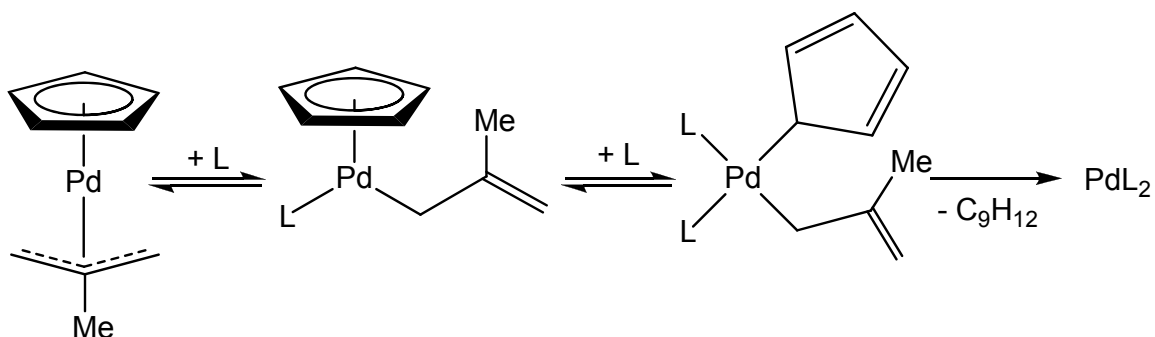
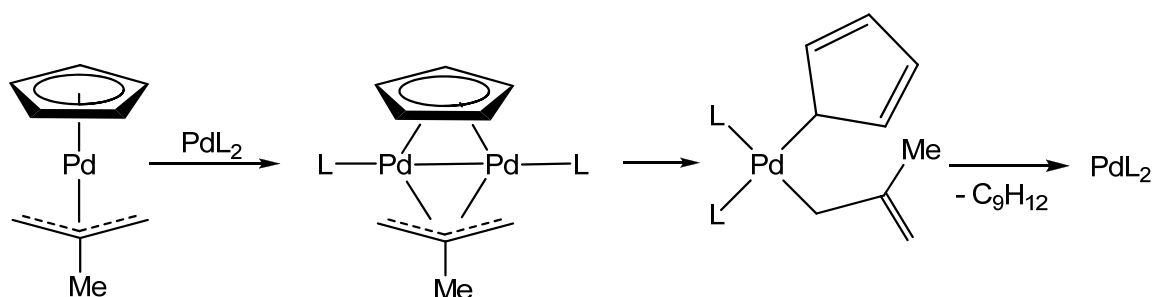


Figure 26. Proposed mechanism for the formation of  $\text{PdL}_2$  from  $\text{Pd}(\eta^5\text{-C}_5\text{H}_5)(\eta^3\text{-2-Me-C}_3\text{H}_4)$

The  $\eta^1\text{-C}_5\text{H}_5$  intermediate has not been identified and is therefore a postulated structure. The hydrocarbon product,  $\text{C}_9\text{H}_{12}$ , exists as a mixture of isomers.<sup>41b</sup>

Attempts to isolate the  $\sigma$ -allyl intermediate for the  $L = PPh_3$  system led to the formation of an unexpected species, identified as  $Pd_2(PPh_3)_2(\mu-C_5H_5)(\mu-2-Me-C_3H_4)$  by X-ray crystallography.<sup>41a,b</sup> Similar dinuclear species were subsequently prepared for other  $L$ , typically by reacting  $Pd(\eta^5-C_5H_5)(\eta^3-2-Me-C_3H_4)$  with one molar equivalent of  $L$ .<sup>41b</sup> In an attempt to account for the formation of this complex under the reaction conditions previously investigated (two molar equivalents of  $L$ ), the mechanism in Figure 27 was proposed. This hypothesis was confirmed by separate experiments in which dinuclear compounds were generated quantitatively from reactions of equimolar amounts of  $PdL_2$  ( $L = PBu^t_3, PPr^i_3$ ) and  $Pd(\eta^5-C_5H_5)(\eta^3-2-Me-C_3H_4)$ .<sup>41b</sup>



**Figure 27. Proposed mechanism for the generation of  $Pd_2(PPh_3)_2(\mu-C_5H_5)(\mu-2-Me-C_3H_4)$**

E. A. Mitchell further investigated the  $R = H$  system, reacting  $Pd(\eta^5-C_5H_5)(\eta^3-C_3H_5)$  with two equivalents  $L$  ( $L = PCy_3, PMeBu^t_2, PBu^t_3$ ) in order to determine the minimum time necessary at a temperature of 25-77 °C to quantitatively generate  $Pd(0)L_2$ .<sup>44</sup> Her studies found that while the compound

was a successful precursor for compounds of the type  $\text{PdL}_n$ , the volatility and thermal instability previously discussed make the compound difficult to synthesize, store and handle. She therefore began preliminary studies on the much more robust  $\text{Pd}(\eta^5\text{-C}_5\text{H}_5)(\eta^3\text{-1-Ph-C}_3\text{H}_4)$  compound.

Mitchell's preliminary studies found that  $\text{Pd}(0)\text{L}_n$  could be generated from  $\text{Pd}(\eta^5\text{-C}_5\text{H}_5)(\eta^3\text{-1-Ph-C}_3\text{H}_4)$  in the presence of L, proceeding through the  $\sigma$ -allyl and dinuclear-type intermediates initially proposed by Werner (Figure 28). These studies also indicated that the asymmetry in the allyl group led to two isomers of the dinuclear species, one with the phenyl group *syn* and one with the phenyl group *anti* to the unique H(2) proton. Each dinuclear species generated a distinct AB quartet in the  $^{31}\text{P}$  NMR spectra.

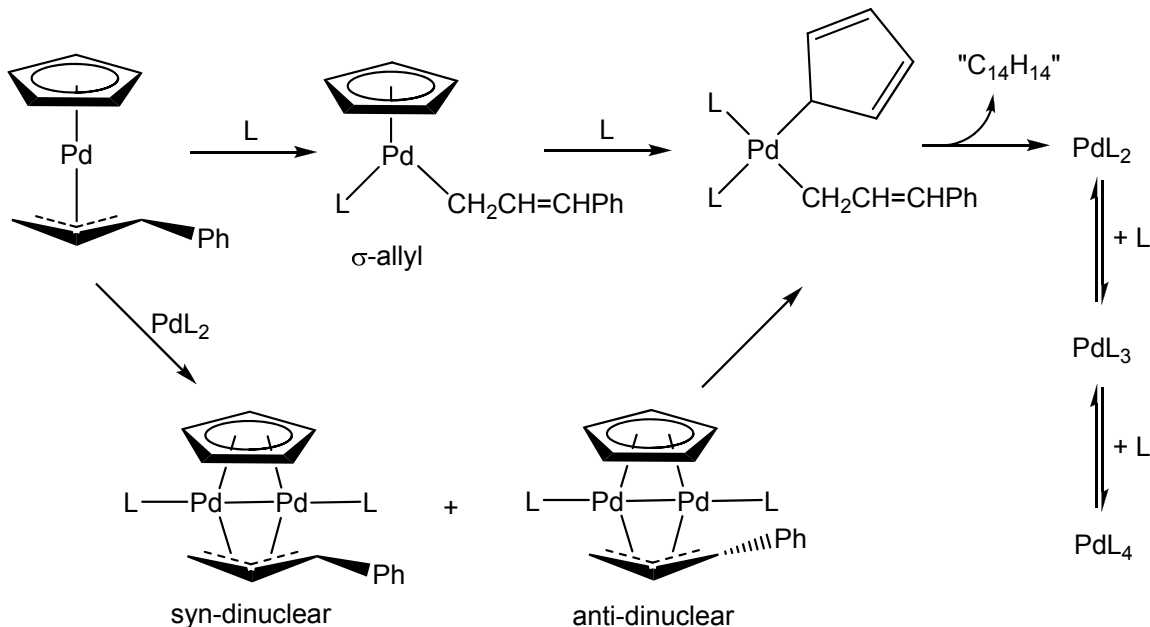


Figure 28. Proposed mechanism of  $\text{PdL}_n$  formation from  $\text{Pd}(\eta^5\text{-C}_5\text{H}_5)(\eta^3\text{-1-Ph-C}_3\text{H}_4)$

The current line of research looked to determine the minimum time at a reasonable temperature to generate Pd(0)L<sub>n</sub> from Pd(η<sup>5</sup>-C<sub>5</sub>H<sub>5</sub>)(η<sup>3</sup>-1-Ph-C<sub>3</sub>H<sub>4</sub>) and a variety of monodentate phosphine ligands. Typical experiments involved combining toluene-d<sub>8</sub> solutions of Pd(η<sup>5</sup>-C<sub>5</sub>H<sub>5</sub>)(η<sup>3</sup>-1-Ph-C<sub>3</sub>H<sub>4</sub>) (3.4 x 10<sup>-5</sup> mol) and L (6.8 x 10<sup>-5</sup> mol), and monitoring the reactions by <sup>1</sup>H and <sup>31</sup>P NMR spectroscopy at 25, 50 or 75 °C. A ligand to Pd(η<sup>5</sup>-C<sub>5</sub>H<sub>5</sub>)(η<sup>3</sup>-1-Ph-C<sub>3</sub>H<sub>4</sub>) ratio of 2:1 was selected in an attempt to favour the formation of the unsaturated, catalytically active PdL<sub>2</sub> species, although the ratio was probably never achieved exactly because of the small amounts being weighed. The timelines to Pd(0)L<sub>n</sub> formation are summarized in Table 4.

**Table 4. Timelines for the formation of Pd(0)L<sub>n</sub> from monodentate phosphines L**

L	L: Pd	Time (T) to complete conversion to Pd(0) products <sup>a</sup>		
		25 °C	50 °C	75 °C
PPh <sub>3</sub>	2:1	> 24 h	5 h < T < 20 h	30 min
PPh <sub>3</sub>	3:1	90 min	NI	NI
PMePh <sub>2</sub>	2:1	> 48 h	5 h < T < 24 h	30 min
PMePh <sub>2</sub>	3:1	10 min	NI	NI
PCy <sub>3</sub>	2:1	> 48 h	5 h < T < 18 h	1 h
PMeBu <sup>t</sup> <sub>2</sub>	2:1	> 48 h	45 min	NI
PBu <sup>t</sup> <sub>3</sub>	2:1	5 h < T < 24 h	3 h	1 h

a. NI = not investigated

These timelines, as well as the presence of σ-allyl and dinuclear intermediates, will be discussed in greater detail below. The intermediates were identified by monitoring corresponding changes in the <sup>1</sup>H and <sup>31</sup>P NMR spectra,

as well as use of COSY to correlate the allyl protons. Integration of the proton resonances acted not only as confirmation of the allyl assignments, but also allowed assignment of the Cp resonances to each set of allyl resonances.

### 3.1.2.1 L = PMeBu<sup>t</sup><sub>2</sub>

A reaction of Pd( $\eta$ -C<sub>5</sub>H<sub>5</sub>)( $\eta$ <sup>3</sup>-1-Ph-C<sub>3</sub>H<sub>4</sub>) with two equivalents of PMeBu<sup>t</sup><sub>2</sub> at 25 °C produced a sharp singlet at  $\delta$  61.7 in the <sup>31</sup>P NMR spectrum within minutes of mixing. The <sup>1</sup>H resonances of this species were obscured by those of the reductive elimination products, and therefore a separate sample of Pd( $\eta$ -C<sub>5</sub>H<sub>5</sub>)( $\eta$ <sup>3</sup>-1-Ph-C<sub>3</sub>H<sub>4</sub>) and two equivalents of PMeBu<sup>t</sup><sub>2</sub> was prepared at -70 °C. A <sup>1</sup>H NMR spectrum (Figure 29) taken at -20 °C allowed the <sup>31</sup>P singlet to be assigned to the  $\sigma$ -allyl intermediate. The <sup>1</sup>H assignments (Table 5) were made based on a COSY spectrum, which showed correlation between the resonances at  $\delta$  6.44 and 6.83, as well as between the resonances at  $\delta$  6.83 and 2.71. These correlations allowed the resonance at  $\delta$  6.83 to be assigned to H(2). The resonance at  $\delta$  2.71 is a doublet of doublets, indicating that in addition to coupling to H(2), it also couples to phosphorus. This along with the fact that the resonance integrates to 2H, allowed the resonance to be assigned to H(3). The remaining resonance at  $\delta$  6.44 was assigned to H(1) and this assignment is supported by the integration to 1H. The assignments are supported by the chemical shifts of the resonances, with H(1) and H(2) being observed in the expected region for vinylic protons. Of note, <sup>3</sup>J<sub>H(1)H(2)</sub> is 15.5 Hz, indicating a *trans* geometry across the double bond.



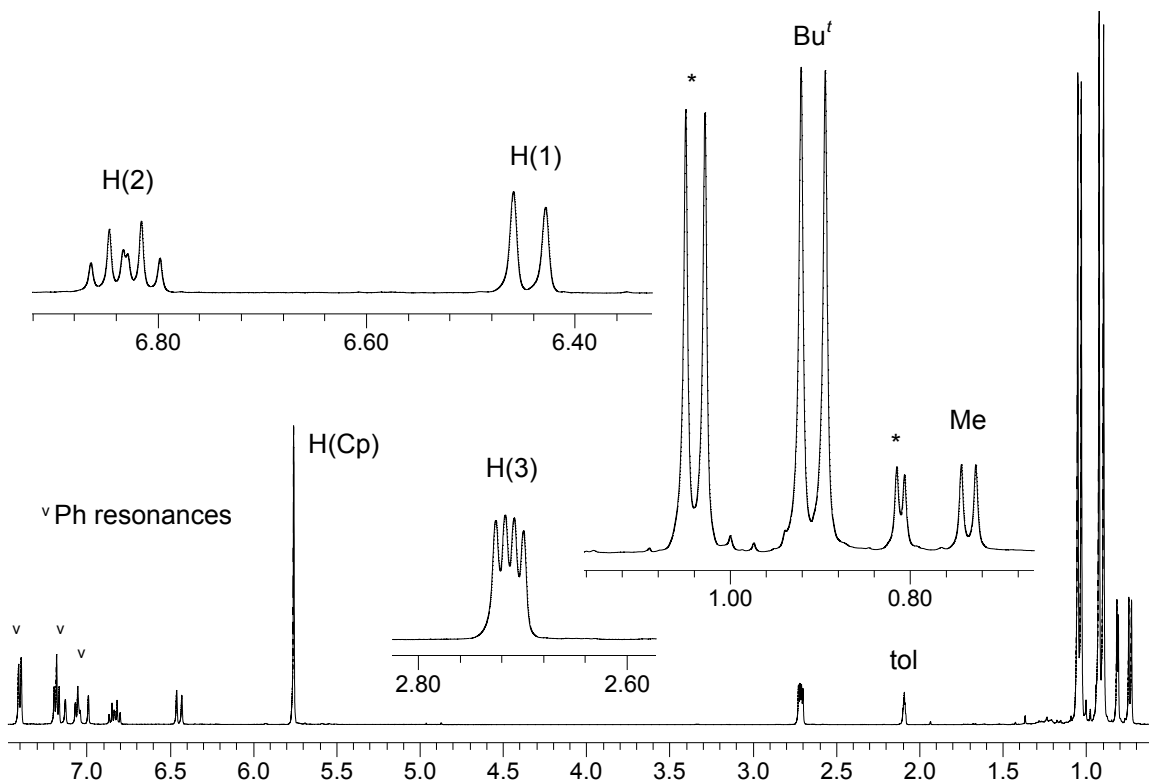


Figure 29.  $^1\text{H}$  NMR ( $-20\text{ }^\circ\text{C}$ , 500 MHz,  $\text{tol-}d_8$ ) of  $\sigma$ -allyl intermediate produced from the reaction of  $\text{Pd}(\eta^5\text{-C}_5\text{H}_5)(\eta^3\text{-1-Ph-C}_3\text{H}_4)$  with two equivalents  $\text{PMeBu}^t_2$  (\* free  $\text{PMeBu}^t_2$ )

Table 5.  $^1\text{H}$  and  $^{31}\text{P}$  NMR chemical shifts of  $\eta^5\text{-CpPd}(\eta^1\text{-1-Ph-C}_3\text{H}_4)(\text{PMeBu}^t_2)$  in toluene- $d_8$

Structure	Assignment
	H(1): $\delta$ 6.44 (d; $^3J_{\text{HH}}$ 15.5 Hz)
	H(2): $\delta$ 6.83 (dt; $^3J_{\text{HH}}$ 15.5, 8.8 Hz)
	H(3): $\delta$ 2.71 (dd; $^3J_{\text{HH}}$ 8.8; $^3J_{\text{PH}}$ 4.4 Hz)
	H(Cp): $\delta$ 5.76 (s)
	Me: $\delta$ 0.74 (d; $^2J_{\text{PH}}$ 8.1 Hz)
	Bu: $\delta$ 0.91 (d; $^3J_{\text{PH}}$ 13.5 Hz)
	Ph: $\delta$ 7.05 (t; $^3J_{\text{HH}}$ 7.6 Hz, <i>p</i> ); 7.18 (t; $^3J_{\text{HH}}$ 7.6 Hz, <i>m</i> ); 7.40 (d; $^3J_{\text{HH}}$ 7.6 Hz, <i>o</i> )
	$^{31}\text{P}$ : $\delta$ 61.7

At 25 °C, the  $\sigma$ -allyl species was the major species after 1 h and remained identifiable in the  $^1\text{H}$  and  $^{31}\text{P}$  NMR spectra past 51 h. At that point a broad resonance around  $\delta$  41, associated with  $\text{Pd}(\text{PMeBu}^t_2)_2$ , had appeared in the  $^{31}\text{P}$  NMR spectrum (lit.  $\delta$  41.9).<sup>40</sup> No dinuclear species were ever identified in the NMR spectra.

For a similar reaction at 50 °C, a  $^{31}\text{P}$  NMR spectrum after 30 min revealed a broad resonance around  $\delta$  42, corresponding to  $\text{Pd}(\text{PMeBu}^t_2)_2$ , along with a minor resonance associated with the  $\sigma$ -allyl intermediate. By 45 min, the resonances associated with the  $\sigma$ -allyl intermediate had disappeared from the  $^1\text{H}$  and  $^{31}\text{P}$  NMR spectra, yielding a sharpened resonance at  $\delta$  42.2 corresponding to  $\text{Pd}(\text{PMeBu}^t_2)_2$ .

### 3.1.2.2 L = $\text{PBu}^t_3$

After 5 min at 25 °C, the  $^1\text{H}$  NMR spectrum of a reaction of  $\text{Pd}(\eta\text{-C}_5\text{H}_5)(\eta^3\text{-1-Ph-C}_3\text{H}_4)$  with two equivalents of  $\text{PBu}^t_3$  revealed a significant amount of unreacted  $\text{Pd}(\eta^5\text{-C}_5\text{H}_5)(\eta^3\text{-1-Ph-C}_3\text{H}_4)$  and free  $\text{PBu}^t_3$ , as well as a small amount of the  $\sigma$ -allyl species. The  $^1\text{H}$  assignments of the  $\sigma$ -allyl intermediate were made in the same fashion as were those in 3.1.2.1 and can be found in Table 6. The  $\text{Bu}^t$  resonance was obscured by the resonances of the reductive elimination products and of free  $\text{PBu}^t_3$ . Of note, the Cp resonance at  $\delta$  5.68 was a doublet ( $^3J_{\text{PH}}$  1.6 Hz), consistent with Werner's studies of other  $\sigma$ -allyl species.<sup>41c,d</sup>

**Table 6.**  $^1\text{H}$  and  $^{31}\text{P}$  NMR chemical shifts of  $\eta^5\text{-CpPd}(\eta^1\text{-1-Ph-C}_3\text{H}_4)(\text{P}^t\text{Bu}_3)$  in toluene- $d_8$

Structure	Assignment
	H(1): $\delta$ 6.57 (d; $^3J_{\text{HH}}$ 15.5 Hz)
	H(2): $\delta$ 6.80 (dt; $^3J_{\text{HH}}$ 15.5, 8.8 Hz)
	H(3): $\delta$ 3.09 (dd; $^3J_{\text{HH}}$ 8.8; $^3J_{\text{PH}}$ 3.3 Hz)
	H(Cp): $\delta$ 5.68 (d; $^3J_{\text{PH}}$ 1.6 Hz)
	Ph: $\delta$ 7.00-7.40 (m)
	$^{31}\text{P}$ : $\delta$ 97.4

After 5 min, the  $^{31}\text{P}$  NMR spectrum (Figure 30) showed a major resonance at  $\delta$  62.2 corresponding to free  $\text{P}^t\text{Bu}_3$ , with minor resonances corresponding to the  $\sigma$ -allyl species at  $\delta$  97.4 and  $\text{Pd}(\text{P}^t\text{Bu}_3)_2$  at  $\delta$  84.8 (lit  $\delta$  84.7).<sup>40</sup>  $^1\text{H}$  NMR spectra indicated that the  $\sigma$ -allyl species disappeared within 3 h, while unreacted  $\text{Pd}(\eta^5\text{-C}_5\text{H}_5)(\eta^3\text{-1-Ph-C}_3\text{H}_4)$  was present past 7 h. At 24 h, this starting material was completely reacted although free  $\text{P}^t\text{Bu}_3$  was still present. As there was no longer starting material or intermediates present in solution for this  $\text{P}^t\text{Bu}_3$  to react with, it was believed that an excess of ligand was present in the system.

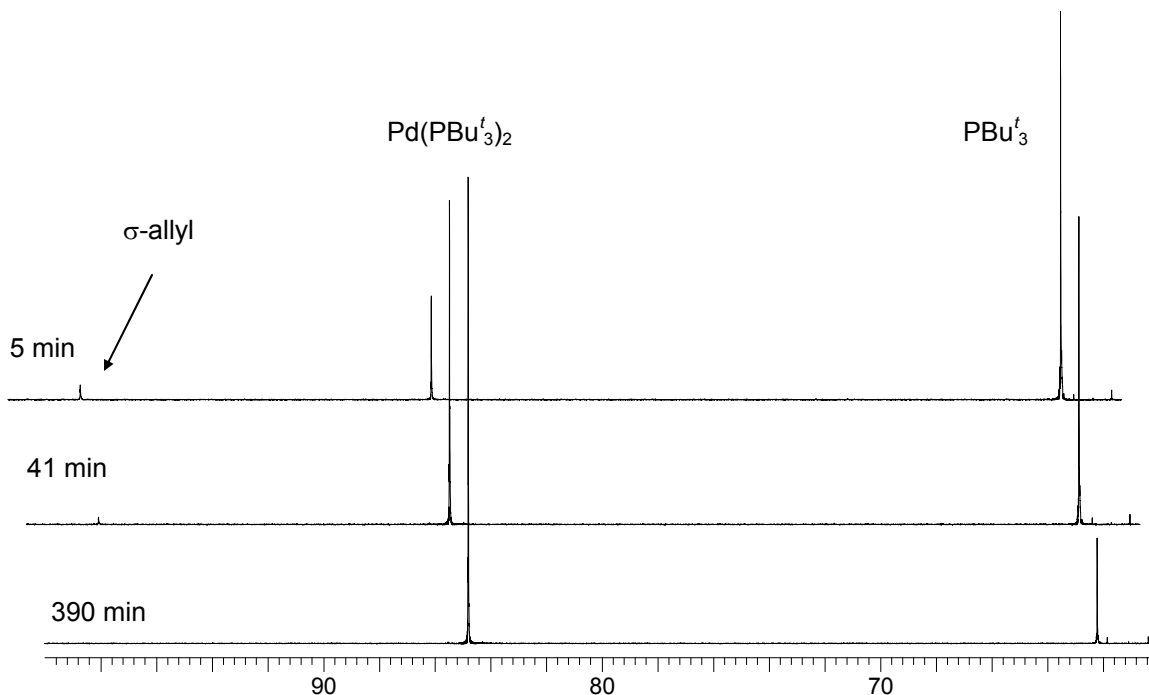


**Figure 30. Stacked plots of  $^{31}\text{P}$  NMR spectra (202.3 MHz,  $\text{tol-d}_8$ ) for the reaction of  $\text{Pd}(\eta^5\text{-C}_5\text{H}_5)(\eta^3\text{-1-Ph-C}_3\text{H}_4)$  with two equivalents of  $\text{PBU}^t_3$  at 25 °C**

When the system was investigated at 50 °C, a  $^1\text{H}$  NMR spectrum after 6 min revealed unreacted  $\text{Pd}(\eta^5\text{-C}_5\text{H}_5)(\eta^3\text{-1-Ph-C}_3\text{H}_4)$  and free  $\text{PBU}^t_3$ . The  $^{31}\text{P}$  NMR spectrum at that time showed that  $\text{Pd}(\text{PBU}^t_3)_2$  was the major species existing in solution and confirmed the presence of free  $\text{PBU}^t_3$ . The resonances corresponding to  $\text{Pd}(\eta^5\text{-C}_5\text{H}_5)(\eta^3\text{-1-Ph-C}_3\text{H}_4)$  and free  $\text{PBU}^t_3$  decreased in intensity, with a growth in the intensity of the resonance corresponding to  $\text{Pd}(\text{PBU}^t_3)_2$ , until the 3 h mark when only  $\text{Pd}(\text{PBU}^t_3)_2$  was present. The reaction proceeded in a similar fashion at 75 °C, with complete  $\text{Pd}(\text{PBU}^t_3)_2$  formation within 1 h.

### 3.1.2.3 L = PPh<sub>3</sub>

At 25 °C, a reaction of Pd( $\eta^5$ -C<sub>5</sub>H<sub>5</sub>)( $\eta^3$ -1-Ph-C<sub>3</sub>H<sub>4</sub>) with two equivalents of PPh<sub>3</sub> completely consumed the Pd( $\eta^5$ -C<sub>5</sub>H<sub>5</sub>)( $\eta^3$ -1-Ph-C<sub>3</sub>H<sub>4</sub>) starting material within 15 min. A <sup>31</sup>P NMR spectrum taken after 20 min (Figure 31) showed the major resonance to be a broad singlet at  $\delta$  22.9 which corresponds well to the known resonance for Pd(PPh<sub>3</sub>)<sub>3</sub> (lit.  $\delta$  22.6).<sup>47a</sup> Three other species were identified in the <sup>31</sup>P NMR spectrum: a sharp singlet at  $\delta$  45.7, and two AB quartets at  $\delta$  24.5 and 26.2 (95 Hz, b), and  $\delta$  23.0 and 26.8 (139 Hz, a).

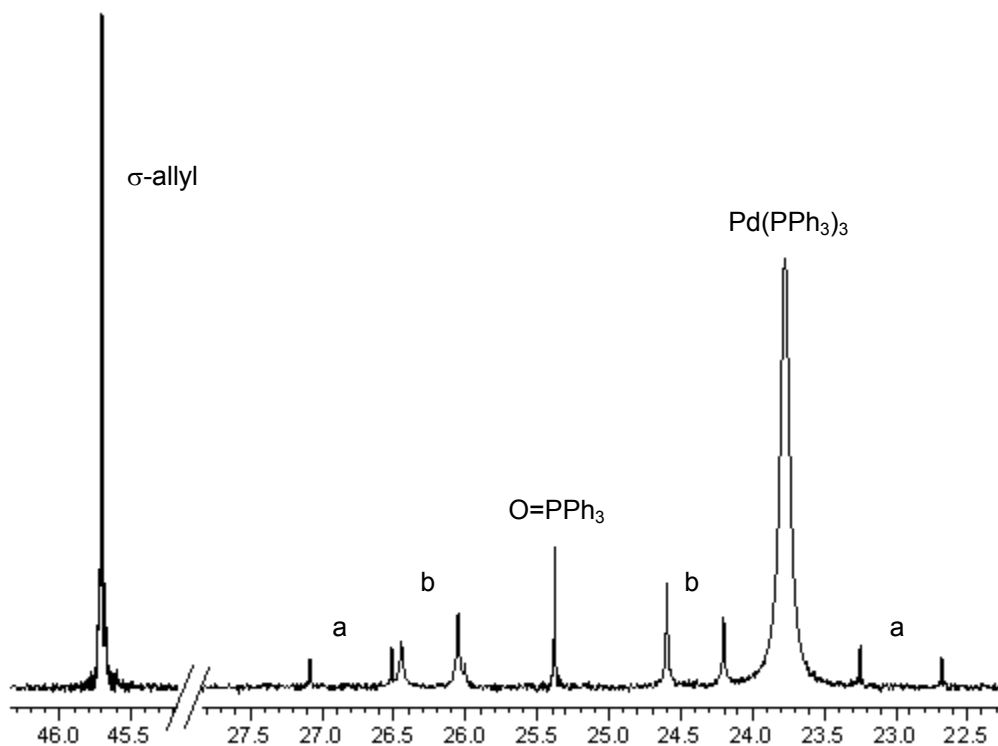


Figure 31. <sup>31</sup>P NMR spectrum (242.9 MHz, tol-d<sub>8</sub>) of a reaction of Pd( $\eta^5$ -C<sub>5</sub>H<sub>5</sub>)( $\eta^3$ -1-Ph-C<sub>3</sub>H<sub>4</sub>) with two equivalents PPh<sub>3</sub> at 25 °C (20 min after mixing)

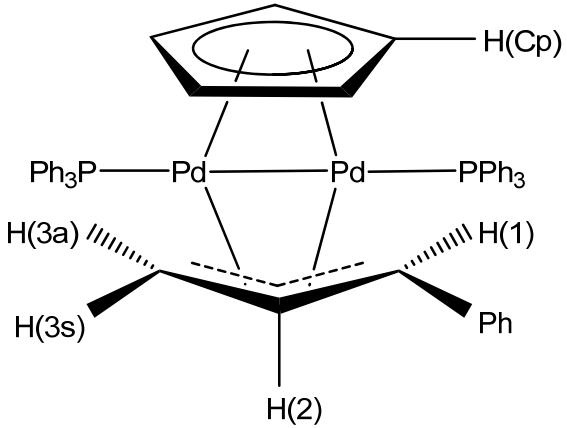
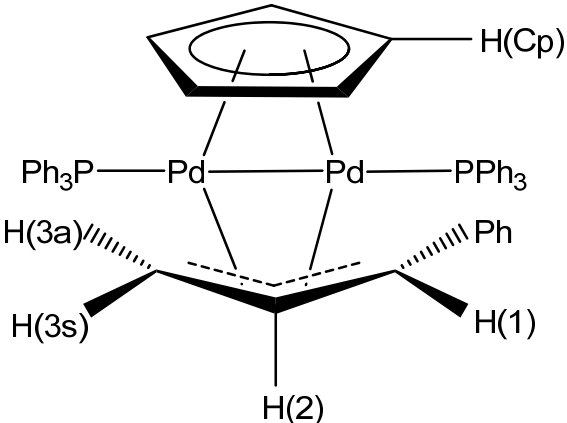
The resonance at  $\delta$  45.7 was assigned to the  $\sigma$ -allyl intermediate in a manner similar to that in 3.1.2.1. The  $^1\text{H}$  assignments can be found in Table 7.

**Table 7.**  $^1\text{H}$  and  $^{31}\text{P}$  NMR chemical shifts of  $\eta^5\text{-CpPd}(\eta^1\text{-1-Ph-C}_3\text{H}_4)(\text{PPh}_3)$  in toluene- $\text{d}_8$

Structure	Assignment
	<p>H(1): <math>\delta</math> 5.66 (d; <math>^3J_{\text{HH}}</math> 15.6 Hz)</p> <p>H(2): <math>\delta</math> 6.59 (dt; <math>^3J_{\text{HH}}</math> 15.6, 8.8 Hz)</p> <p>H(3): <math>\delta</math> 2.66 (dd; <math>^3J_{\text{HH}}</math> 8.8; <math>^3J_{\text{PH}}</math> 5.6 Hz)</p> <p>H(Cp): <math>\delta</math> 5.77 (d; <math>^3J_{\text{PH}}</math> 1.2 Hz)</p> <p><math>^{31}\text{P}</math>: <math>\delta</math> 45.7</p>

The same  $^1\text{H}$  NMR spectrum could not be used to identify the AB quartets due to a significant amount of overlap between the reductive elimination products and the allyl protons of the dinuclear species. A separate sample was prepared by reacting  $\text{Pd}(\eta^5\text{-C}_5\text{H}_5)(\eta^3\text{-1-Ph-C}_3\text{H}_4)$  with one equivalent  $\text{PPh}_3$  in hexanes. This led to the precipitation of the dinuclear species, and therefore the creation of a sample containing a reduced amount of the reductive elimination products. The  $^1\text{H}$  and  $^{31}\text{P}$  assignments can be found in Table 10.

**Table 8.  $^1\text{H}$  and  $^{31}\text{P}$  NMR chemical shifts of  $\text{Pd}_2(\text{PPh}_3)_2(\mu\text{-C}_5\text{H}_5)(\mu\text{-1-Ph-C}_3\text{H}_4)$  in toluene- $d_8$**

Structure	Assignment
 <p style="text-align: center;">Syn-dinuclear</p>	<p>H(1): <math>\delta</math> 3.16 (dd; <math>^3J_{\text{HH}}</math> 9.8 Hz; <math>J_{\text{PH}}</math> 7.7 Hz)</p> <p>H(2): <math>\delta</math> 3.41 (dddd; <math>^3J_{\text{HH}}</math> 13.6 Hz, 9.8 Hz, 7.4 Hz; <math>^3J_{\text{PH}}</math> 2.9 Hz)</p> <p>H(3s): <math>\delta</math> 2.98 (dd; <math>^3J_{\text{HH}}</math> 7.4 Hz; <math>^3J_{\text{PH}}</math> 12.7 Hz)</p> <p>H(3a): <math>\delta</math> 1.04 (dd; <math>^3J_{\text{HH}}</math> 13.6 Hz; <math>^3J_{\text{PH}}</math> 1.6 Hz)</p> <p>H(Cp): <math>\delta</math> 5.62 (t; <math>^3J_{\text{PH}}</math> 1.5 Hz)</p> <p><math>^{31}\text{P}</math>: <math>\delta</math> 24.5 (d, 95 Hz), 26.2 (d, 95 Hz)</p>
 <p style="text-align: center;">Anti-dinuclear</p>	<p>H(1): <math>\delta</math> 4.15 (dd; <math>^3J_{\text{HH}}</math> 8.2 Hz; <math>J_{\text{PH}}</math> 12.2 Hz)</p> <p>H(2): <math>\delta</math> 3.72 (dddd; <math>^3J_{\text{HH}}</math> 12.5 Hz, 8.9 Hz, 8.2 Hz; <math>J_{\text{PH}}</math> 3.1 Hz)</p> <p>H(3s): <math>\delta</math> 1.74 (ddd; <math>^2J_{\text{HH}}</math> 2.4 Hz; <math>^3J_{\text{HH}}</math> 8.9 Hz; <math>J_{\text{PH}}</math> 11.0 Hz)</p> <p>H(3a): <math>\delta</math> 1.64 (ddd; <math>^2J_{\text{HH}}</math> 2.4 Hz; <math>^3J_{\text{HH}}</math> 12.5 Hz; <math>J_{\text{PH}}</math> 4.2 Hz)</p> <p>H(Cp): <math>\delta</math> 5.93 (t; <math>J_{\text{PH}}</math> 1.8 Hz)</p> <p><math>^{31}\text{P}</math>: <math>\delta</math> 23.0 (d, 139 Hz), 26.8 (d, 139 Hz)</p>

The first step in the assignment was to identify all allyl resonances for each dinuclear species. The unique splitting pattern of the H(2) protons made them easy to distinguish in the  $^1\text{H}$  NMR spectrum (Figure 32), and therefore the assignment began by using a COSY spectrum (Figure 33) to correlate the H(2) protons to the rest of the allyl resonances within the species. Integration allowed the Cp resonances and the AB quartets of the  $^{31}\text{P}$  NMR to be assigned to each

set of allyl resonances. Determination of the *syn* and *anti* orientation was based on  ${}^3J_{\text{H}_1\text{H}_2}$ , with  $J_{\text{HH}}$  couplings being distinguished from  $J_{\text{PH}}$  couplings using  ${}^1\text{H}\{{}^{31}\text{P}\}$  NMR. In the *syn* isomer, this is a *trans* coupling of 9.8 Hz versus the *cis* coupling of 8.2 Hz in the *anti* isomer. While the difference is not considerable, the assignments were supported by NOESY, which showed a spatial interaction between H(1) and H(2) for the *anti* isomer. Also, Werner's studies on other dinuclear species found smaller  $J_{\text{PH}}$  couplings for *anti* protons and larger  $J_{\text{PH}}$  couplings for *syn* protons.<sup>41d</sup> H(1) is in the *anti* position in the *syn* dinuclear species and has the smaller  $J_{\text{PH}}$  coupling of 7.7 Hz, as compared to H(1) in the *syn* position in the *anti* dinuclear species with the larger  $J_{\text{PH}}$  coupling of 12.2 Hz. Based on these assignments and the unequal amounts of the two species in the sample, the AB quartet with the smaller of the two couplings ( $J$  95 Hz) was identified as the *syn* isomer and the AB quartet with the larger coupling ( $J$  139 Hz) was identified as the *anti* isomer.



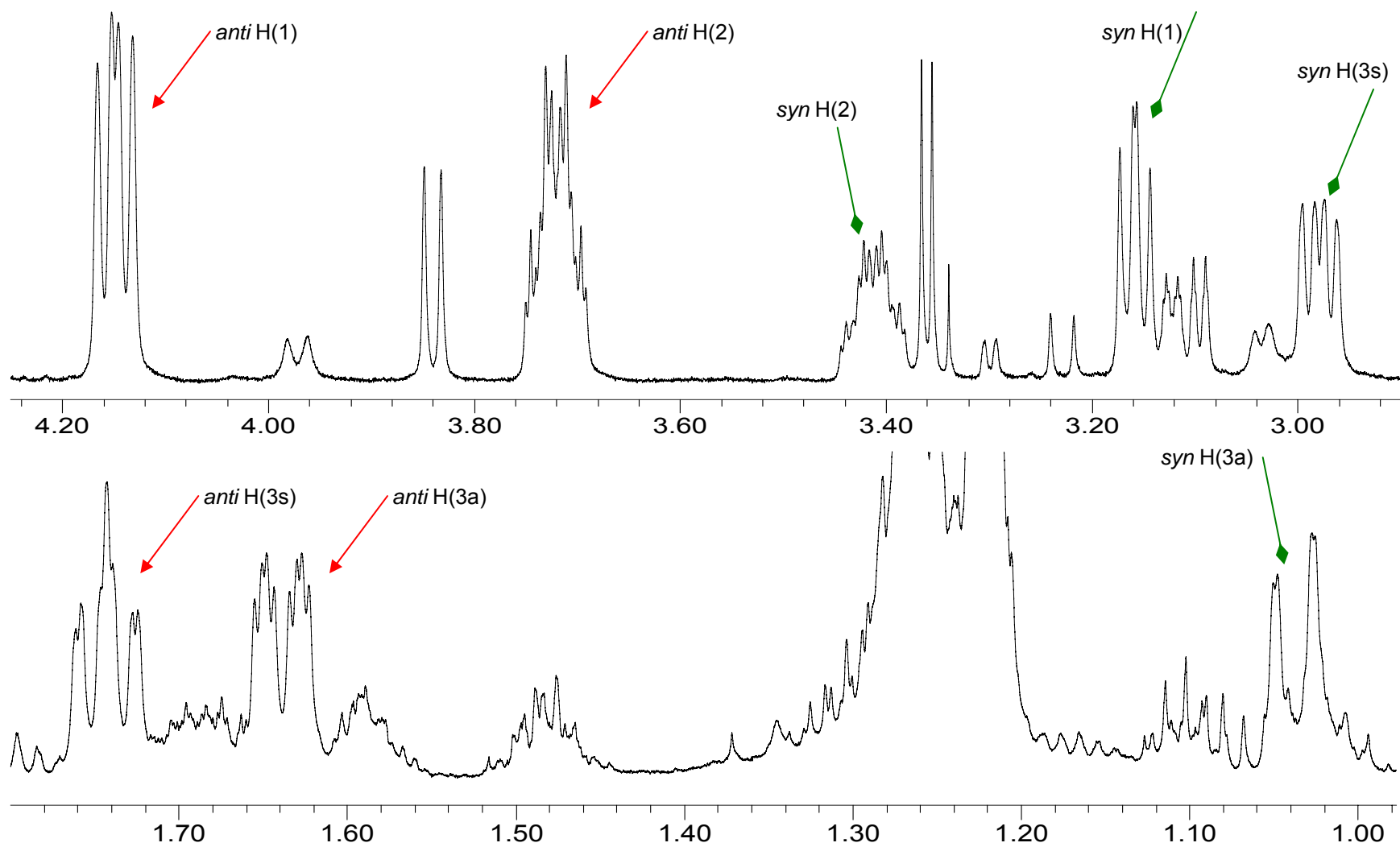


Figure 32.  $^1\text{H}$  NMR spectra (600 MHz,  $\text{C}_7\text{D}_8$ ) of the allyl region of a crude sample of  $\text{Pd}_2(\text{PPh}_3)_2(\mu\text{-C}_5\text{H}_5)(\mu\text{-1-Ph-C}_3\text{H}_4)$

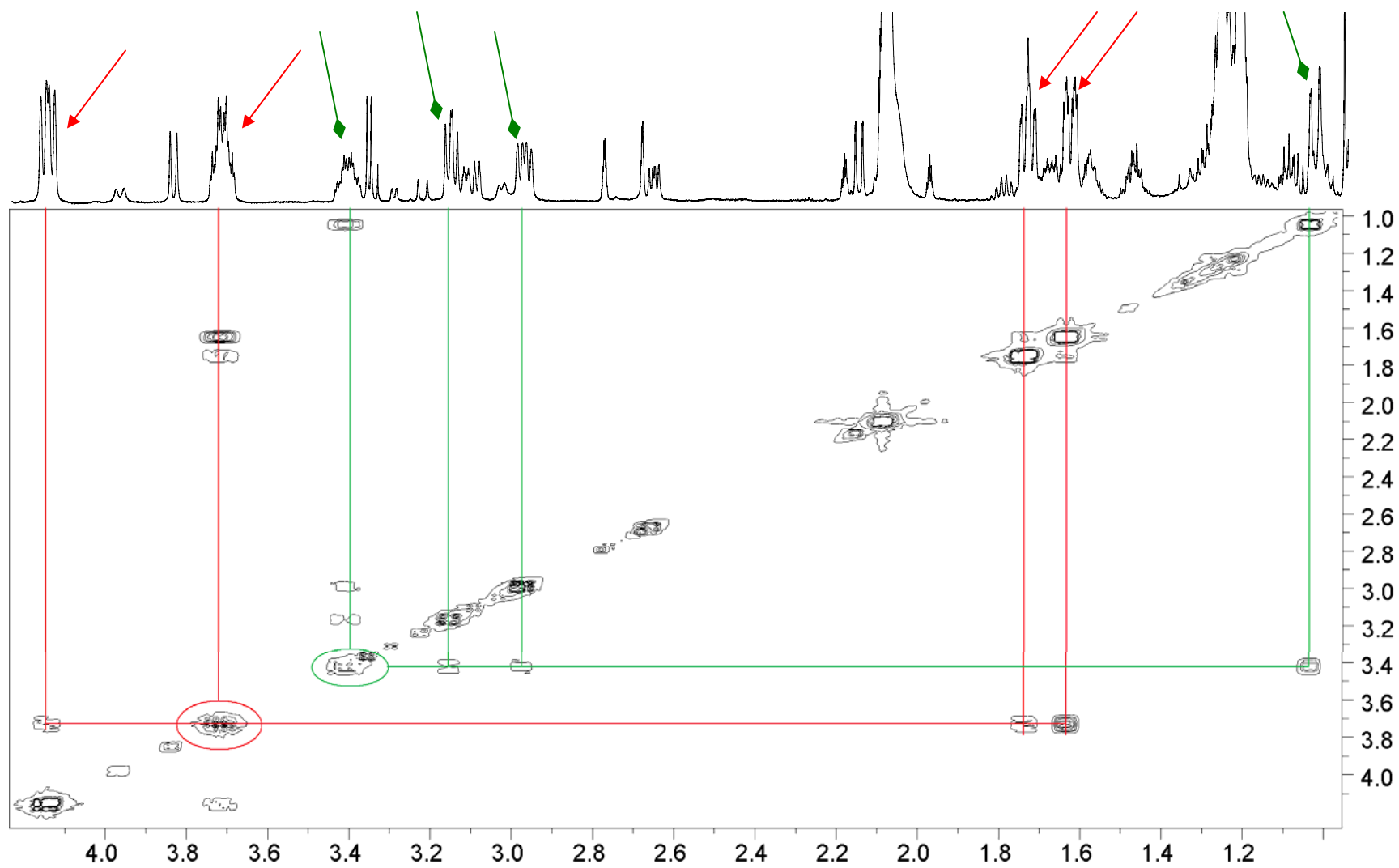


Figure 33. COSY spectrum (600 MHz,  $\text{tol-d}_8$ ) of the allyl region of a crude sample of  $\text{Pd}_2(\text{PPh}_3)_2(\mu\text{-C}_5\text{H}_5)(\mu\text{-1-Ph-C}_3\text{H}_4)$

For the sample generated by reacting two equivalents  $\text{PPh}_3$  with  $\text{Pd}(\eta^5\text{-C}_5\text{H}_5)(\eta^3\text{-1-Ph-C}_3\text{H}_4)$  at 25 °C, the resonances of the  $\sigma$ -allyl and *syn* dinuclear species disappeared within 3 and 24 h, respectively, while the resonances associated with the *anti* isomer increased in intensity relative to  $\text{Pd}(\text{PPh}_3)$ . Complete  $\text{Pd}(\text{PPh}_3)_3$  formation did not occur within 24 h at this temperature, as the *anti*-dinuclear species was still present beyond that time.

All three intermediates had formed by 5 min when  $\text{Pd}(\eta^5\text{-C}_5\text{H}_5)(\eta^3\text{-1-Ph-C}_3\text{H}_4)$  was reacted with two equivalents  $\text{PPh}_3$  at 50 °C. The rate of the reaction was elevated and the resonances associated with the  $\sigma$ -allyl and *syn*-dinuclear species dropped out of the NMR spectra by 30 min and 1 h, respectively. Unlike at 25 °C, the *anti*-dinuclear species dropped out sometime after 5 h, but before 20 h, to yield only  $\text{Pd}(\text{PPh}_3)_3$  ( $^{31}\text{P}$   $\delta$  23.7).

At 75 °C, the  $\sigma$ -allyl and *syn*-dinuclear species were not present in solution at 5 min, the time of the first NMR experiments. A small amount of the *anti*-dinuclear species was identifiable at this time, but  $\text{Pd}(\text{PPh}_3)_3$  ( $^{31}\text{P}$   $\delta$  23.7) was the major species present after 30 min.

During the course of the experiments, Pd metal was seen to precipitate from the 2:1 solutions when the samples were heated. This was attributed to a deficiency of ligand, as once all the available  $\text{PPh}_3$  had coordinated to form  $\text{Pd}(\text{PPh}_3)_3$ , heating forced the remaining  $\text{Pd}(\eta^5\text{-C}_5\text{H}_5)(\eta^3\text{-1-Ph-C}_3\text{H}_4)$  to reductively eliminate  $\text{C}_{14}\text{H}_{14}$  and produce Pd metal. Precedents for this is set by the  $\text{Pd}(\eta^5\text{-C}_5\text{H}_5)(\eta^3\text{-C}_3\text{H}_5)$  system for which the reductive elimination of  $\text{C}_8\text{H}_{10}$  is

observed in the absence of ligand.<sup>48</sup> Experiments were therefore also performed using three equivalents of PPh<sub>3</sub>. After 10 min at 25 °C, the major species was Pd(PPh<sub>3</sub>)<sub>3</sub>, identified by a broad singlet at  $\delta$  22.8 in the <sup>31</sup>P NMR spectrum. Small amounts of the  $\sigma$ -allyl species were also identifiable in the <sup>1</sup>H and <sup>31</sup>P NMR spectra, but these disappeared within 90 min to yield only Pd(PPh<sub>3</sub>)<sub>3</sub>. Neither dinuclear species were ever identified in the NMR spectra nor was Pd metal formed in the reaction.

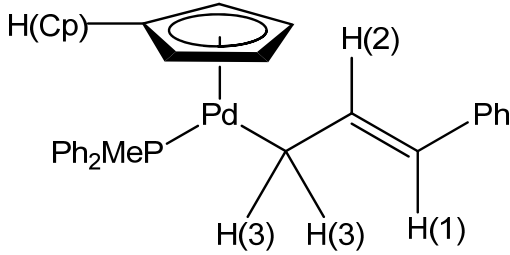
It was thought that the broad singlets assigned to Pd(PPh<sub>3</sub>)<sub>3</sub> might be time-averaged signals corresponding to equilibria between Pd(PPh<sub>3</sub>)<sub>n</sub> (n = 2, 3, 4) species; therefore, a 3:1 sample was analyzed at -80 °C in an attempt to slow the exchange. While the <sup>31</sup>P NMR spectrum at 25 °C showed only a single resonance at  $\delta$  22.8, this shifted downfield to  $\delta$  24.1 at -80 °C, remaining broad. If this exchange was still occurring, it remained too fast on the NMR time scale, even at -80 °C, for separate species to be identified.

#### 3.1.2.4 L = PMePh<sub>2</sub>

The reaction of two equivalents PMePh<sub>2</sub> with Pd( $\eta$ -C<sub>5</sub>H<sub>5</sub>)( $\eta^3$ -1-Ph-C<sub>3</sub>H<sub>4</sub>) was very similar to the PPh<sub>3</sub> system. After 8 min at 25 °C, the <sup>1</sup>H NMR spectrum showed that the Pd( $\eta$ -C<sub>5</sub>H<sub>5</sub>)( $\eta^3$ -1-Ph-C<sub>3</sub>H<sub>4</sub>) starting material had fully reacted and three new Cp resonances had appeared at  $\delta$  5.62, 5.72 and 5.85. A <sup>1</sup>H NMR spectrum taken at -70 °C allowed the Cp resonance at  $\delta$  5.72 to be assigned to the  $\sigma$ -allyl intermediate. The <sup>1</sup>H resonances (Table 9) of this species were assigned in the same manner as in 3.1.2.1. Monitoring corresponding changes

in the  $^1\text{H}$  and  $^{31}\text{P}$  (Figure 34) NMR spectra, allowed the singlet at  $\delta$  26.2 in the  $^{31}\text{P}$  NMR to be assigned to the  $\sigma$ -allyl intermediate.

**Table 9.**  $^1\text{H}$  and  $^{31}\text{P}$  NMR chemical shifts of  $\eta^5\text{-CpPd}(\eta^1\text{-1-Ph-C}_3\text{H}_4)(\text{PMePh}_2)$  in toluene- $d_8$

Structure	Assignment
	H(1): $\delta$ 5.63 (d; $^3J_{\text{HH}}$ 15.5 Hz)
	H(2): $\delta$ 6.70 (dt; $^3J_{\text{HH}}$ 15.5, 8.5 Hz)
	H(3): $\delta$ 2.61 (dd; $^3J_{\text{HH}}$ 8.5; $^3J_{\text{PH}}$ 5.7 Hz)
	H(Cp): $\delta$ 5.81 (s)
	H(Me): $\delta$ 1.55 (d; $^3J_{\text{PH}}$ 9.1 Hz)
	$^{31}\text{P}$ : $\delta$ 26.2

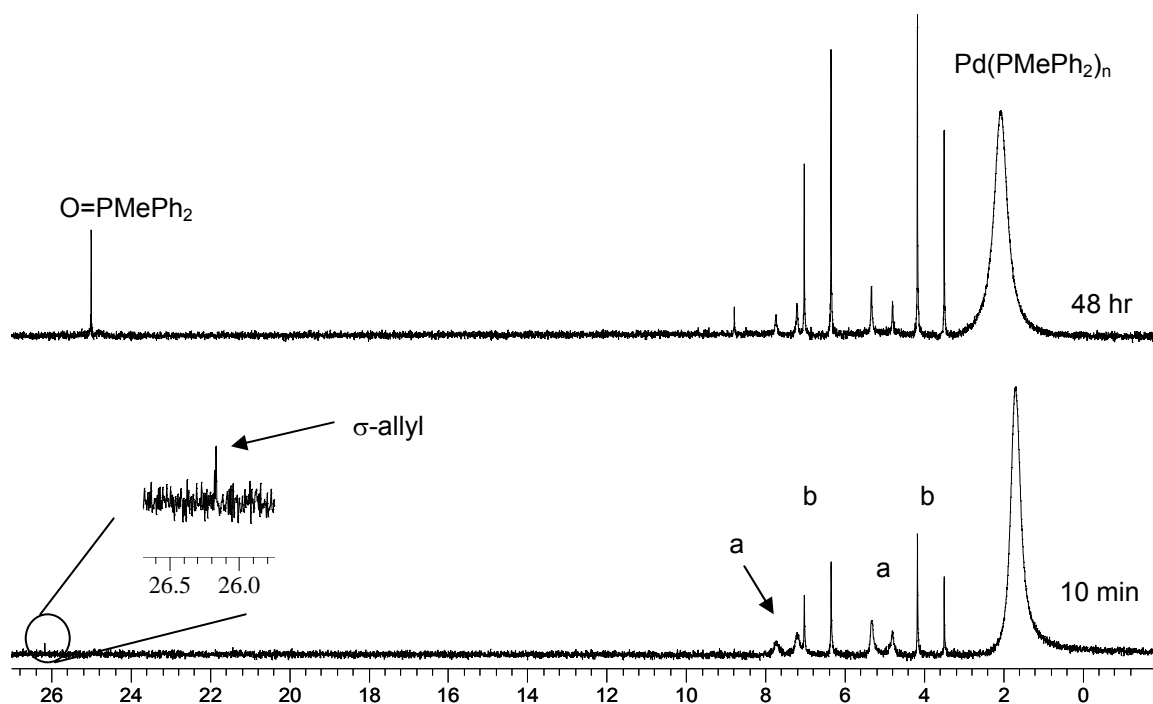


**Figure 34.** Stacked plots of  $^{31}\text{P}$  NMR spectrum (202.3 MHz) of reaction of  $\text{Pd}(\eta^5\text{-C}_5\text{H}_5)(\eta^3\text{-1-Ph-C}_3\text{H}_4)$  with two equivalents  $\text{PMePh}_2$  at  $25^\circ\text{C}$

The  $^{31}\text{P}$  NMR spectrum (Figure 34) taken after 10 min also showed two AB quartets at  $\delta$  5.1 and 7.4 ( $J_{\text{PP}}$  107 Hz, labeled a) and  $\delta$  3.9 and 6.6 ( $J_{\text{PP}}$  136 Hz, labeled b). Attempts to assign these resonances to their respective dinuclear species were unsuccessful; however, the Cp resonances at  $\delta$  5.62 and 5.85 could be attributed to the species giving rise to the AB quartets with  $J_{\text{PP}} = 107$  Hz and  $J_{\text{PP}} = 136$  Hz, respectively. As was seen in the  $\text{PPh}_3$  system, the resonances of the species with the smaller coupling were initially of greater intensity and the resonances of the species with the larger coupling persisted longer in solution. Therefore, it was believed that the *syn* isomer was associated with the smaller coupling and the *anti* isomer was associated with the larger coupling, although this could not be confirmed.

The major  $^{31}\text{P}$  resonance after 10 min at 25 °C was a broad singlet at  $\delta$  1.8, assigned to " $\text{Pd}(\text{PMePh}_2)_n$ ".<sup>47a</sup> The resonances of the  $\sigma$ -allyl species disappeared from the NMR spectra by 25 min; however, both dinuclear species remained past 48 h at 25 °C. At this time, the singlet assigned to  $\text{Pd}(\text{PMePh}_2)_n$  had broadened and shifted slightly downfield to  $\delta$  2.1. According to the literature, the only stable Pd(0) species of  $\text{PMePh}_2$  is  $\text{Pd}(\text{PMePh}_2)_4$ , with a resonance at  $\delta$  -4.2.<sup>47a</sup> This discrepancy was believed to be due to exchange with other species present in the solution, a hypothesis supported by the broadness of the resonance, as well as the broad Me singlet at  $\delta$  1.64 in the  $^1\text{H}$  NMR spectrum.

For a similar reaction at 50 °C, the  $^1\text{H}$  NMR spectra showed the Cp resonances of both dinuclear species up to 90 min; however, only the dinuclear

species with the larger coupling could be clearly identified in the  $^{31}\text{P}$  NMR spectra. Both dinuclear species dropped out of the NMR spectra within 24 h to yield only a broad resonance associated with  $\text{Pd}(\text{PMePh}_2)_n$  at  $\delta$  1.7.

At 75 °C, the  $^1\text{H}$  NMR spectrum contained Cp resonances corresponding to both dinuclear species at 7 min, but again only the dinuclear species with the larger coupling could be identified in the  $^{31}\text{P}$  NMR spectrum. By 30 min, both species had dropped out of the NMR spectra, yielding only a broad  $^{31}\text{P}$  resonance at  $\delta$  2.2 associated with  $\text{Pd}(\text{PMePh}_2)_n$ .

As was seen in the  $\text{PPh}_3$  systems, Pd metal precipitated out of solution during the investigation of the 2:1  $\text{PMePh}_2$  systems at elevated temperatures, and therefore a reaction with three equivalents of ligand was investigated. After 10 min at 25 °C, the only major species appearing in either the  $^1\text{H}$  or  $^{31}\text{P}$  NMR was  $\text{Pd}(\text{PMePh}_2)_n$ . The Me resonance for this species was a broad singlet at  $\delta$  1.61 in  $^1\text{H}$  NMR spectrum. The broad  $^{31}\text{P}$  NMR resonance for this species was  $\delta$  -1.8, which is downfield from the resonance produced from two equivalents of ligand and upfield from the literature reported resonance for  $\text{Pd}(\text{PMePh}_2)_4$ .

Due to the broadness of the  $\text{Pd}(\text{PMePh}_2)_n$  resonances, low temperature NMR experiments were run in an attempt to characterize an exchange between  $\text{Pd}(\text{PMePh}_2)_n$  ( $n = 2, 3, 4$ ) species. While the  $^{31}\text{P}$  resonances of the 2:1 and 3:1 systems differed at 25 °C, spectra (Figure 35) at -80 °C revealed the same resonances in both systems. A large number of unidentified minor resonances occurred in the range of  $\delta$  4.9-9.0, with the amounts relative to the main

resonance at  $\delta -1.3$  being greater in the 2:1 system. The major  $\text{Pd}(\text{PMePh}_2)_n$  resonance still did not correspond to the literature reported value of  $\delta -4.2$ , suggesting that a lower ligated Pd species was formed.

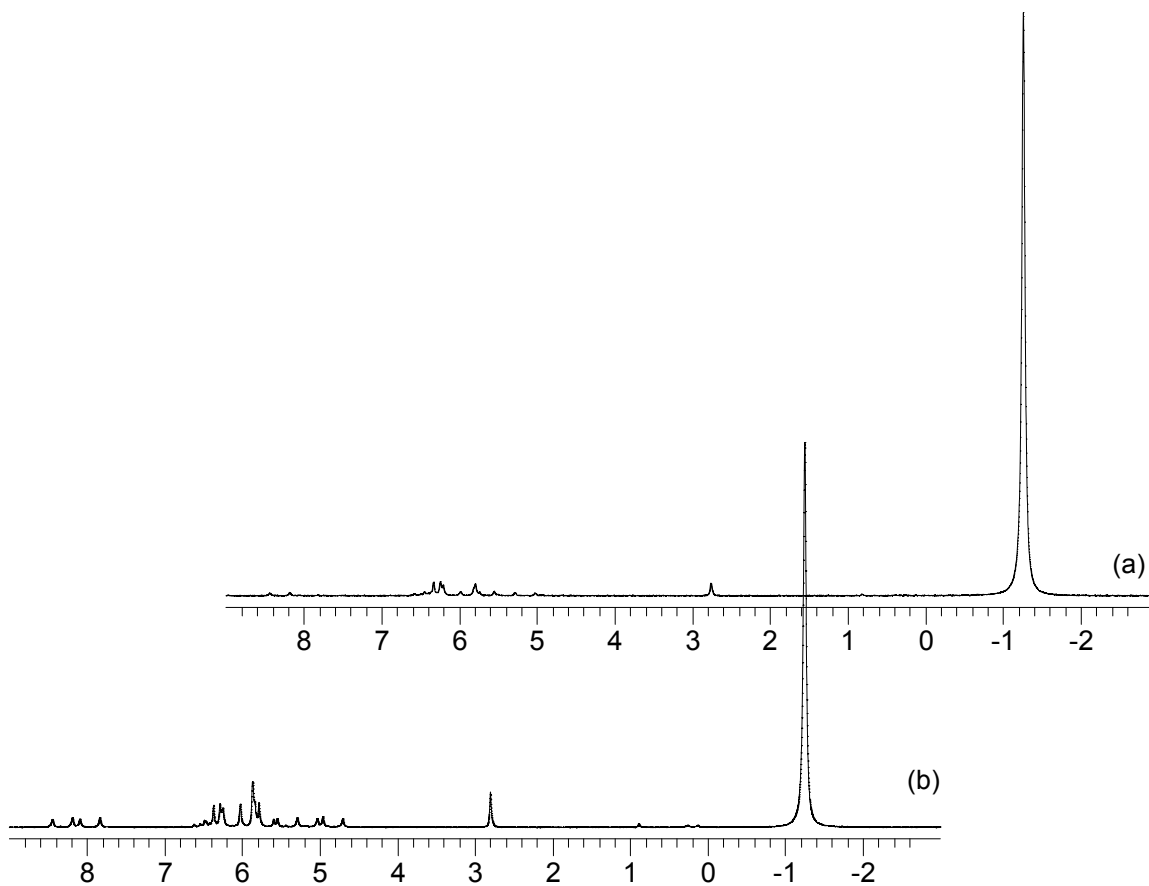


**Figure 35. Stacked  $^{31}\text{P}$  NMR (202.5 MHz,  $\text{tol-d}_8$ ) spectra of (a) the 3:1 and (b) the 2:1  $\text{PMePh}_2$  systems at  $-80^\circ\text{C}$**

### 3.1.2.5 L = $\text{PCy}_3$

At  $25^\circ\text{C}$ , a reaction of  $\text{Pd}(\eta\text{-C}_5\text{H}_5)(\eta^3\text{-1-Ph-C}_3\text{H}_4)$  with two equivalents of  $\text{PCy}_3$  was considerably slower than both the  $\text{PPh}_3$  and  $\text{PMePh}_2$  systems.  $^1\text{H}$



(Figure 36) and  $^{31}\text{P}$  NMR spectra revealed the  $\sigma$ -allyl species to be the only intermediate for over 12 h. The  $^1\text{H}$  resonances (Table 10) for this intermediate were assigned as described in 3.1.2.1.

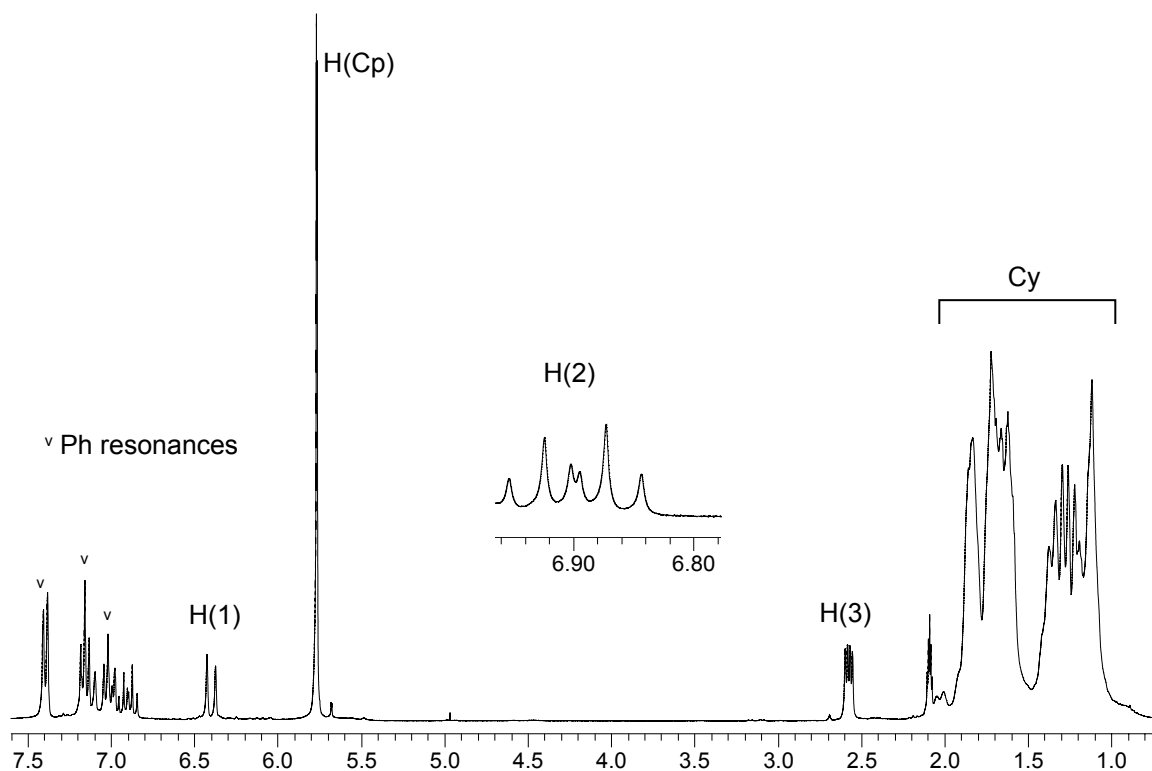


**Figure 36.**  $^1\text{H}$  NMR spectrum (300 MHz,  $\text{tol-d}_8$ ) of the  $\sigma$ -allyl species, produced in the reaction of  $\text{Pd}(\eta^5\text{-C}_5\text{H}_5)(\eta^3\text{-1-Ph-C}_3\text{H}_4)$  with two equivalents  $\text{PCy}_3$  at 25 °C (3 h after mixing)

**Table 10.**  $^1\text{H}$  and  $^{31}\text{P}$  NMR chemical shifts of  $\eta^5\text{-CpPd}(\eta^1\text{-1-Ph-C}_3\text{H}_4)(\text{PCy}_3)$  in toluene- $d_8$

Structure	Assignment
	H(1): $\delta$ 6.40 (d; $^3J_{\text{HH}}$ 15.4 Hz)
	H(2): $\delta$ 6.90 (dt; $^3J_{\text{HH}}$ 15.4, 8.8 Hz)
	H(3): $\delta$ 2.58 (dd; $^3J_{\text{HH}}$ 8.8, $^3J_{\text{PH}}$ 4.4 Hz)
	H(Cp): $\delta$ 5.77 (d; $^3J_{\text{PH}}$ 1.3 Hz)
	Ph: $\delta$ 7.02 (t; $^3J_{\text{HH}}$ 7.3 Hz, <i>p</i> ); 7.12 (t; $^3J_{\text{HH}}$ 7.3 Hz, <i>m</i> ); 7.39 (d; $^3J_{\text{HH}}$ 7.3 Hz, <i>o</i> )
	$^{31}\text{P}$ : $\delta$ 55.8

After 36 h at 25 °C, the  $\sigma$ -allyl species was still present in the system; however, the  $^{31}\text{P}$  NMR spectrum showed minor resonances corresponding to both dinuclear species ( $\delta$  27.1 and 33.4 ( $J$  107 Hz);  $\delta$  22.4 and 27.0 ( $J$  126 Hz)) and the major resonance, a broad singlet at  $\delta$  40, corresponding to  $\text{Pd}(\text{PCy}_3)_2$  (lit.  $\delta$  39.2).<sup>40</sup> The  $^1\text{H}$  resonances of the dinuclear species could not be assigned due to the presence of reductive elimination products and Cy resonances obscuring the  $^1\text{H}$  NMR.

At 50 °C, the  $^{31}\text{P}$  NMR spectrum after 1 h showed resonances attributed to the  $\sigma$ -allyl and both dinuclear intermediates, as well  $\text{Pd}(\text{PCy}_3)_2$ . The resonances associated with  $\sigma$ -allyl and dinuclear species disappeared from the NMR by 3 h and 14 h, respectively, yielding only a sharp  $^{31}\text{P}$  resonance at  $\delta$  40.2 assigned to  $\text{Pd}(\text{PCy}_3)_2$ .

After 8 minutes at 75 °C, the  $^{31}\text{P}$  NMR spectrum revealed the presence of  $\text{Pd}(\text{PCy}_3)_2$  and one dinuclear species ( $J$  126 Hz). This dinuclear species

remained for approximately 1 h, at which point the sharp  $^{31}\text{P}$  resonance of  $\text{Pd}(\text{PCy}_3)_2$  was the only resonance remaining in the  $^{31}\text{P}$  NMR spectrum.

### 3.1.3 Reactions of $\text{Pd}(\eta^5\text{-C}_5\text{H}_5)(\eta^3\text{-1-Ph-C}_3\text{H}_4)$ with Bidentate Phosphines

While the reactions of  $\text{Pd}(\eta^5\text{-C}_5\text{H}_5)(\eta^3\text{-R-C}_3\text{H}_4)$  type compounds with monodentate phosphine ligands to form  $\text{Pd}(0)\text{L}_n$  species have been well studied, the same cannot be said of the reactions with bidentate ligands. Experiments were therefore carried out using both one and two equivalents of ligand ( $\text{L} = \text{dppe}, \text{dppp}, \text{dppf}$ ). Typical 1:1 experiments involved combining toluene- $\text{d}_8$  solutions of  $\text{Pd}(\eta^5\text{-C}_5\text{H}_5)(\eta^3\text{-1-Ph-C}_3\text{H}_4)$  ( $3.4 \times 10^{-5}$  mol) and  $\text{L}$  ( $3.4 \times 10^{-5}$  mol), and monitoring the reactions by  $^1\text{H}$  and  $^{31}\text{P}$  NMR spectroscopy at either 25, 50 or 75 °C. For 2:1 experiments,  $5.4 \times 10^{-5}$  mol  $\text{L}$  was combined with  $2.7 \times 10^{-5}$  mol  $\text{Pd}(\eta^5\text{-C}_5\text{H}_5)(\eta^3\text{-1-Ph-C}_3\text{H}_4)$  in toluene- $\text{d}_8$ .

The reactions of  $\text{Pd}(\eta^5\text{-C}_5\text{H}_5)(\eta^3\text{-1-Ph-C}_3\text{H}_4)$  with one equivalent of bidentate ligand at 25-75 °C often produced an array of new singlets in the region of  $\delta$  5.3-6.0, thought to be new Cp resonances, in the  $^1\text{H}$  NMR spectra with no corresponding resonances in the  $^{31}\text{P}$  NMR spectra. These intermediates could not be identified in the  $^1\text{H}$  NMR spectra due to the considerable amount of overlap with other intermediates and reductive elimination products. The same reactions with two equivalents of ligand were also uninformative, as the reactions were generally completed by the time the NMR spectra were run. Therefore, the focus was placed solely on determining the minimum time at a reasonable

temperature to quantitatively produce Pd(0)L<sub>n</sub> compounds. The reaction times presented in Table 11 represent the time at which all Cp resonances disappeared from the <sup>1</sup>H NMR spectra.

**Table 11. Timelines for the formation of Pd(0)L<sub>2</sub> from bidentate phosphines L**

L	L: Pd	Time (T) to complete conversion to Pd(0) products <sup>a</sup>		
		25 °C	50 °C	75 °C
dppe	1:1	> 4 days	> 24 h	3 h
dppe	2:1	< 5 min	NI	NI
dppp	1:1	90 min	< 15 min	< 10 min
dppp	2:1	< 5 min	NI	< 5 min
dppf	1:1	> 24 h	NI	> 24 h
dppf	2:1	> 1 h	NI	< 1 h

a. NI = not investigated

For both the dppe and dppp systems, sharp singlets at  $\delta$  32.1 and 4.8, respectively, were the only significant resonances that appeared in the <sup>31</sup>P NMR spectra regardless of time, temperature or number of equivalents of ligand. These resonances correspond well to the literature resonances of Pd(dppe)<sub>2</sub> and Pd(dppp)<sub>2</sub> ( $\delta$  30.4 and 4.0,<sup>47b</sup> respectively, in THF-d<sub>8</sub>). In the 1:1 systems, a number of minor, unidentified resonances appeared in the <sup>31</sup>P NMR spectra, which did not appear in the spectra of the 2:1 systems.

The dppf system presented several difficulties in that the NMR instruments could not be shimmed to the samples, most likely due to the existence of paramagnetic species present in solution. Because of this, the <sup>1</sup>H NMR spectra

provided no valuable information and therefore  $^{31}\text{P}$  NMR spectra were solely used to monitor the reaction. For the 1:1 system, none of the resonances in the  $^{31}\text{P}$  NMR spectra could be identified. The 2:1 system, however, produced a singlet at  $\delta$  8.1 after 1 h at 75 °C; this corresponds to  $\text{Pd}(\text{dppf})_2$  (lit.  $\delta$  7.4 in  $\text{THF-d}_8$ ).<sup>47b</sup>

$\text{Pd}$  metal precipitated from all 1:1 systems, but none of the 2:1 systems, believed to be due to a deficiency of ligand.

### 3.1.4 Comparison of the Reactivities of $\text{Pd}(\eta^5\text{-C}_5\text{H}_5)(\eta^3\text{-1-Ph-C}_3\text{H}_4)$ and $\text{Pd}(\eta^5\text{-C}_5\text{H}_5)(\eta^3\text{-C}_3\text{H}_5)$ with Monodentate Phosphines

As  $\text{Pd}(\eta^5\text{-C}_5\text{H}_5)(\eta^3\text{-1-Ph-C}_3\text{H}_4)$  is a useful precursor for the synthesis of  $\text{Pd}(0)\text{L}_n$  and has been found to be easier to handle than  $\text{Pd}(\eta^5\text{-C}_5\text{H}_5)(\eta^3\text{-C}_3\text{H}_5)$ , the reactivities of the two compounds were directly compared by examining their timelines to quantitative  $\text{PdL}_n$  formation for  $\text{L} = \text{PPh}_3$ ,  $\text{PCy}_3$ ,  $\text{PMeBu}^t_2$  and  $\text{PBU}^t_3$ . The reaction conditions (concentration, solvent, temperature) used in 3.1.2 to investigate  $\text{Pd}(\eta^5\text{-C}_5\text{H}_5)(\eta^3\text{-1-Ph-C}_3\text{H}_4)$  were identical to those employed in the thesis of E. A. Mitchell to investigate  $\text{Pd}(\eta^5\text{-C}_5\text{H}_5)(\eta^3\text{-C}_3\text{H}_5)$ .<sup>44</sup>  $\text{Pd}(\eta^5\text{-C}_5\text{H}_5)(\eta^3\text{-1-Ph-C}_3\text{H}_4)$  and  $\text{Pd}(\eta^5\text{-C}_5\text{H}_5)(\eta^3\text{-C}_3\text{H}_5)$  reacted at comparable rates with  $\text{PCy}_3$  and  $\text{PBU}^t_3$ , forming  $\text{Pd}(\text{PCy}_3)_2$  and  $\text{Pd}(\text{PBU}^t_3)_2$  within 1 h at 75 °C, while  $\text{Pd}(\eta^5\text{-C}_5\text{H}_5)(\eta^3\text{-1-Ph-C}_3\text{H}_4)$  reacted with  $\text{PPh}_3$  to form  $\text{Pd}(\text{PPh}_3)_3$  in 30 min, about twice as fast as  $\text{Pd}(\eta^5\text{-C}_5\text{H}_5)(\eta^3\text{-C}_3\text{H}_5)$  at 75 °C.  $\text{Pd}(\eta^5\text{-C}_5\text{H}_5)(\eta^3\text{-1-Ph-C}_3\text{H}_4)$  reacted

with  $\text{PMeBu}_2^t$  to form  $\text{Pd}(\text{PMeBu}_2^t)_2$  within 45 min at 50 °C while  $\text{Pd}(\eta^5\text{-C}_5\text{H}_5)(\eta^3\text{-C}_3\text{H}_5)$  required 1 h at 75 °C. Thus  $\text{Pd}(\eta^5\text{-C}_5\text{H}_5)(\eta^3\text{-1-Ph-C}_3\text{H}_4)$  was generally of comparable or greater reactivity than was  $\text{Pd}(\eta^5\text{-C}_5\text{H}_5)(\eta^3\text{-C}_3\text{H}_5)$ .

In an attempt to rationalize the relatively high reactivity of  $\text{Pd}(\eta^5\text{-C}_5\text{H}_5)(\eta^3\text{-1-Ph-C}_3\text{H}_4)$ , the crystal structure was compared to that of  $\text{Pd}(\eta^5\text{-C}_5\text{H}_5)(\eta^3\text{-C}_3\text{H}_5)$ .<sup>49</sup>  $\text{Pd}(\eta^5\text{-C}_5\text{H}_5)(\eta^3\text{-1-Ph-C}_3\text{H}_4)$  exhibits longer Pd-allyl bonds (Pd-C(6) 2.123(3) Å, Pd-C(7) 2.072(3) Å, Pd-C(8) 2.174(3) Å) than has been reported for  $\text{Pd}(\eta^5\text{-C}_5\text{H}_5)(\eta^3\text{-C}_3\text{H}_5)$  (Pd-C(6) 2.07, Pd-C(7) 2.04 Å, Pd-C(8) 2.13 Å), suggesting weaker Pd-allyl bonding in the more reactive  $\text{Pd}(\eta^5\text{-C}_5\text{H}_5)(\eta^3\text{-1-Ph-C}_3\text{H}_4)$ . The data for  $\text{Pd}(\eta^5\text{-C}_5\text{H}_5)(\eta^3\text{-C}_3\text{H}_5)$  were published in 1968 without standard deviations, meaning the differences may not be significant. Possibly more important is the asymmetry in the Pd-allyl bonding in  $\text{Pd}(\eta^5\text{-C}_5\text{H}_5)(\eta^3\text{-1-Ph-C}_3\text{H}_4)$ , with Pd-C(8) being significantly longer than Pd-C(6) such that the metal may be less sterically hindered at one end and hence more susceptible to attack by a phosphine to give a  $\sigma$ -allyl intermediate.

This hypothesis was tested by determining whether  $\text{Pd}(\eta^5\text{-C}_5\text{H}_5)(\eta^3\text{-C}_3\text{H}_5)$  or  $\text{Pd}(\eta^5\text{-C}_5\text{H}_5)(\eta^3\text{-1-Ph-C}_3\text{H}_4)$  was consumed first in the reaction with one equivalent of  $\text{PPh}_3$  under identical conditions. Were the hypothesis correct, complete consumption of  $\text{Pd}(\eta^5\text{-C}_5\text{H}_5)(\eta^3\text{-1-Ph-C}_3\text{H}_4)$  prior to complete consumption of  $\text{Pd}(\eta^5\text{-C}_5\text{H}_5)(\eta^3\text{-C}_3\text{H}_5)$  would be expected. This however was not

the case, as unreacted  $\text{Pd}(\eta^5\text{-C}_5\text{H}_5)(\eta^3\text{-1-Ph-C}_3\text{H}_4)$  lingered in solution for hours as compared to  $\text{Pd}(\eta^5\text{-C}_5\text{H}_5)(\eta^3\text{-C}_3\text{H}_5)$  which reacted within minutes under the same conditions to form the  $\sigma$ -allyl intermediate.

As illustrated in the previous sections, the identities and stabilities of the intermediates formed vary, depending on the phosphine employed, suggesting that the reactions are very complicated. A rationale for the relatively high reactivity of  $\text{Pd}(\eta^5\text{-C}_5\text{H}_5)(\eta^3\text{-1-Ph-C}_3\text{H}_4)$  is therefore not offered as it is likely dependent on the phosphine and the reaction conditions utilized.

### 3.2 Oxidative Addition Experiments

As the  $^{31}\text{P}$  NMR chemical shifts of the  $\text{Pd}(0)\text{L}_n$  products differ somewhat from literature values, possibly due to combinations of solvent and temperature effects as well as experimental error and the presence of small amounts of free ligands giving rise to exchange phenomena, it was deemed prudent to demonstrate that the generated  $\text{PdL}_n$  products could take part in oxidative addition reactions of PhI to give the corresponding Pd(II) compounds of the types *cis*-PdPhIL (L = bidentate phosphine) or *trans*-PdPhIL<sub>2</sub> (L = monodentate phosphine). These experiments did not give any indication as to the exact identity of  $\text{Pd}(0)\text{L}_n$  (did not indicate the value of n), but successful oxidative addition did confirm accessibility to the unsaturated, catalytically active  $\text{Pd}(0)\text{L}_2$  species. This thus verified the ability of  $\text{Pd}(\eta^5\text{-C}_5\text{H}_5)(\eta^3\text{-1-Ph-C}_3\text{H}_4)$  to act as a suitable Pd-source for the generation of Pd-catalysts used in a number of cross-coupling reactions.

#### 3.2.1 Oxidative Addition to *In Situ* Generated $\text{PdL}_n$

The oxidative addition studies involved reacting samples of newly formed  $\text{PdL}_n$  *in situ* with four equivalents of PhI in toluene- $d_8$  at 25 °C. The reactions were deemed complete when the  $^{31}\text{P}$  resonances of the  $\text{PdL}_n$  species had disappeared.

For the  $\text{PPh}_3$  system in the presence of both two and three equivalents of ligand, a beige solid precipitated from solution within minutes of addition of PhI. Its NMR spectrum was therefore obtained in  $\text{CD}_2\text{Cl}_2$  where the  $^{31}\text{P}$  singlet at  $\delta$



24.1 was consistent with the formation of *trans*-PdPhI(PPh<sub>3</sub>)<sub>2</sub> (lit.  $\delta$  24.3 in CDCl<sub>3</sub>).<sup>50a</sup> Oxidative addition was also successful with the PMePh<sub>2</sub> system in the presence of both two and three equivalents of PMePh<sub>2</sub>. As with Pd(PPh<sub>3</sub>)<sub>3</sub>, *trans*-PdPhI(PMePh<sub>2</sub>)<sub>2</sub> precipitated from solution within 3 h, and while the <sup>31</sup>P resonance,  $\delta$  6.9, was significantly upfield from the literature reported value of  $\delta$  11.3 (both in CD<sub>2</sub>Cl<sub>2</sub>),<sup>50b</sup> the identity of the species was confirmed by observation of a virtual methyl triplet for the PMePh<sub>2</sub> ligand at  $\delta$  1.65 (6H, *J* 3.1 Hz) and of Pd-Ph resonances at  $\delta$  6.59 (3H, m) and 6.78 (2H, m).

The formation of *trans*-PdPhI(PCy<sub>3</sub>)<sub>2</sub> occurred within minutes at 25 °C, and although this compound had been reported previously,<sup>28,50c</sup> no NMR data were provided. The dominant singlet in the <sup>31</sup>P NMR spectrum at  $\delta$  21.0 (toluene-d<sub>8</sub>) was, however, very similar to the chemical shift of the bromo analogue ( $\delta$  20.6).<sup>50c</sup> In addition, Pd-Ph resonances were observed at  $\delta$  6.87 (1H, t, *J* 7.3 Hz), 6.99 (2H, t, *J* 7.3 Hz) and 7.56 (2H, d, *J* 7.3 Hz), similar to those of *trans*-PdPhBr(PCy<sub>3</sub>)<sub>2</sub>.<sup>50c</sup> The compound *trans*-PdPhI(PMeBu<sup>t</sup>)<sub>2</sub> does not appear to have been reported previously and thus no precedents for <sup>1</sup>H or <sup>31</sup>P NMR data could be found. Oxidative addition of PhI to Pd(PMeBu<sup>t</sup>)<sub>2</sub> occurred within minutes at 25 °C, producing a single <sup>31</sup>P resonance at  $\delta$  27.2, as well as Pd-Ph resonances at  $\delta$  6.87 (1H, tt, *J* 7.2 Hz, 1.2 Hz), 6.92 (2H, t, *J* 7.2 Hz) and 7.32 (2H, dd, *J* 7.9 Hz, 1.2 Hz), and virtual Bu<sup>t</sup> and Me triplets at  $\delta$  1.40 (36H, t, *J* 6.8 Hz) and 0.23 (6H, t, *J* 3.0 Hz), respectively, in the <sup>1</sup>H NMR spectra (Figure 37). These data are all consistent with identification of the product as *trans*-

$\text{PdPhI}(\text{PMeBu}^t_2)_2$ . The compound was not fully characterized as a pure sample of *trans*- $\text{PdPhI}(\text{PMeBu}^t_2)_2$  could not be obtained due to the compound's high degree of solubility in all solvents tested for recrystallization.

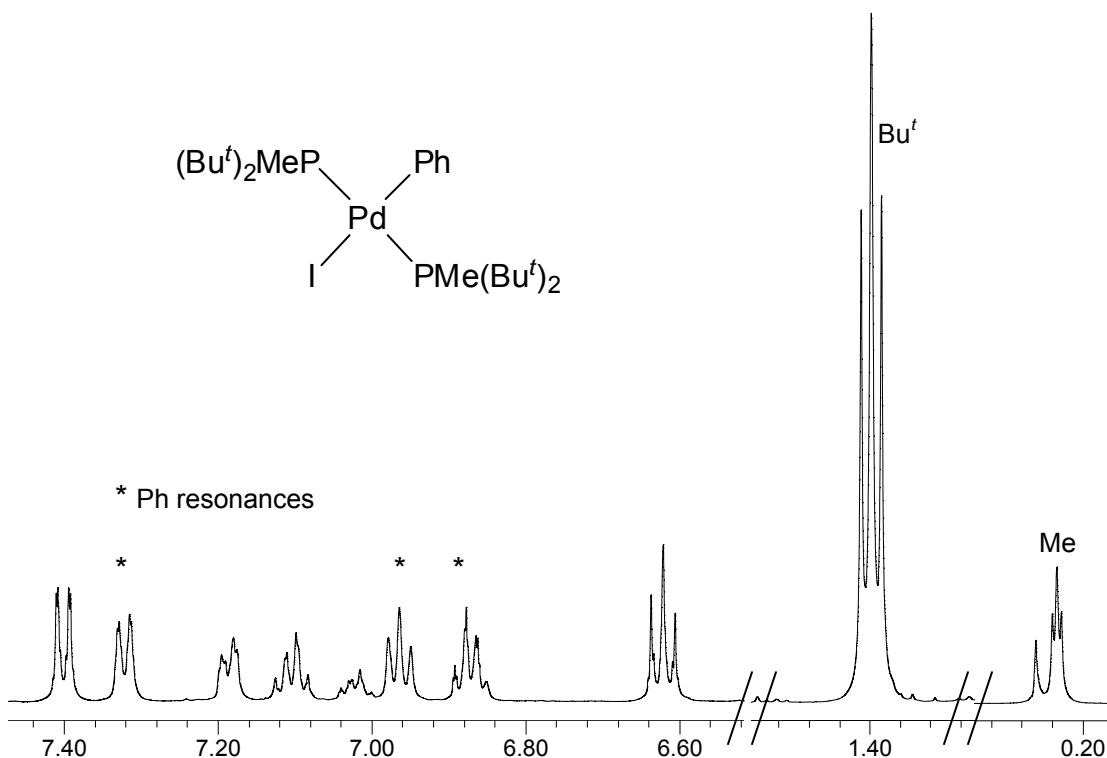


**Figure 37.  $^1\text{H}$  NMR spectrum (500 MHz,  $\text{tol-d}_8$ ) of the reaction of four equivalents PhI with *in situ* generated  $\text{Pd}(\text{PMeBu}^t_2)_3$  10 minutes after mixing**

Oxidative addition of PhI to  $\text{Pd}(\text{PBU}^t_3)_2$  required several days at 25 °C, producing a sharp singlet in the  $^{31}\text{P}$  spectrum at  $\delta$  103.6. This resonance corresponded well to that reported for  $\text{Pd}_2(\mu\text{-I})_2(\text{PBU}^t_3)_2$  (lit.  $\delta$  102.9 in  $\text{C}_6\text{D}_6$ ),<sup>50d</sup> a product subsequently arising from oxidative addition of PhI to the monoligated  $\text{Pd}(\text{PBU}^t_3)$  species (Figure 38). Although the literature provided no  $^1\text{H}$  data for

comparison,<sup>50d</sup> the  $^1\text{H}$  NMR spectrum contained a virtual  $\text{Bu}^t$  triplet at  $\delta$  1.28 ( $J$  6.1 Hz), characteristic of a *trans* geometry to the  $\text{P}(\text{Bu}^t)_3$  ligands. The Ph-region of the  $^1\text{H}$  NMR spectrum was obscured by resonances associated with unreacted PhI and reductive elimination products, preventing the confirmation that biphenyl was formed during the course of the reaction.

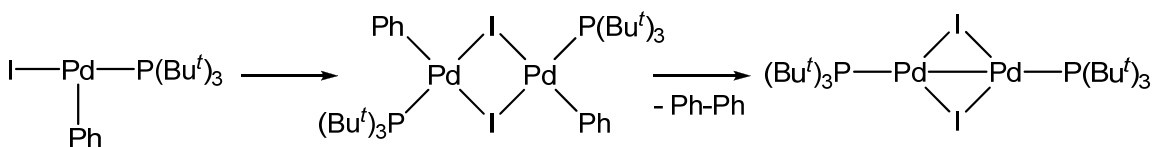


**Figure 38. Proposed pathway for the formation of  $\text{Pd}_2(\mu\text{-I})_2(\text{PBu}^t_3)_2$**

For all three bidentate ligands investigated, the oxidative addition reactions were relatively slow.  $\text{Pd}(\text{dppe})_2$  and  $\text{Pd}(\text{dppp})_2$  required several minutes heating at 75 °C, while  $\text{Pd}(\text{dppf})_2$ , which was insoluble in toluene, was reacted in THF overnight at 25 °C. In all cases, the previously reported (in  $\text{THF-d}_8$ ) compounds *cis*- $\text{PdPhIL}$  were readily identified by the mutually coupled doublets in the  $^{31}\text{P}$  NMR spectra at  $\delta$  34.9 and 49.7 ( $J$  28 Hz) for dppe (lit.  $\delta$  33.9 and 48.9,  $J$  28 Hz)<sup>50e</sup> (Figure 39), at  $\delta$  -8.8 and 12.3 ( $J$  53 Hz) for dppp (lit.  $\delta$  -7.9 and 12.2,  $J$  54 Hz),<sup>50f</sup> and at  $\delta$  8.7 and 26.1 ( $J$  34 Hz) for dppf (lit.  $\delta$  8.1 and 26.6,  $J$  35 Hz).<sup>50e</sup> For  $L = \text{dppe}$ , Pd-Ph resonances at  $\delta$  6.66 (1H, m), 6.72 (2H, m) and 7.04 (2H, m) further confirmed the oxidative addition product. The Pd-Ph resonances for  $L = \text{dppp}$  and dppf were obscured by other Ph resonances.

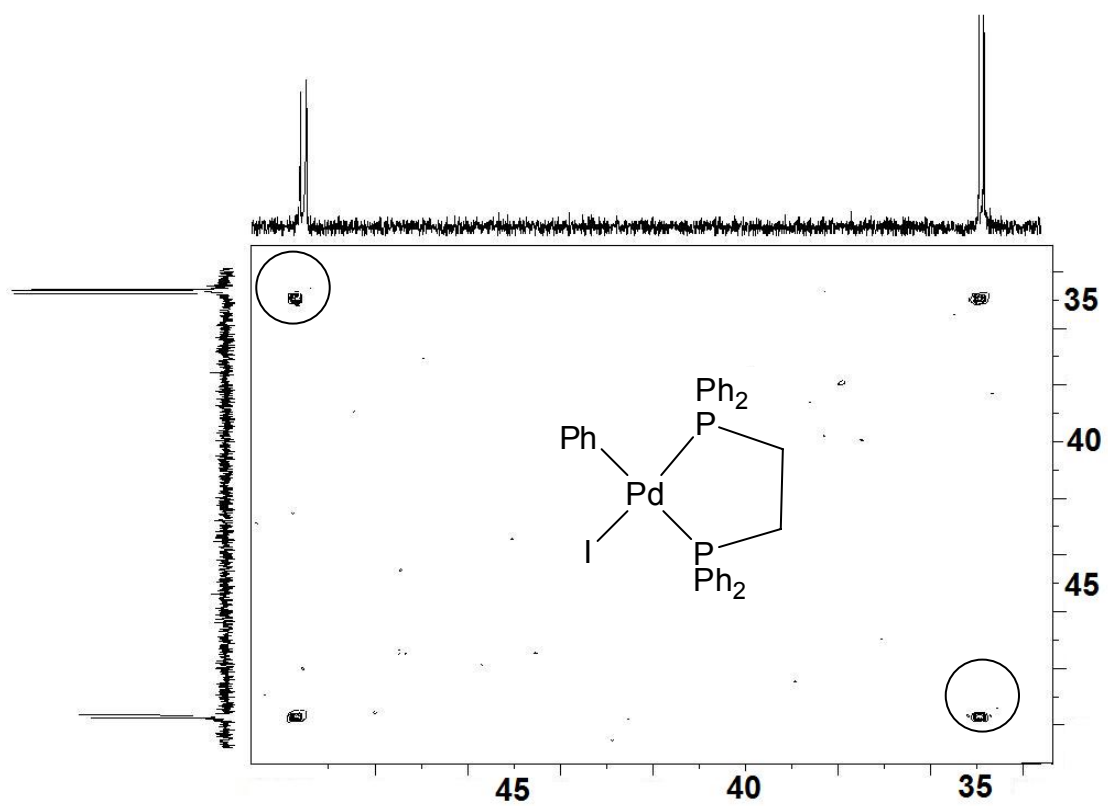
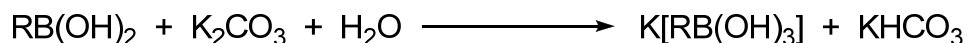


Figure 39.  $^{31}\text{P}$ - $^{31}\text{P}$  correlation spectrum (242.9 MHz,  $\text{CD}_2\text{Cl}_2$ ) of the reaction of four equivalents PhI with *in situ* generated  $\text{Pd}(\text{dppe})_2$

### 3.3 Investigations into the Role of Water in Transmetalation

In Suzuki and Miyaura's original paper,<sup>10a</sup> they reported the first successful coupling of 1-alkenyl halides with 1-alkenyl boranes in the presence of Pd(PPh<sub>3</sub>)<sub>4</sub> and base (Section 1.2, Figure 7). When the couplings were attempted in just the presence of Pd(PPh<sub>3</sub>)<sub>4</sub> in THF or EtOH solutions, a maximum of 2 % yield of the diene product was obtained. However, it was found that with the addition of aqueous sodium methoxide, ethoxide, acetate or hydroxide to the THF or EtOH solutions, yields of up to 80% could be obtained.

As previously discussed in section 1.2.1.2, when working with boronic acids (RB(OH)<sub>2</sub>) and esters (RB(OR')<sub>2</sub>) it is believed that the main role of base is to quaternize the boron in order to effect the transmetalation step.<sup>9c,e,16,17</sup> Aqueous basic salts (Cs<sub>2</sub>CO<sub>3</sub>, K<sub>3</sub>PO<sub>4</sub>, Tl<sub>2</sub>CO<sub>3</sub>, etc) are most often employed in order to generate hydroxide *in situ* which can then coordinate to the boron centre (Figure 40).<sup>9c,51</sup> Stronger bases, such as NaOH, are typically avoided as they have less functional group compatibility.<sup>9c</sup>



**Figure 40. Quaternization of RB(OH)<sub>2</sub> in the presence of aqueous K<sub>2</sub>CO<sub>3</sub>**

Quaternization increases the nucleophilicity of the R group, which allows it to be more effectively transferred to the Pd(II) centre.<sup>9c,e,16,17</sup> DFT calculations and kinetic studies further suggest that the borate complex displaces X<sup>-</sup> from the

coordination sphere of the Pd(II) oxidative addition product, forming a species with a bridging hydroxyl group between boron and palladium (Figure 41).<sup>16c,e</sup>

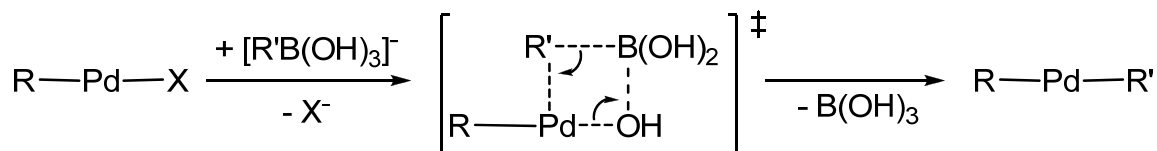
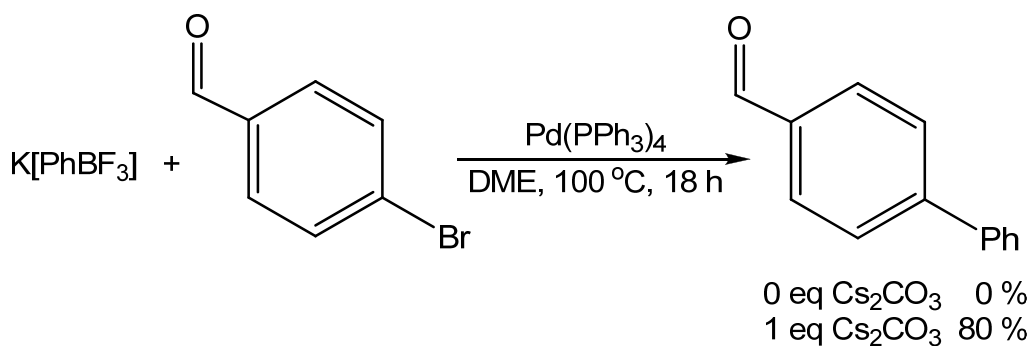


**Figure 41. Proposed four-centered transition state of transmetalation (L omitted)**

These mechanistic proposals surrounding the role of base for boronic acid and ester systems cannot be applied directly to the couplings of aryl trifluoroborates with aryl halides. The trifluoroborate species already contain a tetravalent boron centre and the weakness of palladium-fluorine bonds suggests that bridging will not occur through fluorine.<sup>19</sup> It was proposed that since trifluoroborates already contain a quaternized boron, these couplings would proceed in the absence of a base.<sup>18</sup> Studies found, however, that base was still required in order for the coupling of trifluoroborates and aryl halides to occur smoothly.<sup>18a-d</sup> Quach and Batey were unable to obtain any coupling between  $\text{K}[\text{PhBF}_3]$  and 4-bromobenzaldehyde without the addition of aqueous  $\text{Cs}_2\text{CO}_3$  (Figure 42 a).<sup>18d</sup> Molander and Biolatto found that in coupling  $\text{K}[\text{PhBF}_3]$  and 1-bromonaphthalene, three equivalents  $\text{K}_2\text{CO}_3$  provided a 90 % yield in only 2 h, whereas two equivalents  $\text{K}_2\text{CO}_3$  only provided an 80 % yield in 7 h (Figure 42 b).<sup>18b</sup>

(a) Quach and Batey:



(b) Molander *et al.*:

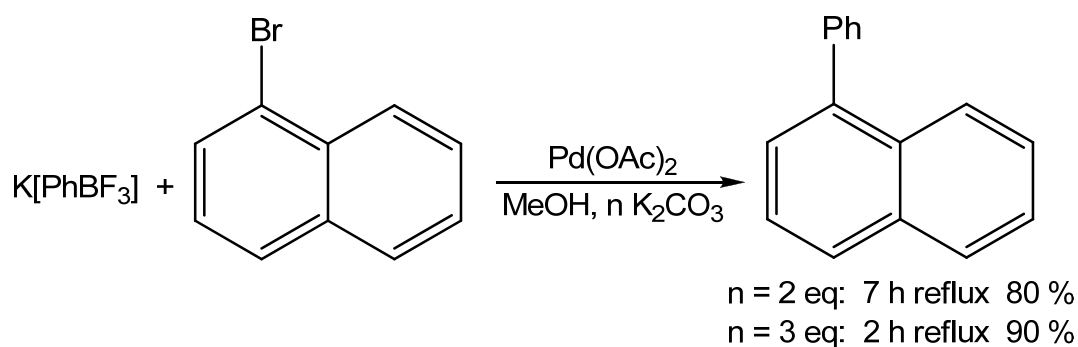


**Figure 42. Representative couplings of  $[\text{ArBF}_3]^-$  with  $\text{ArX}$ , illustrating the necessity of base**

Quach and Batey also investigated the coupling of  $\text{K}[\text{PhBF}_3]$  and 4-bromobenzaldehyde in the presence of  $\text{Cs}_2\text{CO}_3$  in a number of organic solvents (toluene, xylenes, dimethylacetamide, dimethyl ether).<sup>18d</sup> Water was found to be an essential cosolvent, as no coupling occurred under anhydrous conditions. In considering the need for  $\text{Cs}_2\text{CO}_3$  and  $\text{H}_2\text{O}$ , as well as the four-centered transition state proposed by Matos and Soderquist (Figure 41),<sup>16c</sup> Quach and Batey proposed that  $[\text{PhBF}_3]^-$  was not the active species in the reaction. They

proposed that one or more hydroxyl groups must displace fluoride from boron in order for transmetallation to occur.

Molander and Biolatto investigated the extent of  $[\text{RBF}_3]^-$  hydrolysis by refluxing  $\text{K}[\text{PhBF}_3]$  in wet methanol with 0, 1, 2 or 3 equivalents of  $\text{K}_2\text{CO}_3$ , collecting the precipitate that formed and analyzing it by  $^{11}\text{B}$  NMR spectroscopy.<sup>18b</sup> The  $^{11}\text{B}$  NMR spectrum of the sample with no added  $\text{K}_2\text{CO}_3$  exhibited a quartet in the NMR spectrum, consistent with unreacted  $[\text{RBF}_3]^-$ . The spectra of the samples with added  $\text{K}_2\text{CO}_3$  exhibited broad singlets that were shifted downfield in the NMR spectra. It was proposed that the downfield shift was due to  $\text{F}^-$  being displaced by less electron withdrawing groups, such as  $\text{HO}^-$ ,  $\text{MeO}^-$  and/or  $\text{HCO}_3^-$ . In another set of experiments,  $\text{K}[\text{PhBF}_3]$  and  $\text{PhB}(\text{OH})_2$  were separately refluxed in wet methanol- $d_4$  with 3 equivalents of  $\text{K}_2\text{CO}_3$ . The  $^{11}\text{B}$  NMR resonances revealed that the same species had formed in both systems. These results led Molander and Biolatto, like Quach and Batey, to conclude that  $[\text{PhBF}_3]^-$  was not the active species in the transmetallation step.

The research presented herein looked to systematically study how the amount of water affects the transmetallation step of coupling a typical aryl trifluoroborate,  $[\text{NBu}_4][\text{PhBF}_3]$ , with  $\text{Pd}(\text{Tol})(\text{Br})(\text{PCy}_3)_2$  in toluene (Figure 43).



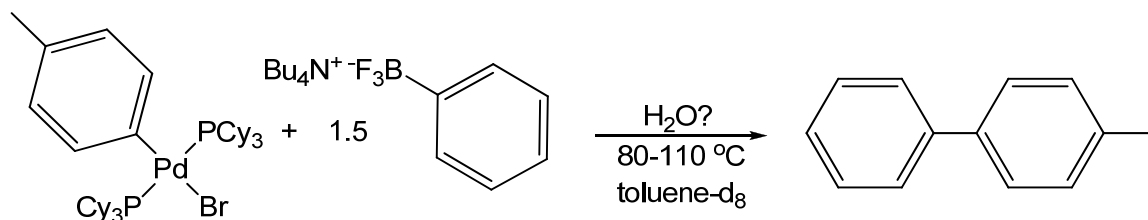


**Figure 43. Cross-coupling reaction of  $\text{Pd}(\text{Tol})(\text{Br})(\text{PCy}_3)_2$  and  $[\text{NBu}_4][\text{PhBF}_3]$**

In order to ensure that the effect of water was in fact attributable to the transmetalation step, the pre-formed oxidative addition product  $\text{Pd}(\text{Tol})(\text{Br})(\text{PCy}_3)_2$  was used. This prevented the observed results from being attributed to either the generation of the catalytically active  $\text{Pd}(0)$  species or the oxidative addition of  $\text{TolBr}$ .

Coupling was attempted in  $\text{toluene-d}_8$  under fully anhydrous conditions, with and without  $\text{K}_2\text{CO}_3$ , and under conditions in which a controlled amount of water was added to the reaction solution. Polar solvents are typically employed for the SM reaction;<sup>9</sup> however, toluene was selected as it is easy to dry and therefore the amount of  $\text{H}_2\text{O}$  in solution could be controlled, as well as to maintain consistency throughout the thesis.  $^1\text{H}$  and  $^{31}\text{P}$  NMR spectroscopy were used to monitor the reactions, and GC was used to determine product yields. Calibration curves and a representative gas chromatograph can be found in Appendix B.

### 3.3.1 Attempts at Anhydrous Cross-Coupling

An anhydrous solution of Pd(Tol)(Br)(PCy<sub>3</sub>)<sub>2</sub> and 1.5 eq [NBu<sub>4</sub>][PhBF<sub>3</sub>] was heated at 80 °C. After 72 h, a <sup>1</sup>H NMR spectrum revealed no change in the solution composition, with still no changes after 24 h at reflux. The reaction was stopped and GC analysis revealed neither the 4-methylbiphenyl product nor either of the homo-coupled byproducts. A second trial revealed the same results after 48 h at 80 °C followed by 96 h at 95 °C.

In considering the studies of Quach and Batey,<sup>18d</sup> and Molander *et al.* (Figure 42),<sup>18a-c</sup> it was deemed prudent to attempt the reaction in the presence of a basic salt. The reaction was therefore repeated with a suspension of four equivalents of dry, powdered K<sub>2</sub>CO<sub>3</sub>. After 48 h at 80 °C followed by 72 h at reflux, no cross-coupling occurred. Pd(Tol)(Br)(PCy<sub>3</sub>)<sub>2</sub> remained in solution, although the phenyl resonances associated with [NBu<sub>4</sub>][PhBF<sub>3</sub>] were no longer visible in the <sup>1</sup>H NMR spectrum. It was possible that K[BF<sub>3</sub>Ph] had precipitated out of solution, although this was difficult to confirm as the solution already contained a white precipitate associated with K<sub>2</sub>CO<sub>3</sub>, and therefore the reaction was repeated with four equivalents of tetrabutylammonium bromide in addition to the K<sub>2</sub>CO<sub>3</sub>. After 48 h at 80 °C followed by 24 h at reflux, [NBu<sub>4</sub>][PhBF<sub>3</sub>] was still present in solution, but the resonances of Pd(Tol)(Br)(PCy<sub>3</sub>)<sub>2</sub> were no longer identifiable in either the <sup>1</sup>H or <sup>31</sup>P NMR spectra. The solution precipitated Pd metal, but neither 4-methylbiphenyl nor either homo-coupled byproducts could be identified.

### 3.3.2 Cross-Coupling with Controlled H<sub>2</sub>O Addition

As the results of section 3.3.1 indicate, the cross-coupling of Pd(Tol)(Br)(PCy<sub>3</sub>)<sub>2</sub> and [NBu<sub>4</sub>][PhBF<sub>3</sub>] did not occur in the absence of water. Experiments were therefore performed in order to determine how the amount of water present in solution would affect the coupling of these compounds. Anhydrous solutions of Pd(Tol)(Br)(PCy<sub>3</sub>)<sub>2</sub> and 1.5 eq [NBu<sub>4</sub>][PhBF<sub>3</sub>] in toluene-d<sub>8</sub> were prepared, and 1.25, 3.75 or ~20 equivalents of water, with respect to [NBu<sub>4</sub>][PhBF<sub>3</sub>], was added. The solutions were heated at 90-95 °C, with the reactions being deemed complete when the resonances of Pd(Tol)(Br)(PCy<sub>3</sub>)<sub>2</sub> were no longer identifiable in the <sup>1</sup>H and <sup>31</sup>P NMR spectra. In all cases, excess [NBu<sub>4</sub>][PhBF<sub>3</sub>] remained in solution. The yields, as determined by GC, can be found in Table 12.

Table 12. Percent yields of 4-methylbiphenyl

Eq. H <sub>2</sub> O	Trial 1	Trial 2	Trial 3	Average
1.25	57	71	40	56
3.75	66	58	50	58
excess <sup>a</sup>	59	56	57	57

a. 0.5 mL toluene can dissolve ~ 1.5 - 2 μL (~ 18 - 25 eq) H<sub>2</sub>O at 90-95 °C<sup>46</sup>

Quantitative generation of 4-methylbiphenyl was not obtained. The homo-coupled product 4,4'-dimethylbiphenyl was not formed in the reactions, and the

formation of toluene could not be determined due to the reactions being performed in toluene. A single experiment performed in  $C_6D_6$  with an excess of water indicated the formation of toluene, therefore providing a likely cause for the reduced yields of 4-methylbiphenyl. Biphenyl was also formed during the reactions; however, since  $[NBu_4][PhBF_3]$  was used in excess, the formation of this product did not contribute to the reduced yields of the desired product.

The successful coupling of  $Pd(Tol)(Br)(PCy_3)_2$  and  $[NBu_4][PhBF_3]$  to form 4-methylbiphenyl in the presence of  $H_2O$ , and the failure to couple the same compounds under anhydrous conditions, indicated that  $H_2O$  was necessary for these coupling reactions to occur. The results presented in Table 12 indicate, however, that the exact amount of  $H_2O$  present in the reaction solution above one equivalent had no significant effect on the yield of 4-methylbiphenyl. Similar to the proposal by Quach and Batey,<sup>18d</sup> it is thought that in the presence of  $H_2O$ ,  $[PhBF_3]^-$  was hydrolyzed to form  $[PhBF_2(OH)]^-$ ,  $[PhBF(OH)_2]^-$  and/or  $[PhB(OH)_3]^-$ , and that any or all of these species were active in the transmetallation step since they would be able to form the bridged transition state illustrated in Figure 41.

In order to determine if the amount of  $H_2O$  had an effect on the rate of cross-coupling, the progress of the reactions at 95 °C was monitored by the disappearance of the  $Pd(Tol)(Br)(PCy_3)_2$  resonances in the  $^1H$  NMR. Monitoring the development of the 4-methylbiphenyl resonances was not suitable as quantitative yields of the product were not obtained. Reactions with an excess of  $H_2O$  consistently went to completion first, followed by reactions with 1.25 eq of

H<sub>2</sub>O and lastly reactions with 3.75 eq of H<sub>2</sub>O. In one particular set of experiments, the timeline to complete consumption of Pd(Tol)(Br)(PCy<sub>3</sub>)<sub>2</sub> was 16-18 h, 19-21 h and 23-25 h, respectively. While the order of reaction completion was consistent over several runs, the reaction times between runs varied by 4-6 h due to fluctuations in the oil bath temperature. Therefore, the observed differences in time for reaction completion may not be significant.

### 3.4 Summary and Conclusions

This thesis reports a superior methodology for the generation of catalytically active Pd(0)L<sub>n</sub> species from Pd( $\eta^5$ -C<sub>5</sub>H<sub>5</sub>)( $\eta^3$ -1-Ph-C<sub>3</sub>H<sub>4</sub>) and both monodentate (L = PMePh<sub>2</sub>, PPh<sub>3</sub>, PCy<sub>3</sub>, PMeBu<sup>t</sup><sub>2</sub>, PBu<sup>t</sup><sub>3</sub>) and bidentate (L = dppe, dppp, dppf) phosphine ligands. All of the palladium(0) species formed were capable of undergoing oxidative addition of PhI.

In the PMePh<sub>2</sub>, PPh<sub>3</sub> and PCy<sub>3</sub> systems, both  $\sigma$ -allyl and dinuclear type intermediates were observed, whereas in the PMeBu<sup>t</sup><sub>2</sub> and PBu<sup>t</sup><sub>3</sub> systems only  $\sigma$ -allyl type intermediates were observed. All monodentate systems reacted within an hour at 75 °C to produce catalytically active PdL<sub>n</sub> species. For PMeBu<sup>t</sup><sub>2</sub>, the reaction was complete within 45 min at 50 °C, whereas the PMePh<sub>2</sub> and PPh<sub>3</sub> systems completely reacted within 10 and 90 min, respectively, at 25 °C when three equivalents of ligand were employed. The additional equivalent of ligand prevented the formation of Pd metal which plagued these systems when only two equivalents of ligand were utilized.

The PdL<sub>2</sub> species produced by the reaction of Pd( $\eta^5$ -C<sub>5</sub>H<sub>5</sub>)( $\eta^3$ -1-Ph-C<sub>3</sub>H<sub>4</sub>) with bidentate ligands occurred almost instantaneously for the dppe and dppp systems when two equivalents of ligand were utilized, whereas an hour at 75 °C was required for dppf. When only one equivalent of dppf was utilized, none of the species formed could be identified. One equivalent of either dppe or dppp still produced PdL<sub>2</sub>; however, Pd metal also precipitated from the reaction solutions.

This thesis also presents a number of experiments which investigated the necessity of water for the cross-coupling of a typical aryl trifluoroborate compound,  $[\text{NBu}_4][\text{PhBF}_3]$ , with a typical aryl halide, 4-bromotoluene. Water was necessary in order for the couplings to occur; however, the amount of water above one equivalent had no significant effect on either the yield of 4-methylbiphenyl or the rate of the cross-coupling reaction. Since it is believed that  $[\text{RBF}_3]^-$  species are hydrolyzed in the presence of water,<sup>18</sup> these results support the proposal that  $[\text{RBF}_2(\text{OH})]^-$ ,  $[\text{RBF}(\text{OH})_2]^-$  and/or  $[\text{RB}(\text{OH})_3]^-$  are active species, while  $[\text{RBF}_3]^-$  is not, in the transmetallation step when coupling aryl trifluoroborate compounds to aryl halides.

## References

1. (a) Tamao, K.; Miyaura, N. *Top. Curr. Chem.*, **2002**, 219, 1. (b) Echavarren, A. M.; Cardenas, D. J. *Metal Catalyzed Cross-Coupling Reactions*, 2<sup>nd</sup> ed.; de Mejiere, A.; Diederich, F., Eds.; John Wiley & Sons: New York, 2004; pp 1 – 40. (c) Negishi, E. *Acc. Chem. Res.*, **1982**, 15, 340. (d) Stanforth, S. P. *Tetrahedron*, **1998**, 54, 263.
2. Jiang, L.; Buchwald, S. L. *Metal Catalyzed Cross-Coupling Reactions*, 2<sup>nd</sup> ed.; de Mejiere, A.; Diederich, F., Eds.; John Wiley & Sons: New York, 2004; pp 699 – 756.
3. Negishi, E. *J. Organomet. Chem.*, **2002**, 653, 34.
4. (a) Tamao, K.; Sumitani, K.; Kumada, M. *J. Am. Chem. Soc.*, **1972**, 94, 4374. (b) Tamao, K.; Zembayashi, M.; Kiso, Y.; Kumada, M. *J. Organomet. Chem.*, **1973**, 55, C91. (c) Corriu, R. J. P.; Masse, J. P. *J. Chem. Soc., Chem. Commun.*, **1972**, 144.
5. Yamamura, M.; Moritani, I.; Murahashi, S. *J. Organomet. Chem.*, **1975**, 91, C39.
6. (a) Kosugi, M.; Shimizu, Y.; Migita, T. *Chem. Lett.*, **1977**, 1423. (b) Kosugi, M.; Hagiwara, I.; Migita, T. *Chem. Lett.*, **1983**, 839.
7. Stille, J. K. *Angew. Chem. Int. Ed.*, **1986**, 25, 508.



8. Calvin, G.; Coates, G. E. *J. Chem. Soc.*, **1960**, 2008.
9. (a) Miyaura, N.; Suzuki, A. *Chem. Rev.*, **1995**, *95*, 2457. (b) Miyaura, N. *Metal Catalyzed Cross-Coupling Reactions*, 2<sup>nd</sup> ed.; de Mejiere, A.; Diederich, F., Eds.; John Wiley & Sons: New York, 2004; pp 41 – 123. (c) Miyaura, N. *Top. Curr. Chem.*, **2002**, *219*, 11 – 59. (d) Littke, A. F.; Fu, G. C. *Angew. Chem. Int. Ed.*, **2002**, *41*, 4176. (e) Kotha, S.; Lahiri, K.; Kashinath, D. *Tetrahedron*, **2002**, *58*, 9633. (f) Suzuki, A. *J. Organomet. Chem.*, **1999**, *576*, 147.
10. (a) Miyaura, N.; Yamada, K.; Suzuki, A. *Tetrahedron Lett.*, **1979**, *36*, 3437. (b) Miyaura, N.; Yanagi, T.; Suzuki, A. *Synth. Commun.*, **1981**, *11*, 513. (c) Miyaura, N.; Yamada, K.; Suginome, H.; Suzuki, A. *J. Am. Chem. Soc.*, **1985**, *107*, 972. (d) Miyaura, N.; Ishiyama, T.; Sasaki, H.; Ishikawa, M.; Satoh, M.; Suzuki, A. *J. Am. Chem. Soc.*, **1985**, *111*, 314.
11. Hills, I. D.; Netherton, M. R.; Fu, G. C. *Angew. Chem. Int. Ed.*, **2003**, *42*, 5749.
12. Amatore, C.; Jutand, A. *J. Organomet. Chem.*, **1999**, *576*, 254.
13. (a) Amatore, C.; Pfluger, F. *Organometallics*, **1990**, *9*, 2278. (b) Casado, A. L.; Espinet, P. *Organometallics*, **1998**, *17*, 954.
14. Crabtree, R. H. *The Organometallic Chemistry of the Transition Metals*, 4<sup>th</sup> ed.; John Wiley & Sons: New Jersey, 2005; pp 159 – 181.
15. Kukushkin, Y. N. *Platinum Metals Rev*, **1991**, *35*, 28.

16. (a) Miyaura, N.; Yamada, K.; Suginome, H.; Suzuki, A. *J. Am. Chem. Soc.*, **1985**, *107*, 972. (b) Aliprantis, A. O.; Canary, J. W. *J. Am. Chem. Soc.*, **1994**, *116*, 6985. (c) Matos, K.; Soderquist, J. A. *J. Org. Chem.*, **1998**, *63*, 461. (d) Miyaura, N. *J. Organometallic Chem.*, **2002**, *653*, 54. (e) Braga, A. A. C.; Morgon, N. H.; Ujaque, G.; Maseras, F. *J. Am. Chem. Soc.*, **2005**, *127*, 9298.
17. Hall, D. G. *Boronic Acids – Preparation and Applications in Organic Synthesis and Medicine*; Hall, D. G, Ed.; John Wiley & Sons: New York, 2005; pp 1 – 99.
18. (a) Molander, G. A.; Ito, T. *Org. Lett.*, **2001**, *3*, 393. (b) Molander, G. A.; Biolatto, B. *J. Org. Chem.*, **2003**, *68*, 4302. (c) Molander, G. A.; Ellis, N. *Acc. Chem. Res.*, **2007**, *40*, 275. (d) Batey, R. A.; Quach, T. D. *Tetrahedron Lett.*, **2001**, *42*, 9099. (e) Thadani, A. N.; Batey, R. A. *Org. Lett.*, **2002**, *4*, 3827.
19. Wright, S. W.; Hageman, D. L.; McClure, L. D. *J. Org. Chem.*, **1994**, *59*, 6095.
20. (a) Miyaura, N.; Tanabe, Y.; Suginome, H.; Suzuki, A. *J. Organometallic Chem.*, **1982**, *233*, C13. (b) Moriya, T.; Miyaura, N.; Suzuki, A. *Synlett.*, **1994**, 149.
21. (a) Fitton, P.; Johnson, M. P.; McKeon, J. E. *Chem. Commun.*, **1968**, 6. (b) Fitton, P.; Rick, E. A. *J. Organomet. Chem.*, **1971**, *28*, 287.
22. Shen, W. *Tetrahedron Lett.*, **1997**, *38*, 5575.

23. (a) Netherton, M. R.; Fu, G. C. *Angew. Chem. Int. Ed.*, **2002**, *41*, 3910. (b) Albaneze-Walker, J.; Raju, R.; Vance, J. A.; Goodman, A. J.; Reeder, M. R. Liao, J.; Maust, M. T.; Irish, P. A.; Espino, P.; Andrews, D. R. *Org. Lett.*, **2009**, *11*, 1463.
24. Roy, A. H.; Hartwig, J. F. *J. Am. Chem. Soc.*, **2001**, *123*, 1232.
25. Hartwig, J. F. *Inorg. Chem.*, **2007**, *46*, 1936.
26. Wolfe, J.P.; Singer, R. A.; Yang, B. H.; Buchwald, S. L. *J. Am. Chem. Soc.*, **1999**, *121*, 9550.
27. Ohzu, Y; Goto, K; Sato, H; Kawashima, T. *J. Organomet. Chem.*, **2005**, *690*, 4175.
28. Galardon, E; Ramdeehul, S; Brown, J; Cowley, A; Hii, K; Jutand, A. *Angew. Chem., Int. Ed.*, **2002**, *41*, 1760
29. Stambuli, J.P.; Kuwano, R.; Hartwig, J.F. *Angew. Chem. Int. Ed.*, **2002**, *41*, 4746.
30. Li, Z.; Fu, Y.; Guo, Q.; Liu, L. *Organometallics*, **2008**, *27*, 4043.
31. Tatsumi, K.; Hoffmann, R.; Yamamoto, A.; Stille, J.K. *Bull. Chem. Soc. Jpn.*, **1981**, *54*, 1857.

32. Choueiry, D.; Negishi, E. *Handbook of Organopalladium Chemistry for Organic Synthesis*; Negishi, E.; de Mejiere, A., Eds.; John Wiley & Sons: New York, 2002; pp 47 - 65.
33. Amatore, C.; Jutand, A.; Khalil, F.; M'Barki, M. A.; Mottier, L. *Organometallics*, **1993**, *12*, 3168.
34. (a) Goodson, F. E.; Wallow, T. I.; Novak, B. M. *J. Am. Chem. Soc.*, **1997**, *119*, 12441. (b) Morita, D. K.; Stille, J. K.; Norton, J. R. *J. Am. Chem. Soc.*, **1995**, *117*, 8576.
35. (a) Amatore, C.; Jutand, A.; M'Barki, M. A. *Organometallics*, **1992**, *11*, 3009. (b) Amatore, C.; Carre, E.; Jutand, A.; M'Barki, M. A. *Organometallics*, **1995**, *14*, 1818. (c) Csákai, Z.; Skoda-Földes, R.; Kollár, L. *Inorg. Chim. Acta*, **1999**, *286*, 93.
36. Amatore, C.; Azzabi, M.; Jutand, A. *J. Am. Chem. Soc.*, **1991**, *113*, 8375.
37. Negishi, E.; Takahashi, T.; Akiyoshi, K. *J. Chem. Soc., Chem. Commun.*, **1986**, 1338.
38. Fiaud, J. C.; De Gournay, A. H.; Larcheveque, M.; Kagan, H. B. *J. Organomet. Chem.*, **1978**, *154*, 175.
39. (a) Amatore, C.; Jutand, A. *Coord. Chem. Rev.*, **1998**, *178-180*, 511. (b) Fairlamb, I. J. S. *Org. Biomol. Chem.*, **2008**, *6*, 3645.

40. Mitchell, E. A.; Baird, M. C. *Organometallics*, **2007**, *26*, 5230.
41. (a) Werner, H.; Tune, d.; Parker, G.; Kruger, C.; Brauer, D. J. *Angew. Chem. Int. Ed.*, **1975**, *14*, 185. (b) Werner, H. *Angew. Chem., Int. Ed.*, **1977**, *16*, 1. (c) Werner, H.; Kühn, A. *Angew. Chem. Int. Ed.*, **1979**, *18*, 416. (d) Kühn, A.; Werner, H. *J. Organomet. Chem.*, **1979**, *179*, 421.
42. (a) Leoni, P. *Organometallics*, **1993**, *12*, 2432. (b) Stauffer, S. R.; Beare, N. A.; Stambuli, J. P.; Hartwig, J. F. *J. Am. Chem. Soc.*, **2001**, *123*, 4641. (c) Grotjahn, D. B.; Gong, Y.; Zakharov, L.; Golen, J. A.; Rheingold, A. L. *J. Am. Chem. Soc.*, **2006**, *128*, 438. (d) Tsukamoto, H.; Ueno, T.; Kondo, Y. *Org. Lett.*, **2007**, *9*, 3033.
43. Littke, A. F.; Dai, C.; Fu, G. C. *J. Am. Chem. Soc.*, **2000**, *122*, 4020.
44. Mitchell, E. A. "Studies in the Optimization of the Suzuki-Miyaura Reaction," PhD dissertation, Department of Chemistry, Queens University, 2008.
45. (a) Tatsuno, Y.; Yoshida, T.; Otsuka, S. *Inorg. Synth.*, **1990**, *28*, 342. (b) Auburn, P. R.; Mackenzie, P. B.; Bosnich, B. *J. Am. Chem. Soc.*, **1985**, *107*, 2033. (c) Murrall, N. W.; Welch, A. J. *J. Organomet. Chem.*, **1973**, *46*, 2819.
46. Marche, C.; Ferronato, C.; De Hemptinne, J.; Jose, J. *J. Chem. Eng. Data*, **2006**, *51*, 355.

47. (a) Mann, B. E.; Musco, A. *J. Chem. Soc., Dalton Trans.*, **1975**, 1673. (b) Broadwood-Strong, G. T. L.; Chaloner, P. A.; Hitchcock, P. B. *Polyhedron*, **1993**, *12*, 721.
48. (a) Liang, C.; Xia, W.; Soltani-Ahmadi, H.; Schlüter, O.; Fischer, R. A.; Muhler, M. *Chem. Comm.*, **2005**, 282. (b) Niklewski, A.; Strunskus, T.; Witte, G.; Wöll, C. *Chem. Mater.*, **2005**, *17*, 861. (c) Xia, W.; Schlüter, O. F. K.; Liang, C.; van den Berg, M. W.E.; Guraya, M.; Muhler, M. *Catal. Today*, **2005**, *102-103*, 34.
49. Minasyants, M. K.; Struchkov, Y. T. *J. Struct. Chem.*, **1968**, *9*, 406.
50. (a) Shmidt, A; Smirnov, V. *Kinetics and Catalysis*, **2002**, *43*, 195. (b) Ozawa, F; Sugimoto, T; Yuasa, Y; Santra, M; Yamamoto, T; Yamamoto, A. *Organometallics*, **1984**, *3*, 683. (c) Stambuli, J. P.; Incarvito, C. D.; Buehl, M.; Hartwig, J. F. *J. Am. Chem. Soc.*, **2004**, *126*, 1184. (d) Durà-Vilà, V.; Mingos, M. P.; Vilar, R.; White, A. J. P.; Williams, D. J. *J. Organomet. Chem.*, **2000**, *600*, 198. (e) Mann, G; Baranano, D; Hartwig, J; Rheingold, A; Guzei, I. *J. Am. Chem. Soc.*, **1998**, *120*, 9205. (f) Brown, J; Guiry, P. *Inorg. Chim. Acta*, **1994**, *220*, 249.
51. Smith, G. B.; Dezeny, G. C.; Hughes, D. L.; King, A. O.; Verhoeven, T. R. *J. Org. Chem.*, **1994**, *59*, 8151.

**Appendix A.** Crystal Structure Data for Pd( $\eta^5$ -C<sub>5</sub>H<sub>5</sub>)( $\eta^3$ -1-Ph-C<sub>3</sub>H<sub>4</sub>)

The crystal structure determination was performed by Dr. Ruiyao Wang in the X-ray Crystallography Laboratory at Queen's University. Diffraction intensity data were collected with a Bruker SMART APEX II X-ray diffractometer with graphite-monochromated Mo  $K_{\alpha}$  radiation ( $\lambda = 0.71073 \text{ \AA}$ ) controlled with Cryostream Controller 700. The space group was determined from systematic absences in the diffraction data. The structure was solved by direct methods. Full-matrix least-square refinements minimizing the function  $\sum w (F_o^2 - F_c^2)^2$  were applied to the compound. All non-hydrogen atoms were refined anisotropically. All of the H atoms were placed in geometrically calculated positions, with C-H = 0.95 (phenyl), 0.99 (allyl-CH<sub>2</sub>), 1.00  $\text{\AA}$  (allyl-CH and Cp), and refined as riding atoms, with  $U_{iso}(H) = 1.2 U_{eqC}$ .



## Crystal Structure of Pd( $\eta^3$ -1-Ph-C<sub>3</sub>H<sub>4</sub>)( $\eta^5$ -C<sub>5</sub>H<sub>5</sub>)

Table 1. Crystal data and structure refinement for Pd( $\eta^3$ -1-Ph-C<sub>3</sub>H<sub>4</sub>)( $\eta^5$ -C<sub>5</sub>H<sub>5</sub>)

Empirical formula	C <sub>14</sub> H <sub>14</sub> Pd	
Formula weight	288.65	
Temperature	180(2) K	
Wavelength	0.71073 Å	
Crystal system	Orthorhombic	
Space group	Pbca	
Unit cell dimensions	a = 9.8908(3) Å	$\alpha = 90^\circ$ .
	b = 12.4381(3) Å	$\beta = 90^\circ$ .
	c = 18.2355(5) Å	$\gamma = 90^\circ$ .
Volume	2243.38(11) Å <sup>3</sup>	
Z	8	
Density (calculated)	1.709 Mg/m <sup>3</sup>	
Absorption coefficient	1.615 mm <sup>-1</sup>	
F(000)	1152	
Crystal size	0.28 x 0.28 x 0.10 mm <sup>3</sup>	
Theta range for data collection	2.86 to 26.00°.	
Index ranges	-9 ≤ h ≤ 12, -15 ≤ k ≤ 11, -22 ≤ l ≤ 19	
Reflections collected	12974	
Independent reflections	2200 [R(int) = 0.0308]	
Completeness to theta = 26.00°	99.9 %	
Absorption correction	Multi-scan	
Max. and min. transmission	0.8500 and 0.6614	
Refinement method	Full-matrix least-squares on F <sup>2</sup>	
Data / restraints / parameters	2200 / 0 / 136	
Goodness-of-fit on F <sup>2</sup>	1.045	
Final R indices [I > 2σ(I)]	R1 = 0.0227, wR2 = 0.0514	
R indices (all data)	R1 = 0.0296, wR2 = 0.0557	
Largest diff. peak and hole	0.550 and -0.495 e.Å <sup>-3</sup>	

Table 2. Atomic coordinates ( $\times 10^4$ ) and equivalent isotropic displacement parameters ( $\text{\AA}^2 \times 10^3$ ) for  $\text{Pd}(\eta^3\text{-1-Ph-C}_3\text{H}_4)(\eta^5\text{-C}_5\text{H}_5)$ .  $U(\text{eq})$  is defined as one third of the trace of the orthogonalized  $U_{ij}$  tensor.

	x	y	z	$U(\text{eq})$
Pd(1)	2851(1)	7751(1)	5876(1)	22(1)
C(1)	2577(3)	6226(3)	6625(1)	34(1)
C(2)	3555(3)	6852(2)	6978(1)	30(1)
C(3)	2970(3)	7858(2)	7129(2)	32(1)
C(4)	1577(3)	7817(3)	6932(2)	38(1)
C(5)	1339(3)	6824(3)	6609(2)	38(1)
C(6)	3520(3)	9173(2)	5345(2)	32(1)
C(7)	3836(3)	8250(2)	4933(2)	33(1)
C(8)	2743(3)	7631(2)	4688(2)	30(1)
C(9)	2875(3)	6598(2)	4296(1)	27(1)
C(10)	4019(3)	5956(2)	4323(2)	34(1)
C(11)	4093(3)	5011(3)	3918(2)	38(1)
C(12)	3024(3)	4696(2)	3484(2)	38(1)
C(13)	1879(3)	5317(2)	3460(2)	35(1)
C(14)	1800(3)	6261(2)	3856(2)	32(1)

Table 3. Bond lengths [ $\text{\AA}$ ] and angles [ $^\circ$ ] for  $\text{Pd}(\eta^3\text{-1-Ph-C}_3\text{H}_4)(\eta^5\text{-C}_5\text{H}_5)$ .

Pd(1)-C(7)	2.072(3)
Pd(1)-C(6)	2.123(3)
Pd(1)-C(8)	2.174(3)
Pd(1)-C(3)	2.293(3)
Pd(1)-C(4)	2.303(3)
Pd(1)-C(5)	2.313(3)
Pd(1)-C(1)	2.353(3)
Pd(1)-C(2)	2.403(3)
C(1)-C(2)	1.398(4)

C(1)-C(5)	1.433(5)
C(1)-H(1A)	1.0000
C(2)-C(3)	1.406(4)
C(2)-H(2A)	1.0000
C(3)-C(4)	1.425(4)
C(3)-H(3A)	1.0000
C(4)-C(5)	1.388(5)
C(4)-H(4A)	1.0000
C(5)-H(5A)	1.0000
C(6)-C(7)	1.408(4)
C(6)-H(6A)	0.9900
C(6)-H(6B)	0.9900
C(7)-C(8)	1.400(4)
C(7)-H(7A)	1.0000
C(8)-C(9)	1.476(4)
C(8)-H(8A)	1.0000
C(9)-C(10)	1.386(4)
C(9)-C(14)	1.396(4)
C(10)-C(11)	1.390(4)
C(10)-H(10A)	0.9500
C(11)-C(12)	1.377(4)
C(11)-H(11A)	0.9500
C(12)-C(13)	1.372(4)
C(12)-H(12A)	0.9500
C(13)-C(14)	1.380(4)
C(13)-H(13A)	0.9500
C(14)-H(14A)	0.9500
C(7)-Pd(1)-C(6)	39.21(11)
C(7)-Pd(1)-C(8)	38.42(11)
C(6)-Pd(1)-C(8)	67.54(11)
C(7)-Pd(1)-C(3)	141.83(11)
C(6)-Pd(1)-C(3)	112.99(11)
C(8)-Pd(1)-C(3)	179.36(11)

C(7)-Pd(1)-C(4)	160.21(12)
C(6)-Pd(1)-C(4)	121.49(11)
C(8)-Pd(1)-C(4)	143.99(11)
C(3)-Pd(1)-C(4)	36.13(11)
C(7)-Pd(1)-C(5)	158.90(11)
C(6)-Pd(1)-C(5)	151.71(12)
C(8)-Pd(1)-C(5)	120.66(11)
C(3)-Pd(1)-C(5)	59.05(10)
C(4)-Pd(1)-C(5)	35.00(11)
C(7)-Pd(1)-C(1)	141.01(11)
C(6)-Pd(1)-C(1)	166.54(11)
C(8)-Pd(1)-C(1)	121.16(11)
C(3)-Pd(1)-C(1)	58.24(10)
C(4)-Pd(1)-C(1)	58.69(11)
C(5)-Pd(1)-C(1)	35.75(11)
C(7)-Pd(1)-C(2)	134.20(11)
C(6)-Pd(1)-C(2)	132.77(11)
C(8)-Pd(1)-C(2)	144.63(10)
C(3)-Pd(1)-C(2)	34.74(10)
C(4)-Pd(1)-C(2)	58.39(10)
C(5)-Pd(1)-C(2)	58.13(10)
C(1)-Pd(1)-C(2)	34.17(10)
C(2)-C(1)-C(5)	108.1(3)
C(2)-C(1)-Pd(1)	74.86(17)
C(5)-C(1)-Pd(1)	70.60(16)
C(2)-C(1)-H(1A)	125.8
C(5)-C(1)-H(1A)	125.8
Pd(1)-C(1)-H(1A)	125.8
C(1)-C(2)-C(3)	107.5(3)
C(1)-C(2)-Pd(1)	70.97(15)
C(3)-C(2)-Pd(1)	68.36(16)
C(1)-C(2)-H(2A)	126.2
C(3)-C(2)-H(2A)	126.2
Pd(1)-C(2)-H(2A)	126.2

C(2)-C(3)-C(4)	108.5(3)
C(2)-C(3)-Pd(1)	76.90(16)
C(4)-C(3)-Pd(1)	72.32(16)
C(2)-C(3)-H(3A)	125.3
C(4)-C(3)-H(3A)	125.3
Pd(1)-C(3)-H(3A)	125.3
C(5)-C(4)-C(3)	107.6(3)
C(5)-C(4)-Pd(1)	72.89(16)
C(3)-C(4)-Pd(1)	71.55(16)
C(5)-C(4)-H(4A)	126.1
C(3)-C(4)-H(4A)	126.1
Pd(1)-C(4)-H(4A)	126.1
C(4)-C(5)-C(1)	108.0(3)
C(4)-C(5)-Pd(1)	72.11(16)
C(1)-C(5)-Pd(1)	73.65(16)
C(4)-C(5)-H(5A)	125.8
C(1)-C(5)-H(5A)	125.8
Pd(1)-C(5)-H(5A)	125.8
C(7)-C(6)-Pd(1)	68.44(16)
C(7)-C(6)-H(6A)	116.8
Pd(1)-C(6)-H(6A)	116.8
C(7)-C(6)-H(6B)	116.8
Pd(1)-C(6)-H(6B)	116.8
H(6A)-C(6)-H(6B)	113.8
C(8)-C(7)-C(6)	116.5(3)
C(8)-C(7)-Pd(1)	74.74(16)
C(6)-C(7)-Pd(1)	72.35(16)
C(8)-C(7)-H(7A)	121.7
C(6)-C(7)-H(7A)	121.7
Pd(1)-C(7)-H(7A)	121.7
C(7)-C(8)-C(9)	124.3(3)
C(7)-C(8)-Pd(1)	66.85(15)
C(9)-C(8)-Pd(1)	122.51(19)
C(7)-C(8)-H(8A)	112.0

C(9)-C(8)-H(8A)	112.0
Pd(1)-C(8)-H(8A)	112.0
C(10)-C(9)-C(14)	118.0(3)
C(10)-C(9)-C(8)	123.8(3)
C(14)-C(9)-C(8)	118.2(3)
C(9)-C(10)-C(11)	120.7(3)
C(9)-C(10)-H(10A)	119.6
C(11)-C(10)-H(10A)	119.6
C(12)-C(11)-C(10)	120.4(3)
C(12)-C(11)-H(11A)	119.8
C(10)-C(11)-H(11A)	119.8
C(13)-C(12)-C(11)	119.5(3)
C(13)-C(12)-H(12A)	120.3
C(11)-C(12)-H(12A)	120.3
C(12)-C(13)-C(14)	120.6(3)
C(12)-C(13)-H(13A)	119.7
C(14)-C(13)-H(13A)	119.7
C(13)-C(14)-C(9)	120.9(3)
C(13)-C(14)-H(14A)	119.6
C(9)-C(14)-H(14A)	119.6

---

Symmetry transformations used to generate equivalent atoms

Table 4. Anisotropic displacement parameters ( $\text{\AA}^2 \times 10^3$ ) for  $\text{Pd}(\eta^3\text{-1-Ph-C}_3\text{H}_4)(\eta^5\text{-C}_5\text{H}_5)$ . The anisotropic displacement factor exponent takes the form:  $-2\pi^2 [h^2 a^{*2} U^{11} + \dots + 2 h k a^* b^* U^{12}]$

	U <sup>11</sup>	U <sup>22</sup>	U <sup>33</sup>	U <sup>23</sup>	U <sup>13</sup>	U <sup>12</sup>
Pd(1)	24(1)	25(1)	18(1)	0(1)	3(1)	0(1)
C(1)	49(2)	32(2)	22(1)	3(1)	3(1)	-9(1)
C(2)	30(1)	43(2)	17(1)	3(1)	0(1)	1(1)
C(3)	37(2)	39(2)	20(1)	-8(1)	5(1)	-2(1)
C(4)	30(2)	58(2)	24(2)	-1(1)	9(1)	6(2)

C(5)	30(2)	62(2)	22(1)	9(1)	1(1)	-16(2)
C(6)	40(2)	28(2)	29(2)	3(1)	1(1)	-2(1)
C(7)	36(2)	35(2)	29(2)	6(1)	7(1)	-4(1)
C(8)	35(2)	35(2)	21(1)	6(1)	2(1)	4(1)
C(9)	36(2)	27(1)	17(1)	4(1)	6(1)	-3(1)
C(10)	32(2)	38(2)	31(2)	2(1)	0(1)	-3(1)
C(11)	38(2)	39(2)	38(2)	2(1)	9(1)	7(1)
C(12)	59(2)	28(2)	27(2)	-1(1)	7(1)	-3(2)
C(13)	43(2)	40(2)	23(2)	4(1)	-2(1)	-11(1)
C(14)	34(2)	37(2)	25(1)	9(1)	4(1)	2(1)

Table 5. Hydrogen coordinates ( $\times 10^4$ ) and isotropic displacement parameters ( $\text{\AA}^2 \times 10^3$ ) Pd( $\eta^3$ -1-Ph-C<sub>3</sub>H<sub>4</sub>)( $\eta^5$ -C<sub>5</sub>H<sub>5</sub>).

	x	y	z	U(eq)
H(1A)	2691	5462	6465	41
H(2A)	4497	6624	7101	36
H(3A)	3412	8451	7412	38
H(4A)	877	8370	7054	45
H(5A)	438	6542	6451	45
H(6A)	2813	9654	5143	39
H(6B)	4287	9560	5573	39
H(7A)	4793	8039	4827	40
H(8A)	2003	8087	4480	36
H(10A)	4762	6164	4621	41
H(11A)	4885	4580	3941	46
H(12A)	3080	4054	3204	46
H(13A)	1133	5096	3169	42
H(14A)	1005	6687	3829	39

Table 6. Torsion angles [°] for Pd( $\eta^3$ -1-Ph-C<sub>3</sub>H<sub>4</sub>)( $\eta^5$ -C<sub>5</sub>H<sub>5</sub>).

C(7)-Pd(1)-C(1)-C(2)	98.8(2)
C(6)-Pd(1)-C(1)-C(2)	16.2(5)
C(8)-Pd(1)-C(1)-C(2)	143.71(17)
C(3)-Pd(1)-C(1)-C(2)	-36.01(17)
C(4)-Pd(1)-C(1)-C(2)	-78.68(18)
C(5)-Pd(1)-C(1)-C(2)	-115.9(2)
C(7)-Pd(1)-C(1)-C(5)	-145.28(19)
C(6)-Pd(1)-C(1)-C(5)	132.2(4)
C(8)-Pd(1)-C(1)-C(5)	-100.38(19)
C(3)-Pd(1)-C(1)-C(5)	79.90(18)
C(4)-Pd(1)-C(1)-C(5)	37.24(17)
C(2)-Pd(1)-C(1)-C(5)	115.9(2)
C(5)-C(1)-C(2)-C(3)	-4.4(3)
Pd(1)-C(1)-C(2)-C(3)	58.79(19)
C(5)-C(1)-C(2)-Pd(1)	-63.21(18)
C(7)-Pd(1)-C(2)-C(1)	-119.9(2)
C(6)-Pd(1)-C(2)-C(1)	-174.91(18)
C(8)-Pd(1)-C(2)-C(1)	-61.1(3)
C(3)-Pd(1)-C(2)-C(1)	118.7(3)
C(4)-Pd(1)-C(2)-C(1)	79.6(2)
C(5)-Pd(1)-C(2)-C(1)	38.23(18)
C(7)-Pd(1)-C(2)-C(3)	121.47(19)
C(6)-Pd(1)-C(2)-C(3)	66.4(2)
C(8)-Pd(1)-C(2)-C(3)	-179.74(18)
C(4)-Pd(1)-C(2)-C(3)	-39.04(18)
C(5)-Pd(1)-C(2)-C(3)	-80.45(19)
C(1)-Pd(1)-C(2)-C(3)	-118.7(3)
C(1)-C(2)-C(3)-C(4)	5.6(3)
Pd(1)-C(2)-C(3)-C(4)	66.02(19)
C(1)-C(2)-C(3)-Pd(1)	-60.44(19)
C(7)-Pd(1)-C(3)-C(2)	-98.3(2)
C(6)-Pd(1)-C(3)-C(2)	-133.05(17)



C(8)-Pd(1)-C(3)-C(2)	13(10)
C(4)-Pd(1)-C(3)-C(2)	114.5(3)
C(5)-Pd(1)-C(3)-C(2)	77.54(19)
C(1)-Pd(1)-C(3)-C(2)	35.41(17)
C(7)-Pd(1)-C(3)-C(4)	147.1(2)
C(6)-Pd(1)-C(3)-C(4)	112.4(2)
C(8)-Pd(1)-C(3)-C(4)	-101(10)
C(5)-Pd(1)-C(3)-C(4)	-37.01(19)
C(1)-Pd(1)-C(3)-C(4)	-79.1(2)
C(2)-Pd(1)-C(3)-C(4)	-114.5(3)
C(2)-C(3)-C(4)-C(5)	-4.6(3)
Pd(1)-C(3)-C(4)-C(5)	64.47(19)
C(2)-C(3)-C(4)-Pd(1)	-69.07(19)
C(7)-Pd(1)-C(4)-C(5)	146.6(3)
C(6)-Pd(1)-C(4)-C(5)	157.73(18)
C(8)-Pd(1)-C(4)-C(5)	63.1(3)
C(3)-Pd(1)-C(4)-C(5)	-115.8(3)
C(1)-Pd(1)-C(4)-C(5)	-38.05(18)
C(2)-Pd(1)-C(4)-C(5)	-78.3(2)
C(7)-Pd(1)-C(4)-C(3)	-97.5(4)
C(6)-Pd(1)-C(4)-C(3)	-86.4(2)
C(8)-Pd(1)-C(4)-C(3)	178.93(18)
C(5)-Pd(1)-C(4)-C(3)	115.8(3)
C(1)-Pd(1)-C(4)-C(3)	77.78(19)
C(2)-Pd(1)-C(4)-C(3)	37.49(17)
C(3)-C(4)-C(5)-C(1)	1.8(3)
Pd(1)-C(4)-C(5)-C(1)	65.42(19)
C(3)-C(4)-C(5)-Pd(1)	-63.6(2)
C(2)-C(1)-C(5)-C(4)	1.6(3)
Pd(1)-C(1)-C(5)-C(4)	-64.41(19)
C(2)-C(1)-C(5)-Pd(1)	66.00(19)
C(7)-Pd(1)-C(5)-C(4)	-148.9(3)
C(6)-Pd(1)-C(5)-C(4)	-43.0(3)
C(8)-Pd(1)-C(5)-C(4)	-142.45(18)

C(3)-Pd(1)-C(5)-C(4)	38.23(18)
C(1)-Pd(1)-C(5)-C(4)	115.7(2)
C(2)-Pd(1)-C(5)-C(4)	79.16(19)
C(7)-Pd(1)-C(5)-C(1)	95.5(3)
C(6)-Pd(1)-C(5)-C(1)	-158.6(2)
C(8)-Pd(1)-C(5)-C(1)	101.89(18)
C(3)-Pd(1)-C(5)-C(1)	-77.44(17)
C(4)-Pd(1)-C(5)-C(1)	-115.7(2)
C(2)-Pd(1)-C(5)-C(1)	-36.50(16)
C(8)-Pd(1)-C(6)-C(7)	-33.44(17)
C(3)-Pd(1)-C(6)-C(7)	146.18(17)
C(4)-Pd(1)-C(6)-C(7)	-174.08(17)
C(5)-Pd(1)-C(6)-C(7)	-146.8(2)
C(1)-Pd(1)-C(6)-C(7)	99.3(5)
C(2)-Pd(1)-C(6)-C(7)	111.61(19)
Pd(1)-C(6)-C(7)-C(8)	62.1(2)
C(6)-Pd(1)-C(7)-C(8)	-125.0(3)
C(3)-Pd(1)-C(7)-C(8)	179.04(17)
C(4)-Pd(1)-C(7)-C(8)	-109.9(3)
C(5)-Pd(1)-C(7)-C(8)	8.9(4)
C(1)-Pd(1)-C(7)-C(8)	76.5(2)
C(2)-Pd(1)-C(7)-C(8)	127.19(17)
C(8)-Pd(1)-C(7)-C(6)	125.0(3)
C(3)-Pd(1)-C(7)-C(6)	-56.0(3)
C(4)-Pd(1)-C(7)-C(6)	15.0(4)
C(5)-Pd(1)-C(7)-C(6)	133.8(3)
C(1)-Pd(1)-C(7)-C(6)	-158.58(18)
C(2)-Pd(1)-C(7)-C(6)	-107.9(2)
C(6)-C(7)-C(8)-C(9)	-175.4(3)
Pd(1)-C(7)-C(8)-C(9)	-114.6(3)
C(6)-C(7)-C(8)-Pd(1)	-60.8(2)
C(6)-Pd(1)-C(8)-C(7)	34.10(18)
C(3)-Pd(1)-C(8)-C(7)	-113(10)
C(4)-Pd(1)-C(8)-C(7)	147.2(2)

C(5)-Pd(1)-C(8)-C(7)	-176.29(18)
C(1)-Pd(1)-C(8)-C(7)	-134.37(18)
C(2)-Pd(1)-C(8)-C(7)	-99.3(2)
C(7)-Pd(1)-C(8)-C(9)	117.1(3)
C(6)-Pd(1)-C(8)-C(9)	151.2(3)
C(3)-Pd(1)-C(8)-C(9)	4(10)
C(4)-Pd(1)-C(8)-C(9)	-95.7(3)
C(5)-Pd(1)-C(8)-C(9)	-59.2(3)
C(1)-Pd(1)-C(8)-C(9)	-17.3(3)
C(2)-Pd(1)-C(8)-C(9)	17.8(3)
C(7)-C(8)-C(9)-C(10)	21.1(4)
Pd(1)-C(8)-C(9)-C(10)	-61.4(3)
C(7)-C(8)-C(9)-C(14)	-157.0(3)
Pd(1)-C(8)-C(9)-C(14)	120.5(2)
C(14)-C(9)-C(10)-C(11)	0.5(4)
C(8)-C(9)-C(10)-C(11)	-177.6(3)
C(9)-C(10)-C(11)-C(12)	-0.2(5)
C(10)-C(11)-C(12)-C(13)	-0.7(4)
C(11)-C(12)-C(13)-C(14)	1.1(4)
C(12)-C(13)-C(14)-C(9)	-0.8(4)
C(10)-C(9)-C(14)-C(13)	0.0(4)
C(8)-C(9)-C(14)-C(13)	178.2(2)

---

Symmetry transformations used to generate equivalent atoms

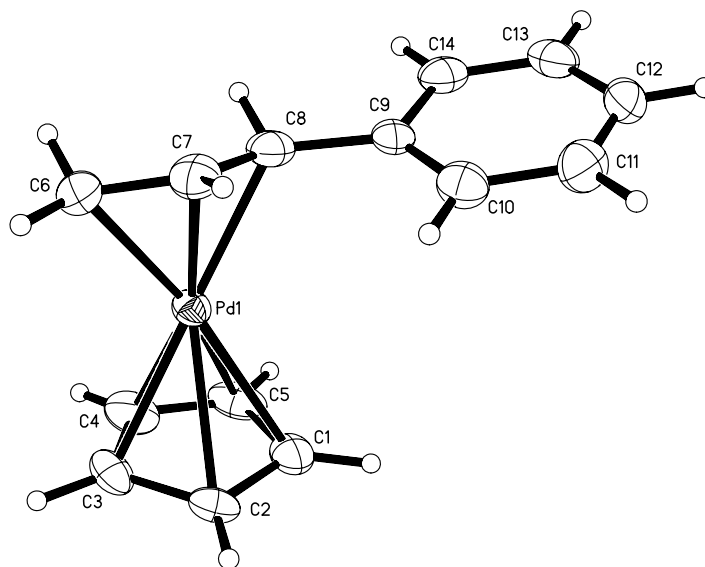
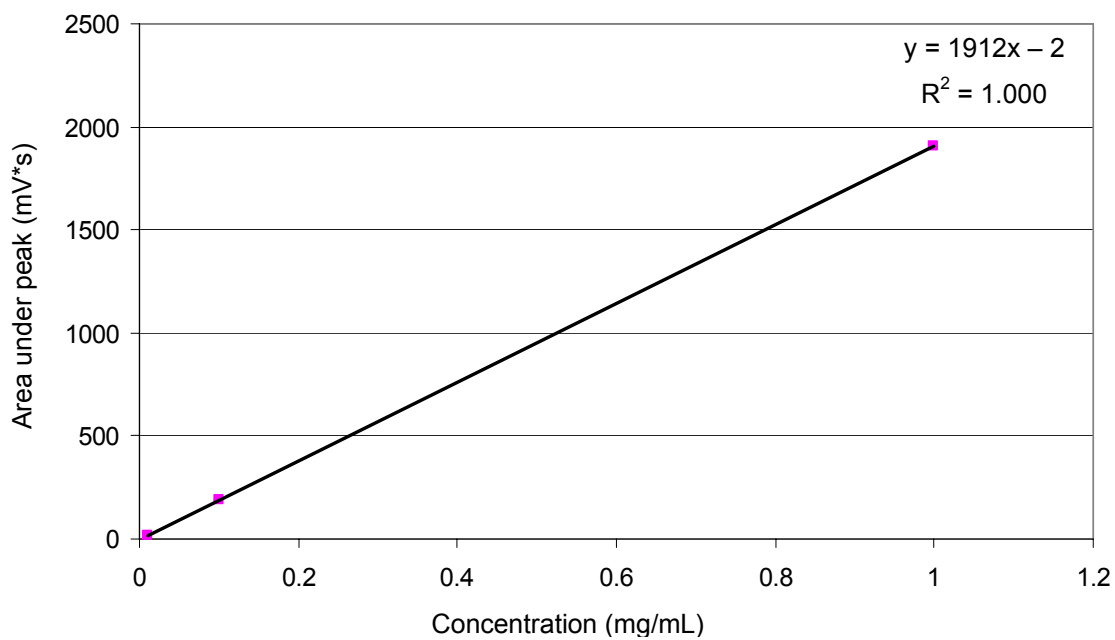
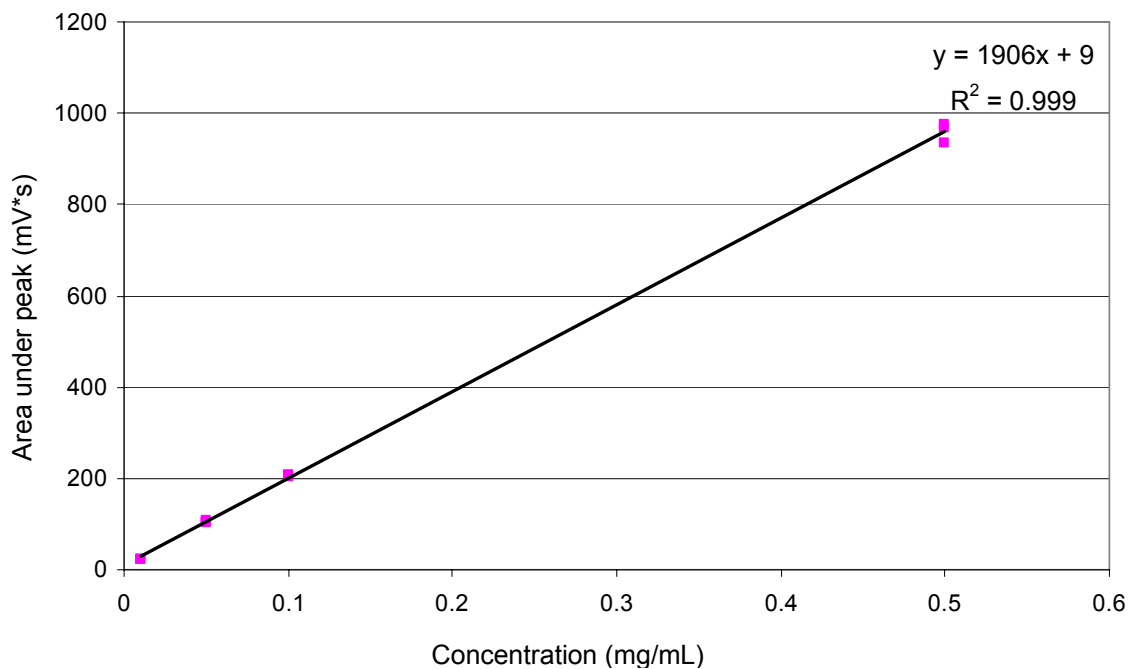


Figure 1. The ORTEP plot of Pd( $\eta^3$ -1-Ph-C<sub>3</sub>H<sub>4</sub>)( $\eta^5$ -C<sub>5</sub>H<sub>5</sub>). Atoms drawn at the 50% probability level.

**Appendix B.** Calibration Curves and a Sample Gas Chromatograph



**Figure 44. Biphenyl Calibration Curve**



**Figure 45. Methylbiphenyl Calibration Curve**

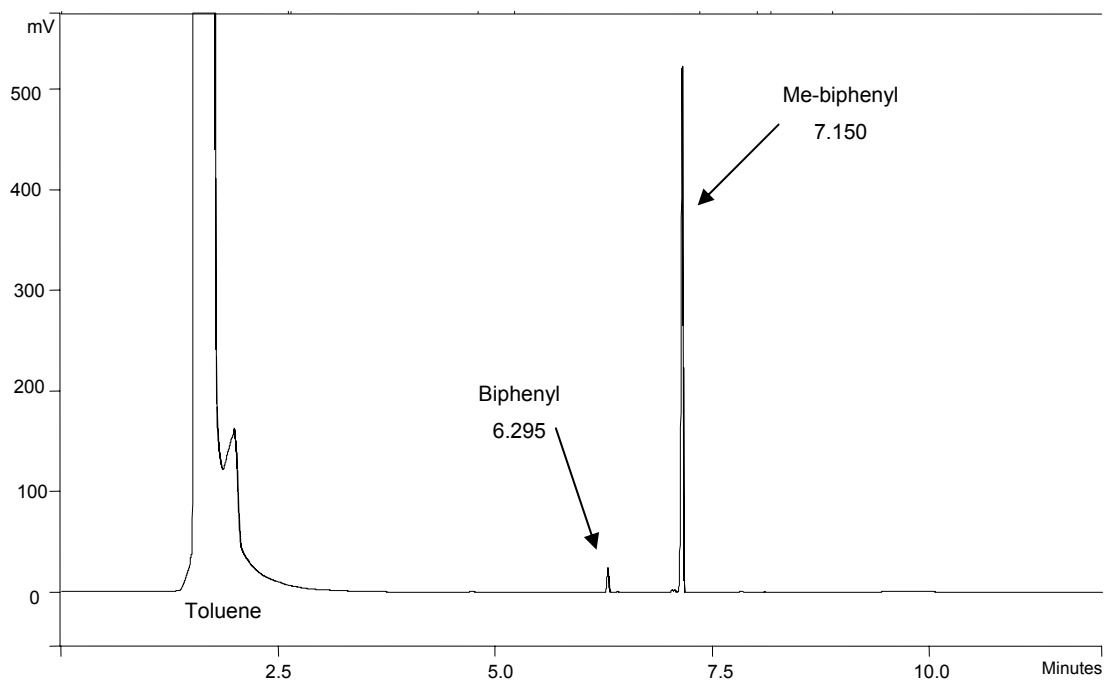


**Figure 46. Representative chromatograph: reaction of Pd(Tol)(Br)(PCy<sub>3</sub>)<sub>2</sub> and [NBu<sub>4</sub>][PhBF<sub>3</sub>] in the presence of 3.75 eq H<sub>2</sub>O (table 1, entry 5)**